

# Complete spectral energy distribution of the hot, helium-rich white dwarf RX J0503.9–2854<sup>★,★★,★★★</sup>

D. Hoyer<sup>1</sup>, T. Rauch<sup>1</sup>, K. Werner<sup>1</sup>, J. W. Kruk<sup>2</sup>, and P. Quinet<sup>3,4</sup>

<sup>1</sup> Institute for Astronomy and Astrophysics, Kepler Center for Astro and Particle Physics, Eberhard Karls University, Sand 1, 72076 Tübingen, Germany

e-mail: rauch@astro.uni-tuebingen.de

<sup>2</sup> NASA Goddard Space Flight Center, Greenbelt, MD 20771, USA

<sup>3</sup> Physique Atomique et Astrophysique, Université de Mons – UMONS, 7000 Mons, Belgium

<sup>4</sup> IPNAS, Université de Liège, Sart Tilman, 4000 Liège, Belgium

Received 10 October 2016 / Accepted 17 October 2016

## ABSTRACT

**Context.** In the line-of-sight toward the DO-type white dwarf RX J0503.9–2854, the density of the interstellar medium (ISM) is very low, and thus the contamination of the stellar spectrum almost negligible. This allows to identify many metal lines in a wide wavelength range from the extreme ultraviolet to the near infrared.

**Aims.** In previous spectral analyses, many metal lines in the ultraviolet spectrum of RX J0503.9–2854 have been identified. A complete line list of observed and identified lines is presented here.

**Methods.** We compared synthetic spectra that had been calculated from model atmospheres in non-local thermodynamical equilibrium, with observations.

**Results.** In total, we identified 1272 lines (279 of them were newly assigned) in the wavelength range from the extreme ultraviolet to the near infrared. 287 lines remain unidentified. A close inspection of the EUV shows that still no good fit to the observed shape of the stellar continuum flux can be achieved although He, C, N, O, Al, Si, P, S, Ca, Sc, Ti, V, Cr, Mn, Fe, Cr, Ni Zn, Ga, Ge, As, Kr, Zr, Mo, Sn, Xe, and Ba are included in the stellar atmosphere models.

**Conclusions.** There are two possible reasons for the deviation between observed and synthetic flux in the EUV may have two reasons. Opacities from hitherto unconsidered elements in the model-atmosphere calculation may be missing, and/or the effective temperature is slightly lower than previously determined.

**Key words.** atomic data – line: identification – stars: abundances – stars: individual: RX J0503.9–2854 – virtual observatory tools

## 1. Introduction

The white dwarf (WD) RX J0503.9–2854 (henceforth RE 0503–289, WD 0501–289 McCook & Sion 1999a,b) was discovered in the ROSAT (ROentgen SATellite) wide field camera all-sky survey of extreme-ultraviolet (EUV) sources (Pounds et al. 1993). Barstow et al. (1993) reported its discovery by the Extreme Ultraviolet Explorer (EUVE), and identified it with a peculiar He-rich DO-type WD, namely MCT 0501–2858 in the Montreal-Cambridge-Tololo survey of southern hemisphere blue stars (Demers et al. 1986). They found that RE 0503–289 is located in a direction with very low density of the interstellar medium (ISM). In the line of sight (LOS) toward RE 0503–289, Vennes et al. (1994) measured a column density of  $\log(N_{\text{HI}}/\text{cm}^{-2}) = 17.75 - 18.00$  using EUVE photometry data. Rauch et al. (2016c) resolved at least two ISM components in the LOS toward RE 0503–289

based on high-resolution and high signal-to-noise ultraviolet (UV) spectroscopy performed by Far Ultraviolet Spectroscopic Explorer (FUSE) and HST/STIS (Hubble Space Telescope / Space Telescope Imaging Spectrograph) and measured a very low ( $E_{B-V} = 0.015 \pm 0.002$ ) interstellar reddening.

The almost negligible contamination by ISM line absorption allows us to identify even weak lines of many species from so far He up to trans-iron elements as heavy as Ba (Table 2). For reliable abundance analyses of these elements, a precise  $T_{\text{eff}}$  and  $\log g$  determination is a prerequisite to keep error propagation as small as possible. An initial constraint of  $T_{\text{eff}} = 60\,000 - 70\,000$  K was given by Vennes et al. (1994) from EUV photometry. The first spectral analysis by means of non-local thermodynamic equilibrium (NLTE) stellar atmosphere models considering opacities of H, He, and C was published by Barstow et al. (1994). They found  $T_{\text{eff}} = 60\,000 - 80\,000$  K and  $\log(g/\text{cm/s}^2) = 7.5 - 8.0$ . Dreizler & Werner (1996) used ultraviolet (UV) spectra in addition and NLTE model atmospheres and determined  $T_{\text{eff}} = 70\,000 \pm 5\,000$  K and  $\log g = 7.5 \pm 0.5$ . Recently, Rauch et al. (2016c) analyzed optical and ultraviolet (FUSE and HST/STIS) spectra and significantly reduced the error limits to  $\pm 2\,000$  K and  $\pm 0.1$ , respectively. Table 1 summarizes previous analyses.

\* Based on observations with the NASA/ESA Hubble Space Telescope, obtained at the Space Telescope Science Institute, which is operated by the Association of Universities for Research in Astronomy, Inc., under NASA contract NAS5-26666.

\*\* Based on observations made with the NASA-CNES-CSA Far Ultraviolet Spectroscopic Explorer.

\*\*\* Based on observations made with ESO Telescopes at the La Silla Paranal Observatory under program IDs 072.D-0362, 165.H-0588, and 167.D-0407.

**Table 1.** History of  $T_{\text{eff}}$  and  $\log g$  determinations (cf., Müller-Ringat 2013). PM denotes photometry.

$T_{\text{eff}}$ /kK	$\log g$	Model atmosphere	Method	Comment	Reference
60–90			EUV, PM	very low $N_{\text{H}1}$	Barstow et al. (1993)
60–80			EUV, OPT	very low $N_{\text{H}1}$	Barstow et al. (1993)
60–80	7.5–8.0	He, HHeC	NLTE, OPT, UV, EUV	EUV problem <sup>a</sup>	Barstow et al. (1994)
60–70			EUV, PM	very low $N_{\text{H}1}$	Vennes et al. (1994)
70 <sup>b</sup>	7.0	HeCNOSiFeNi	LTE, EUV, UV		Polomski et al. (1995)
65 <sup>c</sup>	7.5 <sup>d</sup>	HHeC	NLTE, OPT	no H detectable, upper limit 5% (mass fraction)	Werner (1996)
70	7.5	HHeCNOSi	NLTE, OPT, UV	$M = 0.49 M_{\odot}$	Dreizler & Werner (1996)
66.6–70.4	7.13–7.27	HHe	LTE, UV	$M = 0.40 M_{\odot}$	Vennes et al. (1998)
70 <sup>e</sup>	7.5 <sup>e</sup>		NLTE, diffusion	no good fit achieved	Dreizler (1999)
69–75	7.26–7.63	HHeC	NLTE, OPT, UV, EUV	EUV problem <sup>a</sup>	Barstow et al. (2000)
		HHeCNOSiFeNi			
65–70	7.5 <sup>e</sup>	HeCNi, HeONi	NLTE, EUV	EUV problem <sup>a</sup>	Werner et al. (2001)
70 <sup>e</sup>	7.5 <sup>e</sup>	HHeCNOSiFeNi+PS	NLTE, UV	EUV problem <sup>a</sup>	Barstow et al. (2007)
			LTE		
68–72	7.4–7.6	HeCNOAlSiPS+CaScTiVCrMnFeCrNi+ZnGaGeAsKrZrMoSnXeBa	NLTE, OPT, UV	$M = 0.514^{+0.15}_{-0.05} M_{\odot}$	Rauch et al. (2016c)

**Notes.** <sup>(a)</sup> Sect. 7, <sup>(b)</sup> adopted upper limit of Vennes et al. (1994), <sup>(c)</sup> adopted value close to lower limit of Barstow et al. (1994), <sup>(d)</sup> adopted from Barstow et al. (1994), <sup>(e)</sup> adopted from Dreizler & Werner (1996)

**Table 2.** Photospheric abundances (mass fraction) of RE 0503–289. The reference for the 1<sup>st</sup> line identifications is given in the final column.

Element	Abundance	1 <sup>st</sup> Line identifications
He	$9.73 \times 10^{-1}$	Barstow et al. (1994)
C	$2.22 \times 10^{-2}$	Barstow et al. (1994)
N	$5.49 \times 10^{-5}$	Dreizler & Werner (1996)
O	$2.94 \times 10^{-3}$	Polomski et al. (1995), Dreizler & Werner (1996)
Al	$5.01 \times 10^{-5}$	Rauch et al. (2016a)
Si	$1.60 \times 10^{-4}$	Polomski et al. (1995), Dreizler & Werner (1996)
P	$1.06 \times 10^{-6}$	Vennes et al. (1998); Barstow et al. (2007)
S	$3.96 \times 10^{-5}$	Barstow et al. (2007)
Ni	$7.25 \times 10^{-5}$	Barstow et al. (2000)
Zn	$1.13 \times 10^{-4}$	Rauch et al. (2014a)
Ga	$3.44 \times 10^{-5}$	Werner et al. (2012b), Rauch et al. (2015b)
Ge	$1.58 \times 10^{-4}$	Werner et al. (2012b), Rauch et al. (2012)
As	$1.60 \times 10^{-5}$	Werner et al. (2012b)
Se		Werner et al. (2012b)
Kr	$5.04 \times 10^{-4}$	Werner et al. (2012b), Rauch et al. (2016c)
Zr	$3.00 \times 10^{-4}$	Rauch et al. (2016a)
Mo	$1.88 \times 10^{-4}$	Rauch et al. (2016b)
Sn	$2.06 \times 10^{-4}$	Werner et al. (2012b)
Te		Werner et al. (2012b)
I		Werner et al. (2012b)
Xe	$1.26 \times 10^{-4}$	Werner et al. (2012b), Rauch et al. (2015a), Rauch et al. (2016a)
Ba	$3.57 \times 10^{-4}$	Rauch et al. (2014b)

## 2. Observations

In this paper, we used the observed spectra that are briefly described in the following. If they are compared to synthetic spectra, the latter are convolved with Gaussians to model the respective instrument’s resolution.

Extreme ultraviolet observations by the EUVE observatory were performed using the short-wavelength ( $70 \text{ \AA} < \lambda < 190 \text{ \AA}$ ), the medium-wavelength ( $140 \text{ \AA} < \lambda < 380 \text{ \AA}$ ), and the long-wavelength ( $280 \text{ \AA} < \lambda < 760 \text{ \AA}$ ) spectrometers with a resolving power of  $R \approx 300$ . Details of the data reduction are given by Dupuis et al. (1995).

Far ultraviolet spectra ( $910 \text{ \AA} < \lambda < 1190 \text{ \AA}$ ,  $R \approx 20\,000$ ) were obtained with FUSE. Their data IDs are M1123601 (2000-12-04), M1124201 (2001-02-02), and P2041601 (2000-12-05). The spectra were shifted to rest wavelengths and co-added. For details see Werner et al. (2012b).

Ultraviolet spectroscopy was performed with HST/STIS on 2014-08-14. Two observations with grating E140M ( $1144 \text{ \AA} < \lambda < 1709 \text{ \AA}$ ,  $R \approx 45\,800$ ) and two observations with grating E230M ( $1690 \text{ \AA} < \lambda < 2366 \text{ \AA}$ ,  $2277 \text{ \AA} < \lambda < 3073 \text{ \AA}$ ,  $R \approx 30\,000$ ) were co-added. These observations are retrievable from the Barbara A. Mikulski Archive for Space Telescopes (MAST).

Optical spectra ( $3290 \text{ \AA} < \lambda < 4524 \text{ \AA}$ ,  $4604 \text{ \AA} < \lambda < 5609 \text{ \AA}$ ,  $5673 \text{ \AA} < \lambda < 6641 \text{ \AA}$ ) were obtained on 2000-09-09 and 2001-04-08 in the framework of the Supernova Ia Progenitor Survey project (SPY, Napiwotzki et al. 2001, 2003). The Ultraviolet and Visual Echelle Spectrograph (UVES) attached to the Very Large Telescope (VLT) located at the European Southern Observatory (ESO) on Cerro Paranal in Chile was employed to achieve a resolution of about  $0.2 \text{ \AA}$ . In addition, we use a spectrum taken with the Echelle Multi Mode Instrument (EMMI) attached to the New

**Table 3.** Newly calculated transition probabilities.

Element	Ions	Reference
Zn	IV - V	Rauch et al. (2014a)
Ga	IV - VI	Rauch et al. (2015b)
Ge	V - VI	Rauch et al. (2012)
Kr	IV - VII	Rauch et al. (2016c)
Zr	IV - VII	Rauch et al. (2016a)
Tc	II - VI	Werner et al. (2015)
Mo	IV - VII	Rauch et al. (2016b)
Xe	IV - VII	Rauch et al. (2015a, 2016a)
Ba	V - VII	Rauch et al. (2014b)

Technology Telescope (NTT) (1992-01,  $4094 \text{ \AA} < \lambda < 4994 \text{ \AA}$ , resolution of about  $3.0 \text{ \AA}$ ).

Near infrared spectroscopy ( $9500 \text{ \AA} < \lambda < 13420 \text{ \AA}$ ,  $R \approx 950$ ) was performed on 2003-12-10 using the Son-of-Isaac (SofI) instrument at the NTT. The spectrum used here was digitized with Dexter<sup>1</sup> from Fig. 1 in Dobbie et al. (2005).

### 3. Model atmospheres and atomic data

The stellar model atmospheres used for this paper were calculated with our Tübingen NLTE Model Atmosphere Package (TMAP<sup>2</sup>, Werner et al. 2003, 2012a). They assume plane-parallel geometry, are chemically homogeneous, and in hydrostatic and radiative equilibrium. An adaptation is the New Generation Radiative Transport (NGRT) code (Dreizler & Wolff 1999; Schuh et al. 2002) that can consider diffusion in addition to calculate stratified stellar atmospheres.

The Tübingen Model Atom Database (TMAD<sup>3</sup>) provides ready-to-use model atoms in TMAP format for many species up to Ba. TMAD has been constructed as part of the Tübingen contribution to the German Astrophysical Virtual Observatory (GAVO<sup>4</sup>).

Werner et al. (2012b) discovered lines of trans-iron elements, namely Ga (atomic number  $Z = 31$ ), Ge (32), As (33), Se (34), Kr (36), Mo (42), Sn (50), Te (52), I (53), and Xe (54), in the FUSE spectrum of RE 0503–289. For precise abundance determinations of these species, reliable atomic data is mandatory. For example, reliable transition probabilities are required, not only for lines that are identified in the observation but for the complete model atoms that are considered in the model-atmosphere calculations. Due to the lack of such data, Werner et al. (2012b) were restricted to abundance determinations of Kr and Xe only.

We initiated the calculation of new transition probabilities that were then used to determine the abundance of the respective element. Table 3 gives an overview of the so far calculated data. To provide easy access to this data, the registered Tübingen Oscillator Strengths Service (TOSS) has been created within the GAVO project.

To construct model atoms for the use within TMAP, the elements given in Table 3 require the calculation of so-called super levels and super lines with our Iron Opacity and Interface (IrOnIc, Rauch & Deetjen 2003) due to the very high number

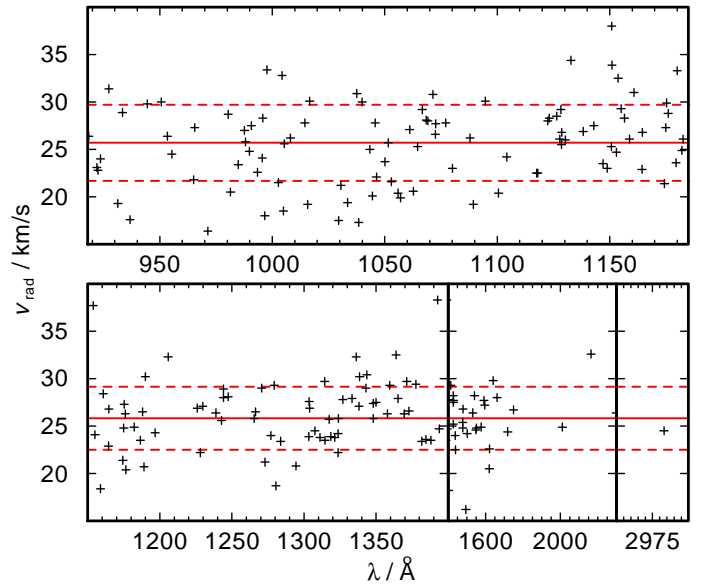


**Fig. 1.** Determination of  $v_{\text{rad}}$  from individual lines in the FUSE (top panel) and HST/STIS observations (bottom). The full horizontal lines indicate the average  $v_{\text{rad}}$  for FUSE and HST/STIS, respectively. The dashed lines show the  $1 \sigma$  error.

of atomic levels and lines. We transferred the TOSS data into Kurucz’s data format<sup>5</sup> that can be read by IrOnIc.

### 4. Radial velocity and gravitational redshift

To shift the observation to rest wavelength, we determined the radial velocity  $v_{\text{rad}}$  of RE 0503–289 from FUSE and HST/STIS spectra. To measure the wavelengths of the line centers, we used IRAF<sup>6</sup> to fit Gaussians to the line profiles. In total, we evaluated 100 lines in the FUSE wavelength range and 103 lines in the STIS wavelength range (Fig. 1). The averages are  $v_{\text{rad}}^{\text{FUSE}} = 25.7 \pm 4.2 \text{ km/s}$  and  $v_{\text{rad}}^{\text{STIS}} = 25.8 \pm 3.7 \text{ km/s}$ . We adopted the mean value of  $v_{\text{rad}} = 25.7^{+3.6}_{-4.0} \text{ km/s}$ . From this value, the gravitational redshift  $z$  has to be subtracted. To calculate  $z$  and the respective radial velocity, we created the GAVO tool Tübingen Gravitational REDshift calculator (TGRED, Fig. C.2). For RE 0503–289, we derive  $v_{\text{rad}}^{\text{gred}} = 15.5^{+6.7}_{-4.6} \text{ km/s}$ . The true radial velocity is then  $v_{\text{rad}}^{\text{RE 0503-289}} = 10.2^{+8.2}_{-8.6} \text{ km/s}$ .

### 5. Line identification

To unambiguously identify lines in our observed spectra (Sect. 2), we used the best synthetic model of Rauch et al. (2016a) and calculated additional spectra with oscillator strengths set to zero for individual elements. This allows to find weak lines, even if they are blended by stronger lines. The detection limit is an equivalent width of  $W_{\lambda} = 2 \text{ m\AA}$ . Table 4 shows the total numbers of lines identified in the four wavelength ranges and the numbers of lines that were suited to determine  $W_{\lambda}$  and  $v_{\text{rad}}$ . The current line lists are presented in Tables A.1 - A.5, a regularly updated version is available at <http://astro.uni-tuebingen.de/~hoyer/objects/RE0503-289>.

<sup>5</sup> <http://kurucz.harvard.edu/atoms.html>

<sup>6</sup> IRAF is distributed by the National Optical Astronomy Observatory, which is operated by the Associated Universities for Research in Astronomy, Inc., under cooperative agreement with the National Science Foundation.

<sup>1</sup> <http://dc.zah.uni-heidelberg.de/sdexter>

<sup>2</sup> <http://astro.uni-tuebingen.de/~TMAP>

<sup>3</sup> <http://astro.uni-tuebingen.de/~TMAD>

<sup>4</sup> <http://www.g-vo.org>

**Table 4.** Statistics of the identified (in brackets: newly identified in this paper) and unidentified lines in the observed spectra. The last two columns give the numbers of lines that were used to measure their equivalent widths  $W_\lambda$  and  $v_{\text{rad}}$  (Fig. 1), respectively.

Wavelength Range	Numbers of lines			$W_\lambda$	$v_{\text{rad}}$
	Total	Identified	Unidentified		
EUV	74	74( 35)	0	0	0
FUV	616	536( 55)	76	148	100
NUV	790	579(120)	211	252	103
optical	83	83( 69)	0	0	0
NIR	2	2( 0)	0	0	0

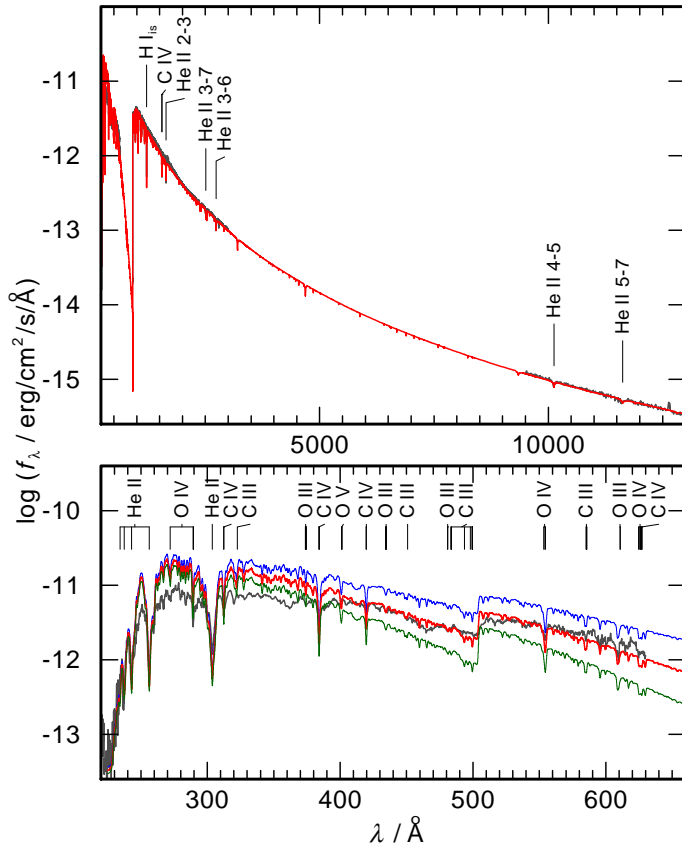


**Fig. 2.** Determination of  $E_{B-V}$ . Top: Reddening with  $E_{B-V}=0.00026$  applied to our synthetic spectrum in the wavelength range from the EUV to the NIR. Bottom: Same like top panel, for  $E_{B-V}=0.00016$  (blue),  $0.00026$  (red), and  $0.00036$  (green) in the EUV wavelength range. Prominent lines are marked.

## 6. Visualization and online line list

In the framework of the Tübingen (GAVO project, we have developed the registered Tübingen VISualization tool (TVIS) that allows the user to plot any data in an easy way on the WWW. The plotter itself is written in HTML5 and Javascript. To strongly increase the security of this web application, no Flash or Java is necessary to use it, meaning that TVIS will even work when Flash is dead and Java applets are blocked by the browsers.

The comparison of our best model spectra with the available observation of RE 0503–289 in the EUV, FUV, NUV, and optical wavelength ranges was realized with TVIS and is shown at <http://astro.uni-tuebingen.de/~TVIS/objects/RE0503-289>. Figures B.1 to B.3 show the FUV to optical range.

## 7. Is there still an EUV problem in RE 0503–289?

To analyze the EUVE observation, Barstow et al. (1995) used NLTE model atmospheres that were calculated with the code that is nowadays called TMAP. A synthetic spectrum (scaled to match the observed EUV flux) that was calculated from a model with  $T_{\text{eff}}=70\,000\text{ K}$ ,  $\log g=7.0$ ,  $C/He = 1\%$ , and  $N/He = 0.01\%$  (the latter being number ratios) reproduced well the observation. A major problem arose, however, from the fact that the model flux (reddened and interstellar neutral hydrogen absorption considered) in the wavelength range  $228\text{ \AA} < \lambda < 400\text{ \AA}$  was about an order of magnitude higher than observed. Only models with  $T_{\text{eff}} < 65\,000\text{ K}$  produced an acceptable fit. He I  $\lambda 5875.62\text{ \AA}$  ( $2p^3P^o - 3d^3D$ ) in the optical wavelength range (e.g., in spectra taken with the TWIN spectrograph at the Calar Alto observatory in SPY spectra, Dreizler & Werner 1996; Rauch et al. 2016c) establishes a stringent constraint of  $T_{\text{eff}} = 70\,000 \pm 2000\text{ K}$ .

Werner et al. (2001) calculated TMAP models that were composed of He, C, O, and the iron-group elements (Ca - Ni). Interstellar He I absorption was applied in addition to that of H I. The flux discrepancy was reduced (model flux three times higher than observed) but the basic problem, finding an agreement at  $T_{\text{eff}} = 70\,000\text{ K}$ , was not solved.

Müller-Ringat (2013) created the Tübingen EUV absorption tool (TEUV, Fig.C.1), that corrects synthetic stellar fluxes for ISM absorption for  $\lambda < 911\text{ \AA}$ . Presently, only radiative bound-free absorption of the lowest ionization states of H, He, C, N, and O is simulated. Opacity Project data (Seaton et al. 1994) is used for the photoionization cross-sections. These consider, for example, autoionization features. For this paper, Si has been added to TEUV. Two interstellar components with different radial and turbulent velocities, temperatures, and column densities can be considered. Müller-Ringat (2013) calculated TMAP models ( $T_{\text{eff}} = 70\,000\text{ K}$ ,  $\log g = 7.5$ ) that included He, C, N, O, and the iron-group elements. Although Kurucz's line lists were strongly extended in 2009 (Kurucz 2009, 2011), and about a factor of ten more iron-group lines were considered, the EUV model flux was about twice as high as that observed. To match the observed EUV flux,  $T_{\text{eff}}$  had to be reduced to  $\leq 65\,000\text{ K}$ .

Rauch et al. (2016a) determined  $T_{\text{eff}} = 70\,000 \pm 2000\text{ K}$  and  $\log g = 7.5 \pm 0.1$  in a detailed reanalysis of optical and UV spectra. They included 27 elements, namely He, C, N, O, Al, Si, P, S, Ca, Sc, Ti, V, Cr, Mn, Fe, Cr, Ni, Zn, Ga, Ge, As, Kr, Zr, Mo, Sn, Xe, and Ba, in their models. From these, we calculated the EUV spectrum ( $228\text{ \AA} \leq \lambda \leq 910\text{ \AA}$ ) with 1601 atomic levels treated in NLTE, considering 2481 lines of the elements He - S and about about 30 million lines of the elements with  $Z \geq 20$ . The frequency grid comprised 174 873 points with  $\Delta\lambda \leq 0.005\text{ \AA}$ .

Figure 2 demonstrates the determination of the interstellar reddening. We apply the reddening data of Morrison & McCammon (1983, provided for  $1.26\text{ \AA} \leq \lambda \leq 413\text{ \AA}$  and extrapolated toward the He I ground-state threshold) and Fitzpatrick (1999,  $\lambda \geq 911\text{ \AA}$ ). Between the He I ground-state edge and the H I Lyman edge, only absorption due to H I is considered. To determine  $E_{B-V}$ , we normalized our models to the 2MASS H brightness ( $14.766 \pm 0.063$ , Cutri et al. 2003a,b). To match the observed flux level between about  $400\text{ \AA}$  to  $600\text{ \AA}$ ,  $E_{B-V} = 0.00026 \pm 0.00003$  is necessary. This is less than  $E_{B-V} = 0.015 \pm 0.002$  that was used by Rauch et al. (2016c) to reproduce the observed FUSE flux level. With the Galactic reddening law of Groenewegen & Lamers (1989,  $\log(N_{\text{H I}}/E_{B-V}) = 21.58 \pm 0.1$ ) and the total cloud column den-

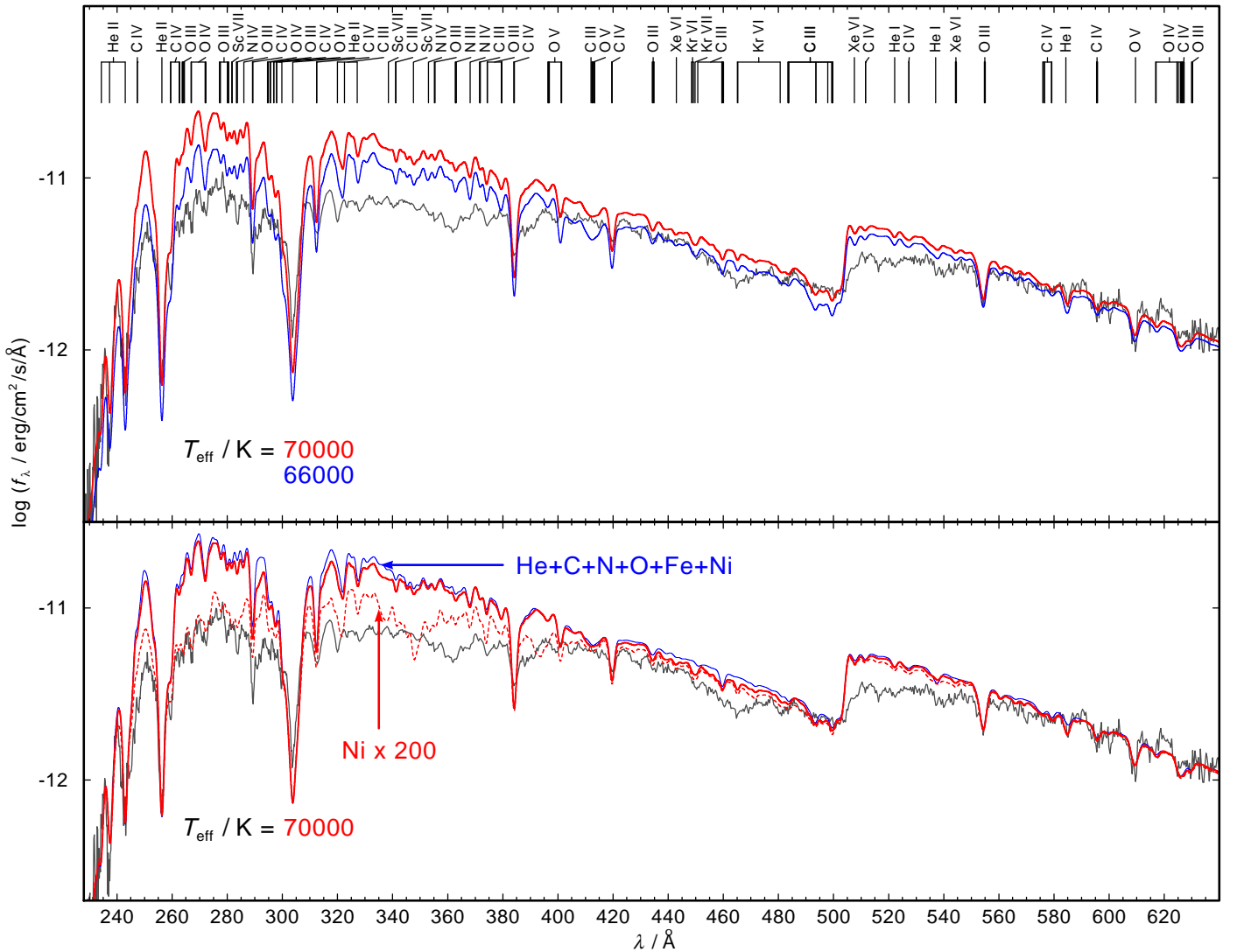


**Fig. 3.** Comparison of the EUVE observation (gray line in both panels) with our models. Top panel: Two models with  $T_{\text{eff}} = 70\,000$  K (red) and  $T_{\text{eff}} = 66\,000$  K (blue). Identified photospheric lines are marked at the top. Bottom panel: Three models with  $T_{\text{eff}} = 70\,000$  K. Red, thick line: model from the top panel, red, dashed line: model with 200 times increased Ni abundance, blue, thin line: model that considered only opacities of He, C, N, O, Fe, and Ni.

sity of interstellar H I of  $1.5 \pm 0.2 \times 10^{18} \text{ cm}^{-2}$  (measured from  $L\beta$ , Rauch et al. 2016c), we can calculate  $E_{B-V} = 0.00039^{+0.00017}_{-0.00012}$  which is within error limits well in agreement with our result.

A close look at the EUV wavelength range shows still a significant difference between model and observation (Fig. 3, top panel), most prominent between  $250 \text{ \AA}$  and  $400 \text{ \AA}$  and between  $504 \text{ \AA}$  and  $550 \text{ \AA}$ . Our present models reduced the deviation by about a factor of two compared the models of Werner et al. (2001). The EUV problem cannot be solved by using a cooler model, even at  $T_{\text{eff}} = 66\,000$  K, which is already outside the error range of  $T_{\text{eff}} = 70\,000 \pm 2000$  K given by Rauch et al. (2016c), no sufficient improvement is achieved. The impact of metal opacities is demonstrated in Fig. 3 by a model that considered only opacities from He, C, N, O, Fe, and Ni with same abundance ratios like our best model. To test the impact of additional opacity, we artificially increased the Ni abundance by factor of 200 to match the model’s flux to the observed between  $250 \text{ \AA}$  and  $280 \text{ \AA}$ . This reduced the flux discrepancy between  $300 \text{ \AA}$  and  $400 \text{ \AA}$  as well while the wavelength region above the He I ground-state threshold is unaffected. However, we conclude that

even in our advanced models opacity is missing from elements that are hitherto not considered. To include, for example, other trans-iron elements requires detailed laboratory measurements of their spectra and the extensive calculation of transition probabilities.

## 8. What is the nature of RE 0503–289?

RE 0503–289 was first classified to be a DO-type WD (Barstow et al. 1993). Its optical spectrum exhibits an absorption trough around C IV  $\lambda\lambda 4646.62 - 4687.95 \text{ \AA}$  and He II  $\lambda 4685.80 \text{ \AA}$ . This trough is the spectroscopic criterion for the H-deficient PG 1159-type stars (e.g., Werner & Herwig 2006). Figure 4 shows the comparison of the wavelength region around this trough for the PG 1159 prototype PG 1159–035 (V★ GW Vir, WD 1159–035,  $T_{\text{eff}} = 140\,000 \pm 5\,000$  K,  $\log g = 7.0 \pm 0.5$ , Jahn et al. 2007) and the O(He)-type WD KPD 0005+5106 (WD 0005+511,  $T_{\text{eff}} = 195\,000 \pm 15\,000$  K,  $\log g = 6.7 \pm 0.2$ , Werner & Rauch 2015). Both objects are at an earlier state of stellar evolution than RE 0503–289. The

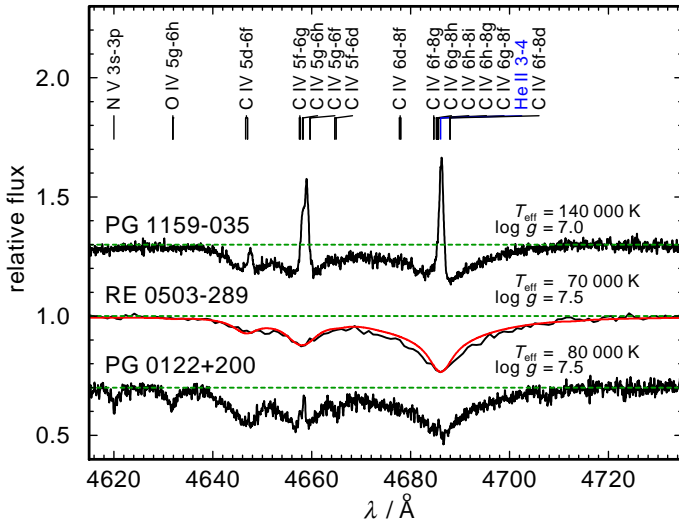


**Fig. 4.** Section of the optical spectra of PG 1159–035 (from SPY, shifted by 0.3 in flux units), RE 0503–289 (EMMI), and PG 0122+200 (KECK, shifted by  $-0.3$ ) (from top to bottom) around the PG 1159 absorption trough. For RE 0503–289, the synthetic spectrum of Rauch et al. (2016a) is overplotted (red line). The green, dashed lines indicate the continuum level.

strengths of the PG 1159 absorption troughs are almost the same for the much hotter PG 1159–035 and RE 0503–289, although their photospheric C abundances are significantly different,  $\approx 48\%$  by mass (Jahn et al. 2007) and  $\approx 2\%$ , respectively. The cool PG 1159-type star PG 0122+200 has about 22% of C in its photosphere (Werner & Rauch 2014).

In a  $\log T_{\text{eff}} - \log g$  diagram (Fig. 5), RE 0503–289 is located at the so-called PG 1159 wind limit (Unglaub & Bues 2000, their Fig. 13, digitized with Dexter) that was predicted for a ten-times-reduced mass-loss rate (line A, calculated with  $\dot{M} = 1.29 \times 10^{-15} L^{1.86}$  from Bloeker 1995; Pauldrach et al. 1988). This line approximately separates the regions that are populated by PG 1159-type stars and DO-type WDs. Lines B and C in Fig. 5 show where the photospheric C content is reduced by factors of 0.5 and 0.1, respectively, when using the mass-loss rate given above. To the right of line D, no PG 1159 star is located.

Werner et al. (2014) suggested a mass ratio  $C/He = 0.02$  to conserve previously assigned spectroscopic classes. However, PG 1159 stars span a wide range of  $C/He$  (0.03 – 0.33, Werner et al. 2014).

RE 0503–289 is located close to line B of Unglaub & Bues (2000) in Fig. 5, that is, its C abundance should be already reduced by a factor of 0.5. Thus, it is likely that RE 0503–289 had a  $C/He \approx 0.05$  in its antecedent PG 1159-star phase. Even now, its  $C/He$  lies a bit higher than 0.02 and RE 0503–289 may be classified as a PG 1159 star as well. This is corroborated by the still high efficiency of radiative levitation that is responsible for the extremely high overabundances of trans-iron elements (Rauch et al. 2016b). However, the transition from a PG 1159-type star to a DO-type star is smooth and RE 0503–289 is an ideal object to study this in detail. Unfortunately, the strong radiative levitation of trans-iron elements wipes out all information about their asymptotic giant branch (AGB) abundances and RE 0503–289 is not suited to constrain AGB nucleosynthesis models.

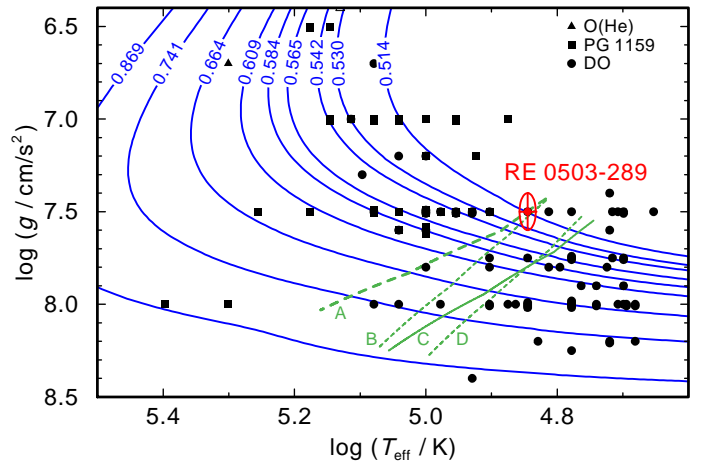


**Fig. 5.** Location of RE 0503–289 and related objects (Hügelmeier et al. 2006; Kepler et al. 2016; Reindl et al. 2014b,a; Werner & Herwig 2006) in the  $\log T_{\text{eff}} - \log g$  plane (cf., <http://www.star.le.ac.uk/~nr152/He.html> for stellar parameters). Evolutionary tracks for H-deficient WDs (Althaus et al. 2009) labeled with their respective masses in  $M_{\odot}$  are plotted for comparison. Transition limits predicted by Unglaub & Bues (2000) are indicated (see text for details).

## 9. Results

RE 0503–289 fulfills criteria of PG 1159 star and of DO-type WD classifications. The presence of the strong PG 1159 absorption trough around  $\text{He II } \lambda 4685.80 \text{ \AA}$  (Fig. 4) shows that RE 0503–289 could be classified as a PG 1159 star, although its C abundance would then be the lowest of this group. It is located close to the so-called PG 1159 wind limit (Fig. 5), meaning that it is close to the regime in which gravitation will dominate and pull metals down, out of the atmosphere. The strongly increased abundances of trans-iron elements, however, indicate that radiative levitation is still efficiently counteracting this process. Thus, RE 0503–289 has not arrived in its final stage of evolution. Formally, due to its  $\log g > 7$ , the DO-type WD classification is right.

In the observed spectra, we identified 1272 lines in the wavelength range from the extreme ultraviolet to the near infrared. 287 lines remain unidentified. The best model of Rauch et al. (2016a) reproduces well most of the identified lines.

The EUV problem (Sect. 7) – the difference between observed and synthetic flux in the EUV is still present. Our advanced model atmospheres include opacities of 27 metals but their flux in the EUV is still partly about a factor of approximately two too high compared with the observation. We expect that missing metal opacities are the reason for this discrepancy.

*Acknowledgements.* DH and TR are supported by the German Aerospace Center (DLR, grants 50 OR 1501 and 05 OR 1507, respectively). The German Astrophysical Virtual Observatory (GAVO) project at Tübingen had been supported by the Federal Ministry of Education and Research (BMBF, 05 AC 6 VTB, 05 AC 11 VTB). Financial support from the Belgian FRS-FNRS is also acknowledged. PQ is research director of this organization. Some of the data presented in this paper were obtained from the Mikulski Archive for Space Telescopes (MAST). STScI is operated by the Association of Universities for Research in Astronomy, Inc., under NASA contract NAS5-26555. Support for MAST for non-HST data is provided by the NASA Office of Space Science via grant NNX09AF08G and by other grants and contracts. We thank Ralf Napiwotzki for putting the reduced ESO/VLT spectra at our disposal. The TEUV tool (<http://astro-uni-tuebingen.de/~TEUV>), the TGRED tool (<http://astro-uni-tuebingen.de/~TGRED>), the TIRO service (<http://astro-uni-tuebingen.de/~TIRO>), the TMAD service (<http://astro-uni-tuebingen.de/~TMAD>), the TOSS service (<http://astro-uni-tuebingen.de/~TOSS>), and the TVIS tool (<http://astro-uni-tuebingen.de/~TVIS>).

astro-uni-tuebingen.de/~TVIS) used for this paper were constructed as part of the activities of the German Astrophysical Virtual Observatory. This work used the profile-fitting procedure OWENS developed by M. Lemoine and the FUSE French Team. This research has made use of NASA's Astrophysics Data System and of the SIMBAD database operated at CDS, Strasbourg, France.

## References

- Althaus, L. G., Panei, J. A., Miller Bertolami, M. M., et al. 2009, *ApJ*, 704, 1605
- Barstow, M. A., Dobbie, P. D., Forbes, A. E., & Boyce, D. D. 2007, in *Astronomical Society of the Pacific Conference Series*, Vol. 372, 15th European Workshop on White Dwarfs, ed. R. Napiwotzki & M. R. Burleigh, 243
- Barstow, M. A., Dreizler, S., Holberg, J. B., et al. 2000, *Monthly Notices of the Royal Astronomical Society*, 314, 109
- Barstow, M. A., Holberg, J. B., Koester, D., Nousek, J. A., & Werner, K. 1995, in *Lecture Notes in Physics*, Berlin Springer Verlag, Vol. 443, *White Dwarfs*, ed. D. Koester & K. Werner, 302
- Barstow, M. A., Holberg, J. B., Werner, K., Buckley, D. A. H., & Stobie, R. S. 1994, *MNRAS*, 267, 653
- Barstow, M. A., Wesemael, F., Holberg, J. B., et al. 1993, *Advances in Space Research*, 13, 281
- Bloecker, T. 1995, *A&A*, 299, 755
- Cutri, R. M., Skrutskie, M. F., van Dyk, S., et al. 2003a, *2MASS All Sky Catalog of point sources*.
- Cutri, R. M., Skrutskie, M. F., van Dyk, S., et al. 2003b, *VizieR Online Data Catalog*, 2246
- Demers, S., Beland, S., Kibblewhite, E. J., Irwin, M. J., & Nithakorn, D. S. 1986, *AJ*, 92, 878
- Dobbie, P. D., Burleigh, M. R., Levan, A. J., et al. 2005, *A&A*, 439, 1159
- Dreizler, S. 1999, *Astronomy and Astrophysics*, 352, 632
- Dreizler, S. & Werner, K. 1996, *A&A*, 314, 217
- Dreizler, S. & Wolff, B. 1999, *A&A*, 348, 189
- Dupuis, J., Vennes, S., Bowyer, S., Pradhan, A. K., & Thejll, P. 1995, *ApJ*, 455, 574
- Fitzpatrick, E. L. 1999, *PASP*, 111, 63
- Groenewegen, M. A. T. & Lamers, H. J. G. L. M. 1989, *A&AS*, 79, 359
- Hügelmeier, S. D., Dreizler, S., Homeier, D., et al. 2006, *A&A*, 454, 617
- Jahn, D., Rauch, T., Reiff, E., et al. 2007, *A&A*, 462, 281
- Kepler, S. O., Pelisoli, I., Koester, D., et al. 2016, *MNRAS*, 455, 3413
- Kurucz, R. L. 1991, in *NATO ASIC Proc. 341: Stellar Atmospheres - Beyond Classical Models*, ed. L. Crivellari, I. Hubeny, & D. G. Hummer, 441
- Kurucz, R. L. 2009, in *American Institute of Physics Conference Series*, Vol. 1171, *American Institute of Physics Conference Series*, ed. I. Hubeny, J. M. Stone, K. MacGregor, & K. Werner, 43–51
- Kurucz, R. L. 2011, *Canadian Journal of Physics*, 89, 417
- McCook, G. P. & Sion, E. M. 1999a, *ApJS*, 121, 1
- McCook, G. P. & Sion, E. M. 1999b, *VizieR Online Data Catalog*, 3210, 0
- Morrison, R. & McCammon, D. 1983, *ApJ*, 270, 119
- Müller-Ringat, E. 2013, *Dissertation*, University of Tübingen, Germany, <http://nbn-resolving.de/urn:nbn:de:bsz:21-opus-67747>
- Napiwotzki, R., Christlieb, N., Drechsel, H., et al. 2001, *Astronomische Nachrichten*, 322, 411
- Napiwotzki, R., Christlieb, N., Drechsel, H., et al. 2003, *The Messenger*, 112, 25
- Pauldrach, A., Puls, J., Kudritzki, R. P., Mendez, R. H., & Heap, S. R. 1988, *A&A*, 207, 123
- Polomski, E. F., Vennes, S., & Chayer, P. 1995, in *Bulletin of the American Astronomical Society*, Vol. 27, *American Astronomical Society Meeting Abstracts*, 1311
- Pounds, K. A., Allan, D. J., Barber, C., et al. 1993, *MNRAS*, 260, 77
- Rauch, T. & Deetjen, J. L. 2003, in *Astronomical Society of the Pacific Conference Series*, Vol. 288, *Stellar Atmosphere Modeling*, ed. I. Hubeny, D. Mihalas, & K. Werner, 103
- Rauch, T., Gamrath, S., Quinet, P., et al. 2016a, *A&A* in prep.
- Rauch, T., Hoyer, D., Quinet, P., Gallardo, M., & Raineri, M. 2015a, *A&A*, 577, A88
- Rauch, T., Quinet, P., Hoyer, D., et al. 2016b, *A&A*, 587, A39
- Rauch, T., Quinet, P., Hoyer, D., et al. 2016c, *A&A*, 590, A128
- Rauch, T., Werner, K., Biéumont, É., Quinet, P., & Kruk, J. W. 2012, *A&A*, 546, A55
- Rauch, T., Werner, K., Quinet, P., & Kruk, J. W. 2014a, *A&A*, 564, A41
- Rauch, T., Werner, K., Quinet, P., & Kruk, J. W. 2014b, *A&A*, 566, A10
- Rauch, T., Werner, K., Quinet, P., & Kruk, J. W. 2015b, *A&A*, 577, A6
- Reindl, N., Rauch, T., Werner, K., et al. 2014a, *A&A*, 572, A117
- Reindl, N., Rauch, T., Werner, K., Kruk, J. W., & Todt, H. 2014b, *A&A*, 566, A116
- Schuh, S. L., Dreizler, S., & Wolff, B. 2002, *A&A*, 382, 164
- Seaton, M. J., Yan, Y., Mihalas, D., & Pradhan, A. K. 1994, *MNRAS*, 266, 805
- Unglaub, K. & Bues, I. 2000, *A&A*, 359, 1042
- Vennes, S., Dupuis, J., Bowyer, S., et al. 1994, *ApJ*, 421, L35
- Vennes, S., Dupuis, J., Chayer, P., et al. 1998, *The Astrophysical Journal*, 500, L41
- Werner, K. 1996, *Astronomy and Astrophysics*, 309, 861
- Werner, K., Deetjen, J. L., Dreizler, S., et al. 2003, in *Astronomical Society of the Pacific Conference Series*, Vol. 288, *Stellar Atmosphere Modeling*, ed. I. Hubeny, D. Mihalas, & K. Werner, 31
- Werner, K., Deetjen, J. L., Rauch, T., & Wolff, B. 2001, in *Astronomical Society of the Pacific Conference Series*, Vol. 226, *12th European Workshop on White Dwarfs*, ed. J. L. Provencal, H. L. Shipman, J. MacDonald, & S. Goodchild, 55
- Werner, K., Dreizler, S., & Rauch, T. 2012a, *TMAP: Tübingen NLTE Model-Atmosphere Package*, *Astrophysics Source Code Library* [record ascl:1212.015]
- Werner, K. & Herwig, F. 2006, *PASP*, 118, 183
- Werner, K. & Rauch, T. 2014, *A&A*, 569, A99
- Werner, K. & Rauch, T. 2015, *A&A*, 583, A131
- Werner, K., Rauch, T., & Kepler, S. O. 2014, *A&A*, 564, A53
- Werner, K., Rauch, T., Kučas, S., & Kruk, J. W. 2015, *A&A*, 574, A29
- Werner, K., Rauch, T., Ringat, E., & Kruk, J. W. 2012b, *ApJ*, 753, L7

## Appendix A: Identified and unidentified lines in the spectrum of RE 0503–289



**Table A.1.** Identified lines in the EUVE observations of RE0503–289. Lower and upper levels are the configuration or the energy ( $\text{cm}^{-1}$ , for elements with an atomic number  $Z \geq 20$ ).  $f$  is the oscillator strength,  $W_\lambda$  the observed equivalent width, and  $v_{\text{rad}}$  the measured radial velocity. “unid.” denotes observed but as yet unidentified lines. The theoretical wavelengths correspond to those given by NIST for He, C, N, O, Si, P, S, As, and Sn, by Kurucz (1991, 2009, 2011) for Fe, and Ni, and by Rauch et al. (2014a, 2015b, 2012, 2016c,a,b, 2015a, 2014b) for Zn, Ga, Ge, Kr, Zr, Mo, Xe, and Ba, respectively.

Ion	Levels		$f$	$W_\lambda / \text{m}\text{\AA}$	Wavelength / $\text{\AA}$		$v_{\text{rad}} / \text{km/s}$	Comment
	Lower	Upper			Theoretical	Observed		
He II	1	6	$7.80 \times 10^{-3}$		234.347			newly identified
He II	1	5	$1.39 \times 10^{-2}$		237.331			Vennes et al. (1998)
He II	1	4	$2.90 \times 10^{-2}$		243.026			Vennes et al. (1998)
C IV	2p $^2\text{P}_{1/2}$	6s $^2\text{S}_{1/2}$	$1.32 \times 10^{-3}$		247.341			newly identified
C IV	2p $^2\text{P}_{3/2}$	6s $^2\text{S}_{1/2}$	$1.32 \times 10^{-3}$		247.407			newly identified
He II	1	3	$7.91 \times 10^{-2}$		256.316			Vennes et al. (1998)
C IV	2p $^2\text{P}_{1/2}^0$	5d $^2\text{D}_{3/2}$	$4.57 \times 10^{-2}$		259.468			
C IV	2p $^2\text{P}_{3/2}^0$	5d $^2\text{D}_{5/2}$	$4.11 \times 10^{-2}$		259.539			
C IV	2p $^2\text{P}_{3/2}^0$	5d $^2\text{D}_{3/2}$	$4.56 \times 10^{-3}$		259.540			
C IV	2p $^2\text{P}_{1/2}$	5s $^2\text{S}_{1/2}$	$2.64 \times 10^{-3}$		262.547			
C IV	2p $^2\text{P}_{3/2}$	5s $^2\text{S}_{1/2}$	$2.64 \times 10^{-3}$		262.621			
O IV	2p <sup>2</sup> $^2\text{D}_{5/2}$	3d $^2\text{D}_{5/2}^0$	$1.48 \times 10^{-1}$		266.931			
O IV	2p <sup>2</sup> $^2\text{D}_{3/2}$	3d $^2\text{D}_{5/2}^0$	$1.60 \times 10^{-2}$		266.941			
O IV	2p <sup>2</sup> $^2\text{D}_{5/2}$	3d $^2\text{D}_{3/2}^0$	$1.07 \times 10^{-2}$		266.971			
O IV	2p <sup>2</sup> $^4\text{P}_{3/2}$	3s $^4\text{P}_{5/2}^0$	$5.18 \times 10^{-2}$		271.990			
O IV	2p <sup>2</sup> $^4\text{P}_{1/2}$	3s $^4\text{P}_{3/2}^0$	$9.58 \times 10^{-2}$		272.076			
O IV	2p <sup>2</sup> $^4\text{P}_{5/2}$	3s $^4\text{P}_{5/2}^0$	$8.05 \times 10^{-2}$		272.127			
O IV	2p <sup>2</sup> $^4\text{P}_{3/2}$	3s $^4\text{P}_{3/2}^0$	$1.53 \times 10^{-2}$		272.173			
O IV	2p <sup>2</sup> $^4\text{P}_{1/2}$	3s $^4\text{P}_{1/2}^0$	$1.91 \times 10^{-2}$		272.176			
O III	2p <sup>2</sup> $^3\text{P}_1$	4s $^3\text{P}_2^0$	$4.61 \times 10^{-3}$		280.109			
O III	2p <sup>2</sup> $^3\text{P}_0$	4s $^3\text{P}_1^0$	$1.11 \times 10^{-2}$		280.234			
O III	2p <sup>2</sup> $^3\text{P}_2$	4s $^3\text{P}_2^0$	$8.30 \times 10^{-3}$		280.261			
O III	2p <sup>2</sup> $^3\text{P}_1$	4s $^3\text{P}_1^0$	$2.77 \times 10^{-3}$		280.323			
O III	2p <sup>2</sup> $^3\text{P}_1$	4s $^3\text{P}_0^0$	$3.69 \times 10^{-3}$		280.408			
O III	2p <sup>2</sup> $^3\text{P}_2$	4s $^3\text{P}_1^0$	$2.76 \times 10^{-3}$		280.474			
N IV	2p $^3\text{P}_0^0$	3d $^3\text{D}_1$	$6.21 \times 10^{-1}$		283.417			newly identified
N IV	2p $^3\text{P}_1^0$	3d $^3\text{D}_2$	$4.59 \times 10^{-1}$		283.465			newly identified
N IV	2p $^3\text{P}_1^0$	3d $^3\text{D}_1$	$1.53 \times 10^{-1}$		283.468			newly identified
N IV	2p $^3\text{P}_2^0$	3d $^3\text{D}_3$	$4.14 \times 10^{-1}$		283.574			newly identified
N IV	2p $^3\text{P}_2^0$	3d $^3\text{D}_2$	$9.20 \times 10^{-2}$		283.581			newly identified
N IV	2p $^3\text{P}_2^0$	3d $^3\text{D}_1$	$6.17 \times 10^{-3}$		283.584			newly identified
C IV	2p $^2\text{P}_{1/2}^0$	4d $^2\text{D}_{3/2}$	$1.22 \times 10^{-1}$		289.141			
C IV	2p $^2\text{P}_{3/2}^0$	4d $^2\text{D}_{5/2}$	$1.01 \times 10^{-1}$		289.292			
C IV	2p $^2\text{P}_{3/2}^0$	4d $^2\text{D}_{3/2}$	$1.22 \times 10^{-2}$		289.231			
O IV	2p <sup>2</sup> $^2\text{P}_{3/2}$	3d $^2\text{P}_{3/2}^0$	$7.07 \times 10^{-2}$		299.853			newly identified

Table A.1. Continued.

Ion	Levels		$f$	$W_\lambda /$ mÅ	Wavelength/Å		$v_{\text{rad}} /$ km/s	Comment
	Lower	Upper			Theoretical	Observed		
He II	1	2	$4.16 \times 10^{-1}$		303.783			newly identified
C IV	2s $^2S_{1/2}$	3p $^2P_{3/2}^o$	$1.36 \times 10^{-1}$		312.420			
C IV	2s $^2S_{1/2}$	3p $^2P_{1/2}^o$	$6.78 \times 10^{-2}$		312.451			
C III	2s <sup>2</sup> $^1S_0$	3s' $^1P_1^o$	$4.51 \times 10^{-2}$		322.574			newly identified
C III	2p $^3P_2^o$	6d $^3D_1$	$2.71 \times 10^{-4}$		327.171			newly identified
C III	2p $^3P_2^o$	6d $^3D_1$	$4.04 \times 10^{-3}$		327.171			newly identified
C III	2p $^3P_2^o$	6d $^3D_1$	$2.56 \times 10^{-2}$		327.171			newly identified
O III	2p <sup>2</sup> $^3P_1$	3s $^3P_0^o$	$2.78 \times 10^{-2}$		374.328			
O III	2p <sup>2</sup> $^3P_2$	3s $^3P_1^o$	$2.08 \times 10^{-2}$		374.432			
C IV	2s $^2P_{1/2}^o$	3d $^2D_{3/2}$	$6.44 \times 10^{-1}$		384.031			
C IV	2s $^2P_{3/2}^o$	3d $^2D_{5/2}$	$5.80 \times 10^{-1}$		384.174			
C IV	2s $^2P_{3/2}^o$	3d $^2D_{3/2}$	$6.43 \times 10^{-2}$		384.190			
C IV	2p $^2P_{1/2}^o$	3s $^2S_{1/2}$	$3.76 \times 10^{-2}$		419.525			
C IV	2p $^2P_{3/2}^o$	3s $^2S_{1/2}$	$3.76 \times 10^{-2}$		419.714			
O III	2p <sup>3</sup> $^3D_2^o$	3s $^3P_2$	$6.86 \times 10^{-3}$		434.320			
O III	2p <sup>3</sup> $^3D_1^o$	3s $^3P_2$	$2.88 \times 10^{-2}$		434.329			
O III	2p <sup>3</sup> $^3D_2^o$	3s $^3P_1$	$6.44 \times 10^{-4}$		434.648			
O III	2p <sup>3</sup> $^3D_1^o$	3s $^3P_1$	$1.60 \times 10^{-2}$		434.657			
O III	2p <sup>3</sup> $^3D_1^o$	3s $^3P_0$	$2.13 \times 10^{-2}$		434.846			
Kr VI	115479	338447	$5.78 \times 10^{-1}$		448.495			newly identified
Kr VI	115479	338364	$1.71 \times 10^{-1}$		448.662			newly identified
Kr VI	115479	338119	1.13		449.156			newly identified
He I	1s $^1S$	4p $^1P^o$	$2.99 \times 10^{-2}$		522.213			newly identified
He I	1s $^1S$	3p $^1P^o$	$7.35 \times 10^{-2}$		537.030			newly identified
O III	2p <sup>3</sup> $^3D_2^o$	3p $^3P_1$	$6.20 \times 10^{-5}$		554.759			newly identified
O III	2p <sup>3</sup> $^3D_1^o$	3p $^3P_1$	$1.52 \times 10^{-3}$		554.773			newly identified
O III	2p <sup>3</sup> $^3D_1^o$	3p $^3P_0$	$2.05 \times 10^{-3}$		555.026			newly identified
He I	1s $^1S$	2p $^1P^o$	$2.76 \times 10^{-1}$		584.334			newly identified
O V	2p' $^3D_1$	4d' $^3D_2^o$	$1.38 \times 10^{-2}$		609.591			newly identified
O IV	2p <sup>2</sup> $^4P_{1/2}$	2p <sup>3</sup> $^4S_{3/2}^o$	$1.26 \times 10^{-1}$		624.619			newly identified
O IV	2p <sup>2</sup> $^4P_{3/2}$	2p <sup>3</sup> $^4S_{3/2}^o$	$1.26 \times 10^{-1}$		625.127			newly identified
O IV	2p <sup>2</sup> $^4P_{5/2}$	2p <sup>3</sup> $^4S_{3/2}^o$	$1.26 \times 10^{-1}$		625.853			newly identified
O IV	3p $^2P_{1/2}^o$	3p' $^2P_{3/2}$	$6.22 \times 10^{-2}$		626.198			newly identified
O IV	3p $^2P_{1/2}^o$	3p' $^2P_{1/2}$	$1.24 \times 10^{-1}$		626.446			newly identified
O IV	3p $^2P_{3/2}^o$	3p' $^2P_{3/2}$	$1.56 \times 10^{-1}$		626.539			newly identified
O IV	3p $^2P_{3/2}^o$	3p' $^2P_{1/2}$	$3.11 \times 10^{-2}$		626.786			newly identified
C IV	3d $^2D_{3/2}$	7f $^2F_{5/2}^o$	$2.58 \times 10^{-2}$		627.102			newly identified
C IV	3d $^2D_{5/2}$	7f $^2F_{5/2}^o$	$1.23 \times 10^{-3}$		627.143			newly identified

Table A.1. Continued.

Ion	Levels		$f$	$W_\lambda /$ mÅ	Wavelength/Å		$v_{\text{rad}} /$ km/s	Comment
	Lower	Upper			Theoretical	Observed		
C iv	3D $^2D_{5/2}$	7f $^2F_{7/2}^o$	$2.45 \times 10^{-2}$		627.144			newly identified

Table A.2. Like Table A.1, for the FUSE observations.

Ion	Levels		$f$	$W_\lambda /$ mÅ	Wavelength/Å		$v_{\text{rad}} /$ km/s	Comment
	Lower	Upper			Theoretical	Observed		
H i	1	25			913.215			ISM multi-component
H i	1	24			913.339			ISM multi-component
H i	1	23			913.480			ISM multi-component
H i	1	22			913.641			ISM multi-component
H i	1	21			913.826			ISM multi-component
H i	1	20			914.039			ISM multi-component
H i	1	19			914.286			ISM multi-component
H i	1	18			914.576			ISM multi-component
H i	1	17			914.919			ISM multi-component
H i	1	16			915.329			ISM multi-component
N ii					915.613			ISM multi-component
H i	1	15			915.834			ISM multi-component
H i	1	14			916.429			ISM multi-component
H i	1	13			917.181			ISM multi-component
H i	1	12			918.129			ISM multi-component
Ge vi	306243	415143	$2.34 \times 10^{-4}$		918.278			
Kr vii	170835	279714.8	$1.39 \times 10^{-1}$	12.2	918.444	918.53	26.4	
H i	1	11			919.351			ISM multi-component
Kr vi	170084	278787	$3.01 \times 10^{-3}$		919.938			
H i	1	10			920.963			ISM multi-component
O iv	2s2p <sup>2</sup> $^2P_{1/2}$	2p <sup>3</sup> $^2P_{3/2}^o$	$5.62 \times 10^{-2}$		921.296			
O iv	2s2p <sup>2</sup> $^2P_{1/2}$	2p <sup>3</sup> $^2P_{1/2}^o$	$1.12 \times 10^{-1}$		921.365			
N iv	2s2p $^3P_1^o$	2p <sup>2</sup> $^3P_2$	$9.38 \times 10^{-2}$	75.7	921.994	922.07	23.1	
N iv	2s2p $^3P_0^o$	2p <sup>2</sup> $^3P_1$	$2.25 \times 10^{-1}$	91.6	922.519	922.59	22.8	
N iv	2s2p $^3P_1^o$	2p <sup>2</sup> $^3P_1$	$5.62 \times 10^{-2}$		923.056			
H i	1	9			923.150			ISM multi-component
N iv	2s2p $^3P_2^o$	2p <sup>2</sup> $^3P_2$	$1.69 \times 10^{-1}$		923.220			
O iv	2s2p <sup>2</sup> $^2P_{3/2}$	2p <sup>3</sup> $^2P_{3/2}^o$	$1.41 \times 10^{-1}$		923.367			
O iv	2s2p <sup>2</sup> $^2P_{3/2}$	2p <sup>3</sup> $^2P_{1/2}^o$	$2.81 \times 10^{-2}$		923.436			
N iv	2s2p $^3P_1^o$	2p <sup>2</sup> $^3P_0$	$7.49 \times 10^{-2}$	69.5	923.676	923.75	24.0	
S v	3s3p $^1P_1^o$	3p <sup>2</sup> $^1S_0$	$1.71 \times 10^{-1}$		924.220			blend with N iv
N iv	2s2p $^3P_2^o$	2p <sup>2</sup> $^3P_1$	$5.61 \times 10^{-2}$		924.284			blend with S v
Ge vi	303696	411886	$2.34 \times 10^{-4}$		924.302			blend with N iv

Table A.2. Continued.

Ion	Levels		$f$	$W_\lambda /$ mÅ	Wavelength/Å		$v_{\text{rad}} /$ km/s	Comment
	Lower	Upper			Theoretical	Observed		
Ba VII	226198	334319	$1.27 \times 10^{-3}$		924.892			newly identified
Ba VII	42514	150634	$1.74 \times 10^{-3}$		924.898			newly identified
H I	1	8			926.226			ISM multi-component
Ge VI	303696	411592	$3.63 \times 10^{-1}$		926.824			
Kr VI	0	107836	$1.58 \times 10^{-3}$	16.5	927.334	927.43	31.4	
Xe VI	$5p^2 \ ^2D_{3/2}$	$5p^3 \ ^2D_{3/2}^o$	$3.53 \times 10^{-2}$		928.371			
Xe VI	$5p^2 \ ^2P_{3/2}$	$5p^3 \ ^2P_{3/2}^o$	$4.87 \times 10^{-2}$		929.141			
O I					929.517			ISM multi-component
Ge VI	313025	420542	$2.44 \times 10^{-1}$		930.082			
Ge VI	306243	413728	$8.07 \times 10^{-4}$		930.366			
H I	1	7			930.748			ISM multi-component
Kr VI	8110	115479	$2.23 \times 10^{-3}$	19.1	931.368	931.43	19.3	
				15.3		931.98		unid.
S VI	$3s \ ^2S_{1/2}$	$3p \ ^2P_{3/2}^o$	$4.36 \times 10^{-1}$	57.9	933.378	933.47	28.9	
O I					936.630			ISM multi-component
Ge IV	190852.5	84102.3	$8.91 \times 10^{-1}$		936.765	936.82	17.6	
Ba VI	36156	142852	$7.40 \times 10^{-3}$		937.241			
Ba VII	15507	122163	$1.08 \times 10^{-2}$		937.595			newly identified
H I	1	6			927.803			ISM multi-component
Ge IV	190601.5	84102.3	$9.89 \times 10^{-2}$		938.973			
Ge V	234219	340296	$8.22 \times 10^{-3}$		942.717			
Ba VII	42514	148547	$3.40 \times 10^{-3}$		943.102			
Kr VI	170084	276011	$3.88 \times 10^{-2}$		944.046			
S VI	$^2S$	$^2P^o$	$2.20 \times 10^{-1}$	59.8	944.523	944.62	29.8	
				14.8		946.06		unid.
Ge VI	306243	411886	$1.28 \times 10^{-1}$		946.589			
Ge VI	303696	409188	$1.15 \times 10^{-1}$		947.937			blend with C IV
C IV	$3s \ ^2S_{1/2}$	$4p \ ^2P_{3/2}^o$	$1.36 \times 10^{-1}$		948.090			
C IV	$3s \ ^2S_{1/2}$	$4p \ ^2P_{1/2}^o$	$6.78 \times 10^{-2}$		948.208			
O I					948.686			ISM multi-component
H I	1	5			949.743			ISM multi-component
P IV	$3s^2 \ ^1S_0$	$3p \ ^1P_1^o$	1.60	33.1	950.655	950.75	30.0	
O I					950.887			ISM multi-component
N I					951.079			ISM multi-component
Ge VI	308657	413728	$1.03 \times 10^{-1}$		951.739			
				40.9		952.90		unid.
Ba VI	23547	128436	$6.95 \times 10^{-3}$	11.0	953.388	953.47	26.4	
N I					953.415			ISM multi-component
N I					953.655			ISM multi-component
N I					953.970			ISM multi-component

Table A.2. Continued.

Ion	Levels		$f$	$W_\lambda /$ mÅ	Wavelength/Å		$v_{\text{rad}} /$ km/s	Comment
	Lower	Upper			Theoretical	Observed		
N IV	2s2p $^1P_1^o$	2p <sup>2</sup> $^1S_0$	$1.33 \times 10^{-1}$	13.6	955.334	954.45	24.5	unid.
Kr VI	222122	326657	$2.68 \times 10^{-2}$	71.8	956.617	955.41		
Ge V	235967	340296	$3.17 \times 10^{-2}$		958.509			
He II	2	9	$5.43 \times 10^{-3}$		958.698			
P I					963.800			ISM multi-component
N I					963.990			ISM multi-component
N I					964.626			ISM multi-component
Kr VI	223040	326657	$1.59 \times 10^{-1}$	25.6	965.093	965.16	21.8	
Ge V	235967	339540	$3.56 \times 10^{-2}$	24.3	965.501	965.59	27.3	
Ge VI	310199	413728	$2.62 \times 10^{-1}$		965.914			
						966.78		unid.
						966.84		unid.
						966.88		unid.
Ge VI	308657	412038	$1.67 \times 10^{-1}$		967.300			newly identified
Xe VI	5p <sup>2</sup> $^2D_{5/2}$	5p <sup>3</sup> $^2D_{3/2}^o$	$1.06 \times 10^{-2}$		967.550			
						968.26		unid.
Ge VI	308657	411886	$1.96 \times 10^{-1}$		968.723			
Kr VI	8110	111193	$4.34 \times 10^{-4}$		970.092			
Ge V	234219	337168	$1.22 \times 10^{-1}$	16.0	971.357	971.41	16.4	
Ge VI	306243	409188	$1.81 \times 10^{-1}$		971.392			blend with Ge v
O I					971.737			ISM multi-component
O I					971.738			ISM multi-component
O I					971.738			ISM multi-component
He II	2	8	$8.04 \times 10^{-3}$		972.111			
D I					972.272			ISM multi-component
H I	1	4			972.537			ISM multi-component
O I					976.448			ISM multi-component
C III					977.020			ISM multi-component
C III	2s3s $^3S_1$	2p( $^2P^o$ )3d $^3P_2^o$	$8.93 \times 10^{-3}$		977.020			
Ge V			$3.56 \times 10^{-3}$		977.798			
N III	2s2p <sup>2</sup> $^2D_{5/2}$	2p <sup>3</sup> $^2D_{3/2}^o$	$9.79 \times 10^{-3}$		979.768			
N III	2p <sup>2</sup> $^2D_{3/2}$	2p <sup>3</sup> $^2D_{3/2}^o$	$1.27 \times 10^{-1}$		979.832			
N III	2s2p <sup>2</sup> $^2D_{5/2}$	2p <sup>3</sup> $^2D_{5/2}^o$	$1.33 \times 10^{-1}$		979.905			
N III	2s2p <sup>2</sup> $^2D_{3/2}$	2p <sup>3</sup> $^2D_{5/2}^o$	$1.44 \times 10^{-2}$		979.969			
Kr VI	222122	324120	$1.31 \times 10^{-1}$	22.7	980.411	980.51	28.7	
C III	3s $^3S_1$	3d' $^3P_2^o$	$8.98 \times 10^{-1}$	24.9	981.462	981.53	20.5	
Ge V	238765	340296	$1.08 \times 10^{-1}$	20.7	984.923	985.00	23.4	
Ge V			$1.13 \times 10^{-3}$		987.064			
As V	4s $^2S_{1/2}$	4p $^2P_{3/2}^o$	$5.28 \times 10^{-1}$	35.7	987.651	987.74	27.0	

Table A.2. Continued.

Ion	Levels		$f$	$W_\lambda /$ mÅ	Wavelength/Å		$v_{\text{rad}} /$ km/s	Comment
	Lower	Upper			Theoretical	Observed		
Fe I					987.687			ISM multi-component
Ge V	235967	337168	$1.00 \times 10^{-1}$	21.6	988.132	988.22	25.8	
O IV	3d $^4F_{3/2}^o$	4f $^4G_{5/2}$	$7.72 \times 10^{-1}$		988.523			
O IV	3d $^4F_{5/2}^o$	4f $^4G_{7/2}$	$6.89 \times 10^{-1}$		988.573			
O I					988.578			ISM multi-component
Fe V	357329.1	256177.9	$5.88 \times 10^{-1}$		988.619			
O IV	3d $^4F_{7/2}^o$	4f $^4G_{9/2}$	$6.87 \times 10^{-1}$		988.627			
O I					988.655			ISM multi-component
O IV	3d $^4F_{9/2}^o$	4f $^4G_{11/2}$	$7.20 \times 10^{-1}$		988.708			
O I					988.773			ISM multi-component
N III	2p $^2P_{1/2}^o$	2s2p $^2D_{3/2}$	$1.23 \times 10^{-1}$	37.0	989.799	989.88	24.8	
Si II					989.873			ISM multi-component
Ge V	234219	335161	$1.13 \times 10^{-1}$	10.8	990.668	990.76	27.5	
N III	2p $^2P_{3/2}^o$	2s2p $^2D_{3/2}$	$1.20 \times 10^{-2}$		991.511			
N III	2p $^2P_{3/2}^o$	2p $^2D_{5/2}$	$1.11 \times 10^{-1}$		991.577			
He II	2	7	$1.27 \times 10^{-2}$		992.363			
Ba VII	21499	122163	$5.38 \times 10^{-3}$	14.2	993.411	993.49	22.6	
Xe VII	5s $^2 S_0$	5p $^3P_1^o$	$2.45 \times 10^{-1}$	26.2	995.511	995.59	24.1	
Mo VI	182404	282826	1.12	12.9	995.806	995.90	28.3	
Xe VII	5p $^2P_{1/2}^o$	5p $^4P_{3/2}$	$5.66 \times 10^{-5}$		996.233			
Se IV				21.7	996.710	996.77	18.0	
P V	3d $^2D_{5/2}$	4p $^2P_{3/2}^o$	$1.50 \times 10^{-1}$	28.5	997.612	997.72	33.4	
				18.5		999.49		unid.
Zn V	231122	331087	$2.69 \times 10^{-2}$		1000.350			uncertain, newly identified
S VI	4d $^2D_{3/2}$	5f $^2F_{5/2}^o$	$6.72 \times 10^{-1}$		1000.372			
Zr V	437678	537502	$1.27 \times 10^{-1}$		1001.765			uncertain
				20.2		1001.99		unid.
C III	3p $^1P_1^o$	6d $^1D_2$	$4.12 \times 10^{-2}$		1001.988			
Zr V	277146	376898	$1.11 \times 10^{-2}$		1002.484			
Kr VI	8110	107836	$3.30 \times 10^{-4}$	16.3	1002.748	1002.82	21.5	
Ge V				33.6	1004.380	1004.49	32.8	
C III	3s $^1S_0$	3d' $^1P_1^o$	$5.49 \times 10^{-2}$		1004.596			
Ge V	238765	338274	$5.41 \times 10^{-2}$	14.0	1004.938	1005.00	18.5	newly identified
Ge V			$5.41 \times 10^{-2}$	15.9	1005.304	1005.39	25.6	
				16.6		1007.15		unid.
Ge V	235967	335161	$1.21 \times 10^{-2}$	11.5	1008.122	1008.21	26.2	
O III	3s $^3P_2^o$	4p $^3D_3$	$5.04 \times 10^{-2}$		1008.384			
				19.6		1008.66		unid.
				20.4		1009.81		unid.

Table A.2. Continued.

Ion	Levels		$f$	$W_\lambda /$ mÅ	Wavelength/Å		$v_{\text{rad}} /$ km/s	Comment
	Lower	Upper			Theoretical	Observed		
Ga v	236072	335089	$7.80 \times 10^{-2}$		1009.928			
Kr vi	275380	374279	$7.23 \times 10^{-3}$		1011.133			
Mo v	157851	256676	$1.52 \times 10^{-1}$		1011.889			
				8.5		1012.44		unid.
						1013.80		unid.
						1014.01		unid.
Ga v	246093	344668	$2.82 \times 10^{-1}$	11.0	1014.456	1014.55	27.8	
Ga v	246133	344668	$2.86 \times 10^{-2}$		1014.868			
				13.0		1015.33		unid.
Ga v	231711	330174	$9.59 \times 10^{-2}$		1015.610			
Kr vi	180339	278787	$7.40 \times 10^{-3}$	12.0	1015.765	1015.83	19.2	
C iii	3p $^3P_0^o$	6d $^3D_1$	$4.74 \times 10^{-2}$		1016.340			
C iii	3p $^3P_1^o$	6d $^3D_1$	$1.19 \times 10^{-2}$		1016.399			
C iii	3p $^3P_1^o$	6d $^3D_2$	$3.56 \times 10^{-2}$		1016.399			
C iii	3p $^3P_2^o$	6d $^3D_1$	$4.78 \times 10^{-4}$		1016.534			
C iii	3p $^3P_2^o$	6d $^3D_2$	$7.13 \times 10^{-3}$		1016.534			
C iii	3p $^3P_2^o$	6d $^3D_3$	$3.98 \times 10^{-2}$		1016.534			
Ge v	241935	340296	$1.95 \times 10^{-1}$	27.9	1016.668	1016.77	30.1	
				10.0		1017.21		unid.
Xe vi	5p <sup>2</sup> $^2P_{1/2}$	5p <sup>3</sup> $^4S_{3/2}$	$1.88 \times 10^{-3}$		1017.265			
Zn v	231831	330069	$3.36 \times 10^{-2}$		1017.935			newly identified
				32.7		1018.13		unid.
				20.3		1018.57		unid.
Ga v	246133	344200	$3.07 \times 10^{-1}$		1019.711			
				9.1		1021.49		unid.
				19.0		1021.73		unid.
He ii	2	6	$2.21 \times 10^{-2}$		1025.272			
D i					1025.440			ISM multi-component
H i	1	3			1025.722			ISM multi-component
				9.9		1027.13		unid.
As v	4s $^2S_{1/2}$	4p $^2P_{1/2}^o$	$2.53 \times 10^{-1}$	36.1	1029.480	1029.54	17.5	
Zn v	231997	329085	$4.38 \times 10^{-2}$		1029.992			
P iv	3p $^3P_1^o$	3p <sup>2</sup> $^3P_1$	$1.20 \times 10^{-1}$	21.8	1030.517	1030.59	21.2	
						1031.22		unid.
						1031.42		unid.
O vi	2s $^2S_{1/2}$	2p $^2P_{3/2}^o$	$1.33 \times 10^{-1}$		1031.912			
O vi					1031.926			ISM multi-component
Zn v	221631	318436	$9.66 \times 10^{-3}$		1033.009			blend with Ge v, newly identified
Ge v	238765	335560	$6.96 \times 10^{-2}$		1033.107			blend with Zn v, newly identified
Ge v			$6.96 \times 10^{-2}$		1033.428			blend with Ca iii

Table A.2. Continued.

Ion	Levels		$f$	$W_\lambda /$ mÅ	Wavelength/Å		$v_{\text{rad}} /$ km/s	Comment
	Lower	Upper			Theoretical	Observed		
Ca III	277380.86	374143.84	$1.03 \times 10^{-5}$	12.4 17.1 16.2	1033.453	1033.52 1034.18 1034.60	19.4	blend with Ge v unid. unid.
Ge v	234219	330791	$1.01 \times 10^{-3}$		1035.504			
Zn v	231831	328369	$1.25 \times 10^{-2}$		1035.859			
Zn v	285885	382420	$5.02 \times 10^{-2}$		1035.887			
N IV	3d $^3D_3$	4f $^3F_4^0$	$8.56 \times 10^{-1}$		1036.119			
N IV	3d $^3D_2$	4f $^3F_3^0$	$8.28 \times 10^{-1}$		1036.149			
N IV	3d $^3D_1$	4f $^3F_2^0$	$9.33 \times 10^{-1}$		1036.196			
N IV	3d $^3D_2$	4f $^3F_2^0$	$1.05 \times 10^{-1}$		1036.237			
N IV	3d $^3D_3$	4f $^3F_3^0$	$7.53 \times 10^{-2}$		1036.239			
C II					1036.337			ISM multi-component
C II					1037.018			ISM multi-component
O VI	2s $^2S_{1/2}$	2p $^2P_{1/2}^0$	$6.60 \times 10^{-2}$	21.0		1037.24	30.9	unid.
O VI					1037.613	1037.72		ISM multi-component
Ge v	241935	338274	$1.45 \times 10^{-1}$	42.3	1037.617			
Mo VI	187331	283611	$9.73 \times 10^{-1}$		1038.430	1038.49	17.3	blend with Zn v
Ga v	214000	310267	$4.38 \times 10^{-2}$		1038.640			blend with Zn v
					1038.778			blend with Mo VI, newly identified
O I						1038.95		unid.
Ge VI	313025	409188	$3.69 \times 10^{-2}$		1039.230			ISM multi-component
S v	3s3d $^1D_2$	3p3d $^1F_3^0$	$3.41 \times 10^{-1}$	21.0	1039.892			blend with S v
O III	2p <sup>3</sup> $^1P_1^0$	3p $^1D_2$	$2.42 \times 10^{-2}$		1039.916	1040.02	30.0	blend with Ge VI
						1040.320		
						1041.03		unid.
						1041.32		unid.
Zn v	286575	382420	$2.54 \times 10^{-1}$	9.8	1043.353	1043.44	25.0	
						1043.80		unid.
Sn IV					19.2	1044.490	20.1	
Kr VI	180339	276011	$5.24 \times 10^{-2}$		1044.56			
O IV	3p $^2P_{1/2}^0$	4s $^2S_{1/2}$	$9.21 \times 10^{-2}$		1045.238			
Ge v	234219	329848	$3.93 \times 10^{-1}$	62.5	1045.364			
O IV	3p $^3P_{3/2}^0$	4s $^2S_{1/2}$	$9.19 \times 10^{-2}$	29.3	1045.713	1045.81	27.8	
						1046.39	22.1	
						1047.02		unid.
Zn v	222940	318436	$2.65 \times 10^{-2}$		1047.164			uncertain, blend with Mo VI, newly identified
Mo VI	187331	282826	$1.07 \times 10^{-1}$		1047.182			blend with Zn v
Ga v	242026	337491	$1.31 \times 10^{-1}$		1047.504			blend with O IV, newly identified
O IV	3s $^2S_{1/2}$	2s2p( $^3P^0$ )3s $^2P_{3/2}^0$	$2.89 \times 10^{-2}$		1047.590			blend with Ga v
Ge v	464652	560097	$1.18 \times 10^{-1}$		1047.730			newly identified



Table A.2. Continued.

Ion	Levels		$f$	$W_\lambda /$ mÅ	Wavelength/Å		$v_{\text{rad}} /$ km/s	Comment
	Lower	Upper			Theoretical	Observed		
Ar I					1048.220			ISM multi-component
Ge V	464077	559463	$2.43 \times 10^{-1}$		1048.371			blend with Zn V, newly identified
Zn V	285523	380902	$1.01 \times 10^{-1}$		1048.448			blend with Ge V, newly identified
				16.9		1048.59		unid.
				34.5		1048.97		unid.
Ge V	241935	337168	$1.55 \times 10^{-1}$		1050.057	1050.14	23.7	
Ga V	210052	305249	$1.95 \times 10^{-1}$		1050.453			blend with O IV
O IV	3s $^2S_{1/2}$	2s2p( $^3P^o$ )3s $^2P^o_{1/2}$	$1.44 \times 10^{-2}$		1050.505			blend with Ga V
				14.4		1051.18		unid.
As V				19.2	1051.600	1051.69	25.7	
Kr VI	183817	278787	$4.76 \times 10^{-3}$	12.8	1052.964	1053.04	21.6	
						1053.24		unid.
Zr VI	427119	522036	$2.20 \times 10^{-1}$		1053.548			
Ge V	235967	330791	$8.93 \times 10^{-2}$		1054.590			
Zn V	221631	316339	$5.31 \times 10^{-2}$	30.4	1055.878	1055.95	20.4	
Se VI				10.7	1056.980	1057.05	19.9	
Ga V	212121	306628	$1.65 \times 10^{-1}$		1058.123			blend with Zn V
Zn V	198962	293463	$6.01 \times 10^{-3}$		1058.185			blend with Ga V, newly identified
				7.9		1059.39		unid.
				28.8		1060.70		unid.
C IV	4p $^2P^o_{3/2}$	10d $^2D_{3/2}$	$1.30 \times 10^{-3}$		1060.740			
C IV	4p $^2P^o_{3/2}$	10d $^2D_{5/2}$	$1.17 \times 10^{-2}$		1060.740			
Kr VI	183817	278062	$6.58 \times 10^{-2}$	25.6	1061.064	1061.16	27.1	
O IV	2s2p( $^3P^o$ )3d $^4D^o_{1/2}$	2s2p( $^3P^o$ )4f $^4F_{3/2}$	$7.40 \times 10^{-1}$		1061.780			
Zn V	221631	315801	$1.40 \times 10^{-2}$		1061.914			newly identified
O IV	2s2p( $^3P^o$ )3d $^4D^o_{5/2}$	2s2p( $^3P^o$ )4f $^4F_{7/2}$	$6.02 \times 10^{-1}$		1062.133			
O IV	2s2p( $^3P^o$ )3d $^4D^o_{7/2}$	2s2p( $^3P^o$ )4f $^4F_{9/2}$	$6.60 \times 10^{-1}$		1062.271			
Ga V	236072	330174	$2.58 \times 10^{-1}$	13.9	1062.677	1062.75	20.6	
Ge V	464853	558877	$8.57 \times 10^{-1}$		1063.554			
Ga V	231711	325713	$3.82 \times 10^{-2}$		1063.807			newly identified
Zn V	222042	316029	$8.15 \times 10^{-2}$		1063.979			
Se VI				25.3	1064.620	1064.71	25.3	
Zr VI	421258	515171	$4.55 \times 10^{-1}$		1064.818			
				24.7		1065.43		unid.
				41.8		1065.69		unid.
Si IV	3d $^2D_{5/2}$	4f $^2F^o_{5/2}$	$4.34 \times 10^{-2}$	64.5	1066.636	1066.74	29.2	
O IV	3d $^2D_{3/2}$	4f $^2F^o_{5/2}$	$7.97 \times 10^{-1}$		1067.768			
O IV	3d $^2D_{5/2}$	4f $^2F^o_{7/2}$	$7.59 \times 10^{-1}$		1067.832			
O IV	3d $^2D_{5/2}$	4f $^2F^o_{5/2}$	$3.80 \times 10^{-2}$		1067.958			

Table A.2. Continued.

Ion	Levels		$f$	$W_\lambda /$ mÅ	Wavelength/Å		$v_{\text{rad}} /$ km/s	Comment
	Lower	Upper			Theoretical	Observed		
Zn v	221631	315239	$5.19 \times 10^{-2}$		1068.284			
Ge v	234219	327891	$6.53 \times 10^{-2}$	25.4	1068.430	1068.53	28.1	
Zr v	378753	472338	$1.68 \times 10^{-1}$		1068.551			blend with Ga v
Ga v	232968	326549	$1.61 \times 10^{-1}$		1068.593			blend with Zr v
Ga v	242026	335605	$1.65 \times 10^{-2}$		1068.616			
Ge v	241935	335560	$8.73 \times 10^{-2}$	27.8	1069.130	1069.23	28.0	
Ge v	461829	555337	$5.02 \times 10^{-1}$		1069.420			blend with Ga v
Ga v	235609	329103	$2.87 \times 10^{-1}$		1069.587			blend with Ge v, newly identified
Zn v	235599	329085	$7.85 \times 10^{-2}$		1069.674			blend with Ga v
Ge v	461815	555299	$6.07 \times 10^{-1}$		1069.703			
Zn v	231997	325476	$3.03 \times 10^{-2}$		1069.764			
Ge v	461829	555299	$1.10 \times 10^{-1}$		1069.859			
				6.2		1070.81		unid.
				19.0		1071.04		unid.
Ga v	235752	329112	$2.75 \times 10^{-1}$		1071.123			
Ga v	235752	329108	$2.34 \times 10^{-1}$		1071.168			
Te vi				65.0	1071.400	1071.51	30.8	blend with Zn v
Zn v	221631	314958	$3.27 \times 10^{-2}$		1071.501			blend with Te vi
Ge v	461418	554658	$9.97 \times 10^{-1}$	17.1	1072.495	1072.59	26.6	
Ge v	241935	335161	$2.52 \times 10^{-1}$	41.4	1072.661	1072.76	27.7	
Zn v	222042	315239	$2.14 \times 10^{-1}$	24.8	1072.992	1073.04		
Ga v	212121	305249	$1.22 \times 10^{-1}$		1073.791			
Zn v	222940	316029	$6.35 \times 10^{-2}$		1074.241			
Ge v	461643	554690	$9.68 \times 10^{-1}$		1074.719			
						1074.93		unid.
Zn v	240446	333455	$3.01 \times 10^{-1}$		1075.171			
Zn v	222042	314958	$1.95 \times 10^{-2}$		1076.239			
				21.3		1076.44		unid.
				20.9		1076.80		unid.
Zn v	222940	315801	$1.56 \times 10^{-1}$		1076.878			
Xe vii	5p $^1P_1^o$	5p <sup>2</sup> $^1D$	$8.10 \times 10^{-1}$	26.1	1077.120	1077.22	27.8	
Ga v	231711	324407	$2.96 \times 10^{-1}$		1078.795			newly identified
O iv	3p $^2P_{3/2}^o$	2s2p( $^3P^o$ )3p $^2D_{5/2}$	$5.18 \times 10^{-2}$		1079.056			
Ga v	214000	306628	$1.56 \times 10^{-1}$		1079.587			
Ga v	215237	307864	$2.23 \times 10^{-1}$		1079.599			
Ga v	231711	324314	$1.29 \times 10^{-2}$		1079.879			
Xe vi	5p $^2P_{1/2}^o$	5p <sup>2</sup> $^4P_1$	$1.90 \times 10^{-3}$	20.0	1080.077	1080.16	23.0	
Zn v	232946	325476	$6.65 \times 10^{-2}$		1080.735			newly identified
O iv	3d $^2D_{3/2}^o$	4f $^2F_{5/2}$	$7.33 \times 10^{-1}$		1080.967			
O iv	3d $^2D_{5/2}^o$	4f $^2F_{7/2}$	$6.98 \times 10^{-1}$		1080.969			

Table A.2. Continued.

Ion	Levels		$f$	$W_\lambda /$ mÅ	Wavelength/Å		$v_{\text{rad}} /$ km/s	Comment
	Lower	Upper			Theoretical	Observed		
O iv	3p $^2P^o_{1/2}$	4p $^2D_{3/2}$	$5.77 \times 10^{-2}$		1081.024			ISM multi-component
N ii					1083.994			
He ii	2	5	$4.47 \times 10^{-2}$		1084.942			
						1086.60		unid.
Ge v	238765	330791	$3.18 \times 10^{-1}$		1086.653			
Ge v	235967	327891	$3.03 \times 10^{-1}$	27.0	1087.855	1087.95	26.2	
Zn v	235730	327581	$2.87 \times 10^{-1}$		1088.709			newly identified
Sn v					1089.350	1089.42	19.2	
Ge v	235967	327753	$1.42 \times 10^{-1}$		1089.491			
Zn v	260880	352553	$2.98 \times 10^{-1}$		1090.831			
Xe vi	5p $^2P^o_{3/2}$	5p <sup>2</sup> $^4P_5$	$2.47 \times 10^{-3}$		1091.632			blend with Ga v
Ga v	221488	313088	$2.70 \times 10^{-1}$		1091.703			blend with Xe vi
Ge v	238765	330333	$1.01 \times 10^{-1}$		1092.089			
O iv	3d $^2D_{5/2}$	2s2p( $^3P^o$ )3d $^2F^o_{7/2}$	$3.78 \times 10^{-2}$		1093.774			
				22.6		1094.00		unid.
Zn v	236969	328369	$2.86 \times 10^{-1}$		1094.088			
				33.6		1094.23		unid.
Ga v	218301	309679	$1.73 \times 10^{-1}$		1094.355			
Ni vi	347278.5	438639.4	$2.27 \times 10^{-1}$		1094.560			
Se v				36.4	1094.680	1094.79	30.1	
Ga v	232968	324314	$6.28 \times 10^{-2}$		1094.739			
Ga v	218301	309616	$1.81 \times 10^{-1}$		1095.110			newly identified
Ge v	464077	555337	$1.53 \times 10^{-2}$		1095.769			
Zn v	285885	377144	$4.69 \times 10^{-2}$		1095.774			blend with Ge v
Zn v	235730	326987	$2.94 \times 10^{-2}$		1095.797			
Zn v	239843	331087	$1.30 \times 10^{-1}$		1095.961			
						1096.28		unid.
O iv	3d $^2D_{3/2}$	2s2p( $^3P^o$ )3d $^2F^o_{5/2}$	$3.95 \times 10^{-2}$		1096.359			
Ge v	464706	555852	$7.69 \times 10^{-1}$		1097.134			
Zn v	235599	326664	$3.51 \times 10^{-2}$		1098.108			newly identified
				15.8		1099.02		unid.
Zr vi	427119	518062	$8.55 \times 10^{-1}$		1099.591			
				11.6		1099.85		unid.
Ga v	243053	333929	$4.24 \times 10^{-1}$		1100.401			newly identified
Ge v	469686	560547	$9.01 \times 10^{-1}$	20.2	1100.585	1100.66	20.4	
Mo v	146977	237760	$2.05 \times 10^{-1}$		1101.530			
Ga v	246133	336909	$2.07 \times 10^{-1}$		1101.613			
Mo v	151195	241965	$2.02 \times 10^{-2}$		1101.690			
Xe vi	5p <sup>2</sup> $^2P_{1/2}$	5p <sup>3</sup> $^2D^o_{3/2}$	$1.88 \times 10^{-3}$		1101.940			
						1102.26		unid.

Table A.2. Continued.

Ion	Levels		$f$	$W_\lambda /$ mÅ	Wavelength/Å		$v_{\text{rad}} /$ km/s	Comment
	Lower	Upper			Theoretical	Observed		
Ga v	242026	332707	$2.39 \times 10^{-1}$		1102.767			
Ga v	210052	300730	$1.12 \times 10^{-1}$		1102.803			
Ga v	212121	302779	$1.34 \times 10^{-1}$		1103.047			
				7.5		1103.37		unid.
				6.4		1103.56		unid.
Zn v	236969	327581	$2.67 \times 10^{-2}$		1103.598			newly identified
Zn v	291107	381670	$2.70 \times 10^{-1}$	34.7	1104.199	1104.29	24.2	newly identified
Ga v	221488	311991	$1.35 \times 10^{-1}$		1104.936			
Ga v	236072	326549	$3.18 \times 10^{-2}$		1105.253			
Ni v	229413	319860.4	$3.02 \times 10^{-4}$		1105.615			blend with Ga v
Ga v	242026	332473	$3.45 \times 10^{-1}$		1105.620			blend with Ni v
C iv					1106.330			forbidden C iv component
C iv					1106.770			forbidden C iv component
C iv	3p $^2P^o_{1/2}$	4d $^2D_{3/2}$	$5.41 \times 10^{-1}$		1107.591			
C iv	3p $^2P^o_{3/2}$	4d $^2D_{5/2}$	$4.86 \times 10^{-1}$		1107.930			
C iv	3p $^2P^o_{3/2}$	4d $^2D_{3/2}$	$5.41 \times 10^{-2}$		1107.979			
Zn v	221631	311796	$1.53 \times 10^{-1}$		1109.078			
Zn v	230614	320772	$5.16 \times 10^{-2}$		1109.166			
Zn v	232946	322969	$2.06 \times 10^{-2}$		1110.821			weak
Zn v	256235	346201	$1.14 \times 10^{-1}$		1111.530			
Zn v	255763	345723	$2.37 \times 10^{-1}$		1111.603			
Zn v	255763	345624	$1.46 \times 10^{-1}$		1112.829			
						1114.19		unid.
Zn v	221631	311359	$2.16 \times 10^{-1}$		1114.482			
Zn v	255482	345146	$1.29 \times 10^{-1}$		1115.266			
Ga v	236072	325713	$1.91 \times 10^{-1}$		1115.561			
Zn v	237032	326664	$2.83 \times 10^{-3}$		1115.668			
Zn v	227195	316827	$1.34 \times 10^{-1}$		1115.680			newly identified
Zn v	256235	345791	$3.51 \times 10^{-1}$		1116.630			
Zn v	198962	288500	$3.70 \times 10^{-1}$		1116.842			blend with Ge v
Ge v	234219	323749	$1.97 \times 10^{-1}$		1116.949			blend with Zn v
				11.3		1117.37		unid.
Zn v	256235	345723	$4.53 \times 10^{-2}$	17.3	1117.466	1117.55	22.5	newly identified
S vi	4f $^2F^o_{5/2}$	5g $^2G_{7/2}$	1.34		1117.756			
S vi	4f $^2F^o_{7/2}$	5g $^2G_{7/2}$	$3.78 \times 10^{-2}$		1117.756			
S vi	4f $^2F^o_{7/2}$	5g $^2G_{9/2}$	1.30		1117.756			
P v	3s $^2S_{1/2}$	3p $^2P^o_{3/2}$	$4.50 \times 10^{-1}$	95.6	1117.976	1118.06	22.5	
P v					1117.977			ISM multi-component
Zr vi	440555	529945	$9.37 \times 10^{-1}$		1118.689			

Table A.2. Continued.

Ion	Levels		$f$	$W_\lambda /$ mÅ	Wavelength/Å		$v_{\text{rad}} /$ km/s	Comment
	Lower	Upper			Theoretical	Observed		
Zr v	382985	472338	$1.42 \times 10^{-1}$		1119.158			uncertain unid. unid.
Zn v	255482	344771	$2.05 \times 10^{-1}$		1119.950			
Zn v	232946	322224	$8.00 \times 10^{-2}$		1120.101			blend with Zn v
I vI					1120.300			blend with I vI
Zn v	226334	315594	$2.23 \times 10^{-1}$		1120.325			blend with I vI
Zn v	239843	329085	$4.82 \times 10^{-2}$		1120.545			newly identified unid.
Zn v	230435	319632	$1.26 \times 10^{-1}$	24.2	1121.109	1120.95		
Zn v	235903	325068	$8.18 \times 10^{-2}$		1121.524			weak
Ge v			$9.44 \times 10^{-2}$		1122.001			blend with S v, very weak
S v	3s3d $^3D_3$	3p3d $^3F_4^0$	$1.73 \times 10^{-1}$		1122.031			blend with Ge v unid.
Si iv	3p $^2P_{1/2}^0$	3d $^2D_{3/2}$	$8.07 \times 10^{-1}$	43.7	1122.485	1122.59	28.0	
Zn v	240446	329533	$1.62 \times 10^{-1}$		1122.502			blend with Si iv unid.
Zn v	230435	319472	$3.03 \times 10^{-2}$	13.2	1122.79			blend with Ga v
Ga v	215237	304272	$2.81 \times 10^{-1}$	16.8	1123.127	1123.26	28.3	unid.
						1123.70		
Ge v	238765	327753	$3.83 \times 10^{-2}$		1123.746			
Zn v	221631	310519	$1.36 \times 10^{-1}$		1125.019			
Zn v	228335	317220	$1.72 \times 10^{-1}$		1125.048			
Zn v	231997	320871	$6.18 \times 10^{-3}$		1125.182			newly identified
Ge v	241935	330791	$1.29 \times 10^{-2}$		1125.424			
C III	3d $^3D_1$	6f $^3F_2^0$	$8.13 \times 10^{-2}$		1125.629			
C III	3d $^3D_2$	6f $^3F_3^0$	$7.22 \times 10^{-2}$		1125.639			
C III	3d $^3D_2$	6f $^3F_2^0$	$9.19 \times 10^{-3}$		1125.643			
C III	3d $^3D_3$	6f $^3F_4^0$	$7.46 \times 10^{-2}$		1125.670			
Mo v	240878	329714	$5.57 \times 10^{-1}$		1125.672			
C III	3d $^3D_3$	6f $^3F_3^0$	$6.57 \times 10^{-3}$		1125.675			
C III	3d $^3D_3$	6f $^3F_2^0$	$1.49 \times 10^{-4}$		1125.679			
Mo v	148949	237760	$5.53 \times 10^{-1}$		1125.988			
Ga v	214000	302779	$2.05 \times 10^{-1}$	27.0	1126.393	1126.50	28.5	
Ga v	235609	324314	$3.96 \times 10^{-2}$		1127.332			
Ga v	215237	303911	$1.41 \times 10^{-1}$		1127.726			
Ga v	246093	334765	$3.63 \times 10^{-1}$	10.8	1127.752	1127.85	26.1	
P v	3s $^2S_{1/2}$	3p $^2P_{1/2}^0$	$2.21 \times 10^{-1}$		1128.006			blend with Ga v
P v					1128.008			ISM multi-component
Ga v	218301	306947	$3.07 \times 10^{-1}$		1128.082			blend with P v

Table A.2. Continued.

Ion	Levels		$f$	$W_\lambda /$ mÅ	Wavelength/Å		$v_{\text{rad}} /$ km/s	Comment
	Lower	Upper			Theoretical	Observed		
Si iv	3p $^2P_{3/2}^o$	3d $^2D_{5/2}$	$7.25 \times 10^{-1}$	53.4	1128.340	1128.45	29.2	
Ga v	212121	300730	$1.94 \times 10^{-1}$	9.6	1128.554	1128.65	25.5	
S v	3d $^3D_2$	3d $^3F_3^o$	$1.74 \times 10^{-1}$	12.1	1128.699	1128.80	26.8	
S v	3d $^3D_3$	3d $^3F_3^o$	$1.55 \times 10^{-2}$		1128.812			
Zn v	255482	344070	$5.38 \times 10^{-2}$		1128.813			newly identified
				8.8		1129.07		unid.
						1129.45		unid.
Zn v	226334	314838	$4.16 \times 10^{-2}$		1129.898			blend with Ga v
Ga v	214000	302499	$1.75 \times 10^{-1}$		1129.956			blend with Zn v
Zn v	228335	316827	$9.66 \times 10^{-2}$		1130.051			
Zn v	222042	310519	$1.55 \times 10^{-1}$	7.1	1130.242	1130.34	26.0	
Ni vi	330141	418553.6	$3.12 \times 10^{-1}$		1131.061			
Zn v	227195	315594	$6.70 \times 10^{-2}$		1131.242			
Ga v	231711	320093	$2.30 \times 10^{-1}$		1131.452			newly identified
Zn v	222940	311296	$1.33 \times 10^{-1}$		1131.788			
Zn v	231122	319472	$1.29 \times 10^{-1}$		1131.863			
Zn v	208715	297033	$1.40 \times 10^{-1}$		1132.271			
Zn v	235599	323886	$3.93 \times 10^{-1}$		1132.659			
Sn v					1132.790	1132.92	34.4	
Zn v	200644	288903	$3.36 \times 10^{-1}$		1133.031			
Zn v	228335	316586	$2.11 \times 10^{-1}$		1133.128			
Zn v	241829	330069	$3.40 \times 10^{-1}$		1133.278			
Zn v	222042	310265	$1.66 \times 10^{-1}$		1133.498			
S v	3s3d $^3D_1$	3p3d $^3F_2^o$	$1.84 \times 10^{-1}$		1133.901			
S v	3s3d $^3D_2$	3p3d $^3F_2^o$	$2.19 \times 10^{-2}$		1133.973			
N ii					1134.165			ISM multi-component
N ii					1134.415			ISM multi-component
N ii					1134.980			ISM multi-component
Zn v	208715	296796	$1.50 \times 10^{-2}$		1135.324			
Zn v	200644	288704	$4.32 \times 10^{-2}$		1135.588			
Ga v	212121	300144	$1.98 \times 10^{-1}$		1136.067			
Zn v	228335	316339	$7.85 \times 10^{-2}$		1136.311			blend with Xe vi, newly identified
Xe vi	5d $^2D_{5/2}$	6p $^2P_{3/2}^o$	$1.91 \times 10^{-1}$		1136.410			blend with Zn v
Zn v	198962	286943	$4.06 \times 10^{-2}$		1136.603			
Zn v	201973	289925	$4.03 \times 10^{-2}$		1136.986			
				18.9		1137.33		unid.
Zn v	235730	323632	$5.74 \times 10^{-2}$		1137.625			
Mo v	151195	239069	$2.98 \times 10^{-1}$		1137.995			
Mo v	151213	239069	$2.30 \times 10^{-1}$		1138.229			blend with Zn v
Zn v	201973	289827	$3.67 \times 10^{-1}$	36.1	1138.248	1138.35	26.9	blend with Mo v

Table A.2. Continued.

Ion	Levels		$f$	$W_\lambda /$ mÅ	Wavelength/Å		$v_{\text{rad}} /$ km/s	Comment
	Lower	Upper			Theoretical	Observed		
Zn v	256235	344070	$1.72 \times 10^{-1}$		1138.497			
Zn v	210973	298801	$1.93 \times 10^{-2}$		1138.586			newly identified
Zn v	230614	318436	$2.59 \times 10^{-2}$		1138.671			newly identified
Zn v	202929	290731	$4.08 \times 10^{-3}$		1138.933			newly identified
Zn v	231831	319632	$3.28 \times 10^{-3}$		1138.937			newly identified
Ge v	235967	323749	$9.14 \times 10^{-3}$		1139.187			blend with Zn v
Zn v	202929	290704	$6.62 \times 10^{-2}$		1139.278			blend with Ge v
Ni VI	347278.5	435011.5	$2.59 \times 10^{-1}$		1139.822			blend with C III
C III	2s3p P <sub>1</sub> <sup>o</sup>	2s5d D <sub>2</sub>	$8.86 \times 10^{-2}$		1139.899			
Zn v	222940	310659	$8.37 \times 10^{-2}$		1139.997			blend with C III, newly identified
Zn v	286575	374241	$3.85 \times 10^{-1}$		1140.703			
Zn v	227195	314838	$9.68 \times 10^{-2}$		1141.003			
Zn v	231997	319632	$9.35 \times 10^{-2}$		1141.095			
Zn v	222042	309658	$7.60 \times 10^{-2}$		1141.344			
						1142.10		unid.
Zn v	228335	315840	$3.27 \times 10^{-2}$		1142.792			
Zn v	202929	290424	$3.99 \times 10^{-1}$	18.6	1142.925	1143.03	27.5	
Zn v	237032	324526	$3.40 \times 10^{-1}$		1142.938			
Zn v	203548	291022	$8.87 \times 10^{-2}$		1143.196			
Fe II					1143.226			ISM multi-component
Ba VII	61083	148547	$2.88 \times 10^{-3}$		1143.317			newly identified
Zn v	255763	343221	$1.16 \times 10^{-1}$		1143.403			
						1143.58		unid.
Zn v	210973	298375	$1.27 \times 10^{-1}$		1144.136			
Ni VI	298130.5	385520.9	$3.52 \times 10^{-1}$		1144.290			
Fe I					1144.938			ISM multi-component
Zn v	222940	310265	$7.64 \times 10^{-2}$		1145.151			
				9.4		1145.55		unid.
Zn v	241829	329085	$6.47 \times 10^{-2}$		1146.057			
Zn v	234582	321830	$3.55 \times 10^{-1}$		1146.149			
Zn v	203548	290731	$4.50 \times 10^{-1}$	25.3	1147.020	1147.11	23.5	
Zn v	203548	290704	$1.63 \times 10^{-1}$		1147.371			
Zn v	255482	342616	$2.00 \times 10^{-1}$		1147.648			newly identified
Mo v	153040	240110	$4.03 \times 10^{-1}$		1148.502			
Zn v	232946	319984	$3.33 \times 10^{-1}$	10.7	1148.922	1149.01	23.0	
Zn v	227195	314197	$1.89 \times 10^{-1}$		1149.398			
Zn v	202929	289925	$2.05 \times 10^{-1}$		1149.486			
Zn v	256235	343221	$1.34 \times 10^{-1}$		1149.608			
Zn v	226334	313300	$3.62 \times 10^{-1}$		1149.873			
Ni VI	330580.5	417538.4	$1.17 \times 10^{-1}$		1149.982			

Table A.2. Continued.

Ion	Levels		$f$	$W_\lambda /$ mÅ	Wavelength/Å		$v_{\text{rad}} /$ km/s	Comment
	Lower	Upper			Theoretical	Observed		
Ni VI	376343.7	463301.5	$2.29 \times 10^{-1}$		1149.983			
Ga V	218301	305249	$2.22 \times 10^{-2}$		1150.113			
Ga V	210052	296992	$2.24 \times 10^{-1}$		1150.219			
				25.1		1150.64		unid.
Zn V	212471	299372	$1.66 \times 10^{-1}$	11.4	1150.743	1150.84	25.3	
O III	$2p^3 \ ^3S_1^o$	$2p^4 \ ^3P_1$	$8.43 \times 10^{-2}$		1150.884	1151.03	38.0	
Se V					1151.000	1151.13	33.9	
Ni V	212095.8	298972.3	$2.34 \times 10^{-2}$		1151.059			
Zn V	255763	342616	$1.16 \times 10^{-1}$		1151.368			
Zn V	230614	317466	$4.50 \times 10^{-2}$		1151.393			newly identified
Zr VI	427649	514487	$2.33 \times 10^{-1}$		1151.571			
Zn V	201973	288704	$2.26 \times 10^{-1}$	19.6	1152.985	1153.08	24.7	
Zn V	222940	309658	$4.82 \times 10^{-2}$		1153.160			
				18.4		1153.56		unid.
O III	$2p^3 \ ^3S_1^o$	$2p^4 \ ^3P_2$	$1.41 \times 10^{-1}$	37.2	1153.775	1153.90	32.5	
Zn V	208715	295293	$7.17 \times 10^{-2}$	3.6	1155.027	1155.14	29.3	
Zn V	232946	319472	$1.27 \times 10^{-1}$		1155.725			
Zn V	285885	372360	$3.17 \times 10^{-1}$		1156.394			newly identified
Ga V	246133	332600	$3.44 \times 10^{-1}$	12.4	1156.511	1156.62	28.3	
Zn V	231997	318436	$2.76 \times 10^{-2}$		1156.885			
Zn V	203548	289925	$2.90 \times 10^{-2}$		1157.725			newly identified
Ni VI	337993.9	424363.7	$1.04 \times 10^{-1}$		1157.812			
				15.7		1158.00		unid.
Zn V	239843	326189	$7.13 \times 10^{-2}$		1158.122			
Zn V	235903	322224	$1.83 \times 10^{-1}$		1158.475			
Zn V	200644	286943	$2.38 \times 10^{-1}$	24.6	1158.759	1158.86	26.1	
				27.3		1159.88		unid.
Zn V	226334	312534	$1.04 \times 10^{-2}$		1160.091			weak
Zn V	234582	320772	$2.88 \times 10^{-1}$		1160.221			
Sn V				37.6	1160.740	1160.86	31.0	blend with Zn v
Zn V	255482	341627	$7.26 \times 10^{-2}$		1160.827			blend with Sn v, newly identified
				40.1		1161.99		unid.
Zn V	210973	297033	$5.56 \times 10^{-2}$		1161.971			
Zn V	291107	377144	$3.72 \times 10^{-1}$		1162.281			
Zn V	230614	316643	$9.18 \times 10^{-2}$		1162.401			
Ge V	241935	327891	$1.29 \times 10^{-2}$		1163.389			
Zn V	230435	316339	$7.96 \times 10^{-2}$		1164.082			
Zn V	212471	298375	$6.62 \times 10^{-2}$		1164.100			newly identified
O IV	3d $^2F_{5/2}^o$	4f $^2G_{7/2}$	$8.50 \times 10^{-1}$	16.7	1164.321	1164.41	22.9	
O IV	3d $^2F_{7/2}^o$	4f $^2G_{9/2}$	$8.26 \times 10^{-1}$	19.9	1164.546	1164.65	26.8	



Table A.2. Continued.

Ion	Levels		$f$	$W_\lambda /$ mÅ	Wavelength/Å		$v_{\text{rad}} /$ km/s	Comment
	Lower	Upper			Theoretical	Observed		
Zn v	255763	341627	$5.07 \times 10^{-2}$		1164.632			
Zn v	228335	314197	$1.72 \times 10^{-2}$		1164.656			newly identified
Zn v	210973	296796	$4.52 \times 10^{-2}$		1165.186			blend with Ge v
Ge v	241935	327753	$1.48 \times 10^{-2}$		1165.259			blend with Zn v
				27.0		1165.40		unid.
Zn v	286575	372360	$4.41 \times 10^{-2}$		1165.706			
Zn v	210973	296757	$5.56 \times 10^{-2}$		1165.716			
Zn v	234846	320618	$3.60 \times 10^{-1}$		1165.880			
C iv	3d $^2D_{3/2}$	4f $^2F_{5/2}^o$	1.02		1168.849			
C iv	3d $^2D_{5/2}$	4f $^2F_{7/2}^o$	$4.88 \times 10^{-2}$		1168.993			
C iv	3d $^2D_{5/2}$	4f $^2F_{5/2}^o$	$9.97 \times 10^{-1}$		1168.993			
Zn v	226334	311796	$1.02 \times 10^{-1}$		1170.105			
C iv					1170.130			forbidden C iv component
C iv					1170.330			forbidden C iv component
Zn v	231831	317220	$7.01 \times 10^{-2}$		1171.106			
Zn v	239843	325068	$3.11 \times 10^{-1}$		1173.366			
Zn v	198962	284116	$3.01 \times 10^{-1}$	24.1	1174.346	1174.43	21.4	
				12.3		1174.75		unid.
C iii	2s2p $^3P_1^o$	2p <sup>2</sup> $^3P_2$	$1.17 \times 10^{-1}$	108.5	1174.933	1175.04	27.3	
Zn v	235599	320709	$1.24 \times 10^{-1}$		1174.945			blend with C iii
C iii	2s2p $^3P_0^o$	2p <sup>2</sup> $^3P_1$	$2.72 \times 10^{-1}$	112.4	1175.263	1175.38	29.9	
C iii	2s2p $^3P_1^o$	2p <sup>2</sup> $^3P_1$	$7.03 \times 10^{-2}$		1175.590			
C iii	2s2p $^3P_2^o$	2p <sup>2</sup> $^3P_2$	$2.11 \times 10^{-1}$		1175.711			
C iii	2s2p $^3P_1^o$	2p <sup>2</sup> $^3P_0$	$9.07 \times 10^{-2}$	98.9	1175.987	1176.10	28.8	
Zn v	226334	311359	$8.10 \times 10^{-2}$		1176.122			blend with C iii
C iii	2s2p $^3P_2^o$	2p <sup>2</sup> $^3P_1$	$7.02 \times 10^{-2}$		1176.370			
Zn v	231831	316827	$7.34 \times 10^{-2}$		1176.527			blend with C iii, newly identified
Ge v	238765	323749	$2.06 \times 10^{-3}$		1176.690			blend with C iii
Zn v	198962	283933	$1.86 \times 10^{-1}$		1176.868			newly identified
Zn v	201973	286936	$1.46 \times 10^{-1}$		1176.980			newly identified
Zn v	226334	311295	$7.56 \times 10^{-2}$		1177.016			newly identified
Zn v	202929	287888	$1.00 \times 10^{-1}$		1177.036			newly identified
Zn v	200644	285603	$1.68 \times 10^{-1}$		1177.044			newly identified
Zn v	231831	316786	$3.06 \times 10^{-1}$		1177.087			newly identified
Zn v	260880	345723	$8.22 \times 10^{-2}$		1178.639			newly identified
Zn v	241829	326664	$1.12 \times 10^{-1}$		1178.759			
Ni v	232655.6	317477.9	$9.35 \times 10^{-3}$		1178.935			
Zn v	236969	321776	$1.93 \times 10^{-1}$		1179.145			
Zn v	230435	315239	$1.10 \times 10^{-1}$		1179.179			
Xe vi	5p $^2P_{3/2}^o$	5p <sup>2</sup> $^4P_3$	$4.65 \times 10^{-4}$	19.9	1179.537	1179.63	23.6	

**Table A.2.** Continued.

Ion	Levels		$f$	$W_\lambda /$ mÅ	Wavelength/Å		$v_{\text{rad}} /$ km/s	Comment
	Lower	Upper			Theoretical	Observed		
Zn v	208715	293463	$2.79 \times 10^{-1}$	17.3	1179.969	1180.10	33.3	
Zn v	260880	345624	$4.73 \times 10^{-2}$		1180.018			
Xe VI	5d $^2D_{3/2}$	6p $^2P_{1/2}^o$	$1.54 \times 10^{-1}$		1181.455			
Zn v	227195	311796	$2.22 \times 10^{-2}$		1182.019			
Mo VI	283610.94	368203.16	$7.44 \times 10^{-1}$	16.1	1182.142	1182.24	24.9	
Zn v	212471	297033	$7.26 \times 10^{-2}$	23.5	1182.567	1182.67	26.1	
Zn v	235730	320257	$1.94 \times 10^{-2}$		1183.041			
Zn v	230435	314958	$3.17 \times 10^{-2}$		1183.100			
Zn v	232946	317466	$2.31 \times 10^{-2}$		1183.158			
Zn v	231831	316339	$2.99 \times 10^{-2}$		1183.314			
Zn v	230614	314958	$8.97 \times 10^{-2}$		1185.619			
Zn v	231997	316339	$5.02 \times 10^{-2}$		1185.645			
Zn v	203548	287888	$1.30 \times 10^{-1}$		1185.676			
Zn v	212471	296796	$3.24 \times 10^{-1}$		1185.898			
Zn v	210973	295293	$1.84 \times 10^{-1}$		1185.948			
Mo v	159857	244170	$7.85 \times 10^{-1}$		1186.050			blend with Zn v
Zn v	235730	320043	$2.18 \times 10^{-1}$		1186.057			blend with Mo v
Mo v	151195	235496	$4.73 \times 10^{-1}$		1186.227			
Mo v	245600	329898	$4.77 \times 10^{-1}$		1186.277			
Zn v	212471	296757	$2.05 \times 10^{-1}$		1186.447			
Mo v	148949	233190	$3.57 \times 10^{-1}$		1187.061			
Zn v	228335	312534	$2.72 \times 10^{-1}$		1187.664			
Zn v	210973	295168	$3.51 \times 10^{-1}$		1187.706			

**Table A.3.** Like Table A.1, for the HST/STIS observations.

Ion	Levels		$f$	$W_\lambda /$ mÅ	Wavelength/Å		$v_{\text{rad}} /$ km/s	Comment
	Lower	Upper			Theoretical	Observed		
						1150.35		unid.
						1151.10		unid.
Zn v	201973	288704	$2.26 \times 10^{-1}$		1152.985			
O III	$2p^3 \ ^3S_1$	$2p^4 \ ^3P_2$	$1.41 \times 10^{-1}$		1153.775	1153.92	37.7	
Zn v	208715	295293	$7.17 \times 10^{-2}$	29.8	1155.027	1155.12	24.1	
Zn v	285885	372360	$3.17 \times 10^{-1}$		1156.394			newly identified
Ga v	246133	332600	$3.44 \times 10^{-1}$		1156.511			
Zn v	231997	318436	$2.76 \times 10^{-2}$		1156.885			
						1158.00		unid.
Zn v	200644	286943	$2.38 \times 10^{-1}$	19.0	1158.759	1158.83	18.4	
						1159.90		unid.

Table A.3. Continued.

Ion	Levels		$f$	$W_\lambda /$ mÅ	Wavelength / Å		$v_{\text{rad}} /$ km/s	Comment
	Lower	Upper			Theoretical	Observed		
Sn v				36.4 25.2	1160.740	1160.85 1161.97	28.4	uncertain unid.
Ge v	241935	327891	$1.29 \times 10^{-2}$		1163.389			
O iv	3d $^2F_{5/2}^o$	4f $^2G_{7/2}$	$8.50 \times 10^{-1}$	17.7	1164.321	1164.41	22.9	
O iv	3d $^2F_{7/2}^o$	4f $^2G_{9/2}$	$8.26 \times 10^{-1}$	44.0	1164.546	1164.65	26.8	
Zn v	255763	341627	$5.07 \times 10^{-2}$		1164.632			
Zn v	228335	314197	$1.72 \times 10^{-2}$		1164.656			newly identified
Zn v	210973	296796	$4.52 \times 10^{-2}$		1165.186			blend with Ge v
Ge v	241935	327753	$1.48 \times 10^{-2}$		1165.259			blend with Zn v
				23.1		1165.40		unid.
Zn v	210973	296757	$5.56 \times 10^{-2}$		1165.716			
Zn v	234846	320618	$3.60 \times 10^{-1}$		1165.880			
C iv	3d $^2D_{3/2}$	4f $^2F_{5/2}^o$	1.02		1168.849			
C iv	3d $^2D_{5/2}$	4f $^2F_{7/2}^o$	$9.97 \times 10^{-1}$		1168.993			
C iv	3d $^2D_{5/2}$	4f $^2F_{5/2}^o$	$4.88 \times 10^{-2}$		1168.993			
				10.2		1169.26		unid.
C iv					1170.130			forbidden C iv component
C iv					1170.330			forbidden C iv component
Zn v	231831	317220	$7.01 \times 10^{-2}$		1171.106			
				15.4		1172.35 1173.37		unid. unid.
Zn v	239843	325068	$3.11 \times 10^{-1}$		1173.366			
Zn v	237032	322224	$7.26 \times 10^{-2}$		1173.823			newly identified
Zn v	230614	315801	$1.79 \times 10^{-1}$		1173.892			newly identified
Zn v	198962	284116	$3.01 \times 10^{-1}$	23.6	1174.346	1174.43 1174.72	21.4	unid.
C iii	2s2p $^3P_1^o$	2p <sup>2</sup> $^3P_2$	$1.17 \times 10^{-1}$	100.0	1174.933	1175.03	24.8	
C iii	2s2p $^3P_0^o$	2p <sup>2</sup> $^3P_1$	$2.72 \times 10^{-1}$	100.0	1175.263	1175.37	27.3	
C iii	2s2p $^3P_1^o$	2p <sup>2</sup> $^3P_1$	$7.03 \times 10^{-2}$		1175.590			
C iii	2s2p $^3P_2^o$	2p <sup>2</sup> $^3P_2$	$2.11 \times 10^{-1}$		1175.711			
C iii	2s2p $^3P_1^o$	2p <sup>2</sup> $^3P_0$	$9.07 \times 10^{-2}$	104.7	1175.987	1176.09	26.3	blend with Zn v
Zn v	226334	311359	$8.10 \times 10^{-2}$		1176.122			blend with C iii
C iii	2s2p $^3P_2^o$	2p <sup>2</sup> $^3P_1$	$7.02 \times 10^{-2}$	130.7	1176.370	1176.45	20.4	blend with Zn v
Zn v	231831	316827	$7.34 \times 10^{-2}$		1176.527			blend with C iii, newly identified
Ge v	238765	323749	$2.06 \times 10^{-3}$		1176.690			blend with C iii
Zn v	198962	283933	$1.86 \times 10^{-1}$		1176.868			newly identified
Zn v	201973	286936	$1.46 \times 10^{-1}$		1176.980			newly identified
Zn v	226334	311295	$7.56 \times 10^{-2}$		1177.016			newly identified
Zn v	202929	287888	$1.00 \times 10^{-1}$		1177.036			newly identified
Zn v	200644	285603	$1.68 \times 10^{-1}$		1177.044			newly identified

Table A.3. Continued.

Ion	Levels		$f$	$W_\lambda /$ mÅ	Wavelength / Å		$v_{\text{rad}} /$ km/s	Comment
	Lower	Upper			Theoretical	Observed		
Zn v	231831	316786	$3.06 \times 10^{-1}$	20.2	1177.087	1178.68		newly identified unid.
Zn v	260880	345723	$8.22 \times 10^{-2}$		1178.639			
Zn v	241829	326664	$1.12 \times 10^{-1}$		1178.759			
Ni v	232655.6	317477.9	$9.35 \times 10^{-3}$		1178.935			
Zn v	236969	321776	$1.93 \times 10^{-1}$		1179.145			
Zn v	230435	315239	$1.10 \times 10^{-1}$		1179.179			
Xe VI	5p $^2P_{3/2}^o$	5p $^2$ $^4P_{3/2}$	$4.65 \times 10^{-4}$		1179.537			
Zn v	208715	293463	$2.79 \times 10^{-1}$		1179.969			
Xe VI	5d $^2D_{3/2}$	6p $^2P_{1/2}^o$	$1.54 \times 10^{-1}$		1181.455			
Xe VI	5d $^2D_{5/2}$	5d $^4F_{7/2}^o$	$6.24 \times 10^{-3}$		1181.474			newly identified
Zn v	227195	311796	$2.22 \times 10^{-2}$		1182.019			
Zn IV	151574	236175	$5.65 \times 10^{-2}$		1182.022			newly identified
Mo VI	283611	368203	$7.44 \times 10^{-1}$	15.0	1182.142	1182.24	24.9	
Zn v	212471	297033	$7.26 \times 10^{-2}$		1182.567			
Zn v	235730	320257	$1.94 \times 10^{-2}$		1183.041			
Zn v	230435	314958	$3.17 \times 10^{-2}$		1183.100			
Zn v	232946	317466	$2.31 \times 10^{-2}$		1183.158			
Zn v	230614	314958	$8.97 \times 10^{-2}$		1185.619			
Zn v	231997	316339	$5.02 \times 10^{-2}$		1185.645			
Zn v	203548	287888	$1.30 \times 10^{-1}$		1185.676			
Zn v	212471	296796	$3.24 \times 10^{-1}$		1185.898			
Zn v	210973	295293	$1.84 \times 10^{-1}$		1185.948			
Zn v	285523	369843	$1.03 \times 10^{-1}$		1185.961			
Zn v	235730	320043	$2.18 \times 10^{-1}$		1186.057			
Zn v	212471	296757	$2.05 \times 10^{-1}$	18.0	1186.447	1186.54	23.5	
				8.9		1187.05		unid.
Zn v	228335	312534	$2.72 \times 10^{-1}$		1187.664			
Zn v	210973	295168	$3.51 \times 10^{-1}$		1187.706			
N IV	2s3s $^1S_0$	2p( $^2P_{3/2}^o$ )3s $^1P_1^o$	$6.02 \times 10^{-1}$	24.8	1188.005	1188.11	26.5	
Ge IV	84102.3	0	$5.52 \times 10^{-1}$	51.7	1189.028	1189.11	20.7	
Zn v	227195	311295	$2.43 \times 10^{-1}$		1189.072			newly identified
Zn v	234846	318927	$2.55 \times 10^{-2}$		1189.331			newly identified
Zn v	235903	319984	$7.13 \times 10^{-2}$		1189.332			newly identified
Sn v				23.3	1189.920	1190.04	30.2	
Zn v	235599	319632	$1.40 \times 10^{-1}$		1190.003			newly identified
Zn v	208715	292722	$3.13 \times 10^{-1}$		1190.376			newly identified
Zn v	202929	286936	$8.34 \times 10^{-2}$		1190.380			newly identified
				83.2		1190.48		unid.
Ga v	235609	319570	$2.23 \times 10^{-2}$		1191.029			newly identified

Table A.3. Continued.

Ion	Levels		$f$	$W_\lambda /$ mÅ	Wavelength/Å		$v_{\text{rad}} /$ km/s	Comment
	Lower	Upper			Theoretical	Observed		
Zn v	260880	344771	$6.24 \times 10^{-2}$	4.9	1192.014	1192.35	newly identified unid.	
Ga iv	153086	236907	$1.87 \times 10^{-1}$		1193.024			
Ga v	235752	319570	$1.20 \times 10^{-1}$	60.1	1193.061	1193.34	newly identified unid.	
Zn v	231997	315801	$1.66 \times 10^{-2}$		1193.260			
C I				3.1	1193.264	1193.45	newly identified ISM multi-component unid.	
Ba vii	157675	241412	$3.06 \times 10^{-3}$		1194.221			
				11.0 20.2		1194.65 1194.99	newly identified unid. unid.	
Zn v	201973	285603	$7.16 \times 10^{-2}$		1195.745			
O iii	3p $^3D_2$	4d $^3F_3^o$	$8.82 \times 10^{-2}$	9.5	1196.753	1196.85	24.3	
O iii	3p $^3D_3$	4d $^3F_4^o$	$9.11 \times 10^{-2}$		1197.239			
O iii	3p $^3D_1$	4d $^3F_2^o$	$9.93 \times 10^{-2}$		1197.331			
					1197.81		unid.	
C iv	3d $^2D_{3/2}$	4p $^2P_{3/2}^o$	$2.76 \times 10^{-3}$		1198.403			
C iv	3d $^2D_{5/2}$	4p $^2P_{3/2}^o$	$1.65 \times 10^{-2}$		1198.554			
C iv	3d $^2D_{3/2}$	4p $^2P_{1/2}^o$	$1.38 \times 10^{-2}$		1198.591			
Ni v	241773.6	325148.4	$1.18 \times 10^{-1}$		1199.403			
N I					1199.550		ISM multi-component	
				27.0		1199.61	unid.	
				22.9		1199.75	unid.	
				13.6		1199.99	unid.	
				18.0		1200.28	unid.	
N I					1200.223		ISM multi-component	
Zn v	200644	283933	$6.25 \times 10^{-2}$		1200.639		newly identified	
Zn v	236969	320257	$3.36 \times 10^{-1}$		1200.643		newly identified	
N I					1200.710		ISM multi-component	
Zr v	453681	536961	$8.10 \times 10^{-1}$		1200.760		blend with Mo vi	
Mo vi	151213	234490	$5.26 \times 10^{-1}$		1200.808		blend with Zr v, newly identified	
				19.5		1201.37	unid.	
							1201.60	unid.
Zn v	234846	317978	$2.38 \times 10^{-1}$		1202.906		newly identified	
Zn v	239843	322969	$4.20 \times 10^{-2}$		1202.983		newly identified	
						1204.72	unid.	
Zn v	231831	314838	$9.24 \times 10^{-2}$		1204.722		newly identified	
						1205.01	unid.	
						1205.36	unid.	
Sn v				14.1	1205.720	1205.85	32.3	
Si iii					1206.500		ISM multi-component	

Table A.3. Continued.

Ion	Levels		$f$	$W_\lambda /$ mÅ	Wavelength / Å		$v_{\text{rad}} /$ km/s	Comment	
	Lower	Upper			Theoretical	Observed			
C III	3d $^1D_2$	6f $^1F_3^o$	$1.01 \times 10^{-1}$		1210.081	1209.56		unid.	
						1213.15		unid.	
						1214.31		unid.	
He II	2	4	$1.19 \times 10^{-1}$		1215.133				
							1219.94		unid.
							1220.07		unid.
							1220.23		unid.
Ge V	241935	323749	$4.91 \times 10^{-3}$		1222.289				
						1222.80		unid.	
Zn IV	160886	242640	$2.88 \times 10^{-1}$		1223.182			newly identified	
N IV	2s3p $^3P_2^o$	2s4s $^3S_1$	$2.03 \times 10^{-2}$		1225.722				
Sb V				9.0	1226.000	1226.11	26.9		
Zn V	235903	317466	$2.59 \times 10^{-2}$		1226.057			newly identified	
Se V					43.7	1227.600	1227.64	9.8	
					6.9		1227.91		unid.
Ga IV	156025	237458	$1.95 \times 10^{-1}$	17.3	1227.999	1228.090	22.2	newly identified	
Xe VI	5p $^2$ $^2P_{3/2}^o$	5p $^3$ $^2D_{5/2}^o$	$3.96 \times 10^{-2}$		1228.426			blend with Zn V, newly identified	
Zn IV	160919	242320	$3.07 \times 10^{-1}$		1228.486			blend with Xe VI, newly identified	
						8.4	1228.93		unid.
						2.6	1229.04		unid.
Ni V	274695.4	356036.3	$1.89 \times 10^{-1}$		1229.394			blend with Mo V	
Mo V	157851	239189	$1.52 \times 10^{-1}$		1229.447			blend with Ni V, newly identified	
						3.7	1229.66		unid.
Ge IV	81311.4	0	$2.66 \times 10^{-1}$	27.7	1229.839	1229.95	27.1		
C IV	3p $^2P_{1/2}^o$	4s $^2S_{1/2}$	$8.14 \times 10^{-2}$		1230.043				
C IV	3p $^2P_{3/2}^o$	4s $^2S_{1/2}$	$8.15 \times 10^{-2}$		1230.521				
Ni V	225200.7	306377.8	$1.26 \times 10^{-1}$		1231.875				
Ni V	208163.7	289298	$7.34 \times 10^{-2}$		12.3	1232.01		unid.	
							1232.73		unid.
Ni V	246240.9	327356.6	$1.68 \times 10^{-1}$		1232.807				
Ni V	263805.8	344911.2	$3.57 \times 10^{-1}$		1232.964				
Ni V	234082.1	315168.2	$1.59 \times 10^{-1}$		1233.257				
Ni V	208164.6	289247.1	$9.35 \times 10^{-2}$		1233.312				
Ni V	274695.4	355765.2	$2.33 \times 10^{-3}$		1233.505				
Ni V	263735.7	344805.3	$3.16 \times 10^{-1}$		1233.508				
Ni V	234125.4	315168.2	$1.10 \times 10^{-1}$		1233.916				
						1234.41		unid.	

Table A.3. Continued.

Ion	Levels		$f$	$W_\lambda /$ mÅ	Wavelength / Å		$v_{\text{rad}} /$ km/s	Comment
	Lower	Upper			Theoretical	Observed		
Ni v	208151.5	289163	$1.33 \times 10^{-1}$		1234.393			
Ni v	233839.2	314756.4	$2.15 \times 10^{-1}$		1235.831			
Ni v	240193.8	321081.9	$3.86 \times 10^{-2}$		1236.276			
Ni v	234412.7	315300.7	$1.12 \times 10^{-1}$		1236.277			
Zn v	230435	311296	$4.58 \times 10^{-2}$		1236.689			newly identified
Zn v	234846	315594	$3.44 \times 10^{-5}$		1238.425			newly identified
Zn v	260880	341627	$1.01 \times 10^{-1}$		1238.430			newly identified
N v	2s $^2S_{1/2}$	2p $^2P_{3/2}^o$	$1.56 \times 10^{-1}$	141.3	1238.821	1238.93	26.4	
Zn v	231831	312534	$2.67 \times 10^{-2}$		1239.108			newly identified
				9.2		1239.82		unid.
Kr v	278928	359544	$2.25 \times 10^{-1}$		1240.449			newly identified
Ni v	243331.5	323908.6	$3.93 \times 10^{-2}$		1241.047			
Ni v	234125.4	314702.2	$3.71 \times 10^{-2}$		1241.052			
Ni v	234275.2	314834.7	$1.28 \times 10^{-1}$		1241.319			
Ni v	233839.2	314392	$6.46 \times 10^{-2}$		1241.422			
						1241.86		unid.
						1241.99		unid.
Ni v	234082.1	314599.2	$1.24 \times 10^{-1}$		1241.972			
Ni v	229408.8	309919.5	$1.85 \times 10^{-1}$		1242.071			
O iv	3d $^2D_{3/2}$	4p $^2P_{3/2}^o$	$8.21 \times 10^{-3}$		1242.176			
O iv	3d $^2D_{5/2}$	4p $^2P_{3/2}^o$	$4.93 \times 10^{-2}$		1242.434			
N v	2s $^2S_{1/2}$	2p $^2P_{1/2}^o$	$7.80 \times 10^{-2}$	132.4	1242.804	1242.91	25.6	blend with O iv
O iv	3d $^2D_{3/2}$	4p $^2P_{1/2}^o$	$4.11 \times 10^{-2}$		1242.838			blend with N v
Ni v	234125.4	314562.8	$1.46 \times 10^{-1}$		1243.203			
Ni vi	337993.9	418368.8	$3.60 \times 10^{-2}$	21.2	1244.170	1244.29	28.9	
Ni v	164525.9	244900.5	$3.97 \times 10^{-1}$	21.2	1244.174	1244.29	28.0	
Ni v	229408.8	309743.6	$1.68 \times 10^{-2}$		1244.791			
Ni v	234275.2	314599.2	$9.70 \times 10^{-2}$		1244.958			
Ni v	216596	296919.3	$3.91 \times 10^{-2}$		1244.969			
Ni v	240193.8	320513.8	$1.23 \times 10^{-1}$		1245.020			
Ni v	234082.1	314392	$2.55 \times 10^{-1}$		1245.176			
Ni v	274695.4	354989.6	$3.46 \times 10^{-1}$		1245.420			
Ga iv	156025	236312	$1.38 \times 10^{-1}$		1245.529			newly identified
				9.5		1245.74		unid.
				10.1		1245.87		unid.
Zr v	491116	571376	$8.57 \times 10^{-3}$		1245.951			
Zr v	457547	537807	$7.85 \times 10^{-1}$		1245.951			
Ni v	263700.9	343905.7	$3.56 \times 10^{-1}$		1246.808			
Zn v	208715	288903	$3.85 \times 10^{-2}$		1247.074			newly identified
C iii	2s2p $^1P_1^o$	2p <sup>2</sup> $^1S_0$	$1.62 \times 10^{-1}$	93.2	1247.383	1247.50	28.1	

Table A.3. Continued.

Ion	Levels		$f$	$W_\lambda /$ mÅ	Wavelength / Å		$v_{\text{rad}} /$ km/s	Comment
	Lower	Upper			Theoretical	Observed		
				12.8		1247.81		unid.
Ni v	208131	288161.6	$1.30 \times 10^{-1}$		1249.522			
Zn v	232946	312967	$5.28 \times 10^{-2}$		1249.675			newly identified
				6.5		1249.98		unid.
Ni v	208163.7	288161.6	$5.58 \times 10^{-2}$		1250.033			
				13.8		1250.40		unid.
Ni v	208046.4	288021.6	$3.50 \times 10^{-1}$		1250.388			blend with Zn v
Zn v	231831	311796	$9.46 \times 10^{-3}$		1250.539			blend with Ni v, newly identified
Ni v	217048.7	296932.9	$2.74 \times 10^{-1}$		1251.812			
Ni v	232910.8	312778.2	$1.69 \times 10^{-1}$		1252.075			
Ni v	208046.4	287906.9	$1.62 \times 10^{-1}$		1252.183			
Ni v	229408.8	309264	$8.26 \times 10^{-2}$		1252.267			
Ni v	217048.7	296897	$2.05 \times 10^{-2}$		1252.375			
Ni v	229440.6	309264	$1.67 \times 10^{-1}$		1252.765			
						1253.38		unid.
Ni v	263700.9	343478.2	$1.77 \times 10^{-1}$		1253.489			
Ni v	208131	287906.9	$4.65 \times 10^{-2}$		1253.511			
Kr v	213932.87	293705	$3.74 \times 10^{-2}$		1253.571			newly identified
Ni v	217129.1	296897	$2.43 \times 10^{-1}$		1253.637			
Ni v	217101	296847.1	$2.52 \times 10^{-1}$		1253.980			
				19.0		1254.22		unid.
				7.4		1255.40		unid.
Ba VII	42514	122163	$6.18 \times 10^{-4}$		1255.520			newly identified
C III	3s $^3S_1$	4p $^3P_2^o$	$4.26 \times 10^{-2}$		1256.466			
C III	3s $^3S_1$	4p $^3P_1^o$	$2.56 \times 10^{-2}$		1256.542			
C III	3p $^1P_1^o$	5s $^1S_0$	$2.55 \times 10^{-2}$		1256.549			
C III	3s $^3S_1$	4p $^3P_0^o$	$8.52 \times 10^{-3}$		1256.577			
				14.1		1256.83		unid.
Ni v	208131	287645.9	$3.46 \times 10^{-1}$		1257.626			
Ni v	243331.5	322820.8	$7.67 \times 10^{-2}$		1258.031			
Ga IV	149512	228953	$4.03 \times 10^{-1}$		1258.801			newly identified
Ni v	229413	308804.1	$9.65 \times 10^{-2}$		1259.587			
Ni v	234082.1	313464.7	$8.37 \times 10^{-2}$		1259.722			
				84.4		1260.47		unid.
Ni v	234125.4	313464.7	$1.98 \times 10^{-1}$		1260.409			blend with ?
Si II					1260.422			ISM multi-component
Zr v	391998	471306	1.05		1260.909			
Ni v	212253.4	291541.7	$6.11 \times 10^{-2}$		1261.220			
Ni v	243331.5	322617.6	$1.13 \times 10^{-1}$		1261.255			
Ni v	235420.6	314702.2	$2.90 \times 10^{-1}$		1261.327			



Table A.3. Continued.

Ion	Levels		$f$	$W_\lambda /$ mÅ	Wavelength/Å		$v_{\text{rad}} /$ km/s	Comment
	Lower	Upper			Theoretical	Observed		
Ni v	279199.5	358475.6	$3.28 \times 10^{-1}$		1261.414			
Ni v	216189.9	295444.3	$3.32 \times 10^{-1}$		1261.760			
Zn v	230435	309658	$3.99 \times 10^{-2}$		1262.252			newly identified
				15.9		1262.38		unid.
Ni v	274738.6	353944.1	$1.81 \times 10^{-1}$		1262.539			
				13.3		1262.81		unid.
				17.7		1263.27		unid.
				10.8		1263.50		unid.
Mo VI	395181	474296	$2.07 \times 10^{-1}$		1263.989			
Mo VI	395184	474297	$2.04 \times 10^{-1}$		1264.023			
				11.0		1264.24		unid.
Ni v	164525.9	243608.5	$2.98 \times 10^{-1}$		1264.501			
Ga IV	150967	230040	$9.57 \times 10^{-2}$		1264.654			newly identified
Ni v	243370.5	322436.4	$1.14 \times 10^{-1}$		1264.768			
Zr v	376898	455925	$8.93 \times 10^{-1}$	11.2	1265.381	1265.49	25.8	
Zn IV	128730	207737	$2.04 \times 10^{-1}$		1265.707			newly identified
				8.5		1266.00		unid.
Ni v	247049.1	326029.9	$1.14 \times 10^{-1}$		1266.131			
Ni v	208163.7	287127.2	$3.11 \times 10^{-1}$	12.3	1266.408	1266.52	26.5	
Ni v	240193.8	319138.7	$7.81 \times 10^{-2}$		1266.706			
Ni v	212455.7	291390	$3.00 \times 10^{-1}$		1266.876			
Ga IV	156025	234940	$1.26 \times 10^{-1}$		1267.189			newly identified
Ni v	229408.8	308317.3	$1.59 \times 10^{-1}$		1267.291			
				8.0		1267.56		unid.
				9.7		1267.77		unid.
Ni v	229440.6	308317.3	$1.60 \times 10^{-1}$		1267.802			
Ni v	236454.1	315326.2	$1.02 \times 10^{-1}$		1267.875			
				18.6		1268.09		unid.
						1268.40		unid.
Ni v	274738.6	353548.7	$2.22 \times 10^{-1}$		1268.873			
Ni v	241082.2	319860.4	$1.63 \times 10^{-1}$		1269.387			
Ni v	242290.4	321018.3	$1.44 \times 10^{-1}$		1270.198			
N IV	2s3p $^3P_2^o$	2p( $^2P^o$ )3p $^3D_3$	$1.39 \times 10^{-1}$		1270.270			
Mo VI	316477	395184	$1.14 \times 10^{-2}$		1270.523			
Ni v	229440.6	308138.8	$3.40 \times 10^{-1}$	14.0	1270.677	1270.80	29.0	
Ni v	234275.2	312889.4	$7.80 \times 10^{-2}$		1272.035			
N IV	2s3p $^3P_1^o$	2p( $^2P^o$ )3p $^3D_2$	$1.23 \times 10^{-1}$		1272.145			
				6.9		1272.52		unid.
Ni v	242504.3	321081.9	$9.12 \times 10^{-2}$		1272.627			
Ni v	208131	286706.6	$1.33 \times 10^{-2}$		1272.660			

Table A.3. Continued.

Ion	Levels		$f$	$W_\lambda /$ mÅ	Wavelength / Å		$v_{\text{rad}} /$ km/s	Comment
	Lower	Upper			Theoretical	Observed		
Ni v	274773.5	353347.1	$8.85 \times 10^{-2}$		1272.692			
Zn iv	130366	208921	$1.65 \times 10^{-1}$	13.8	1272.990	1273.08	21.2	newly identified
Ni v	208164.6	286706.6	$3.51 \times 10^{-1}$		1273.204			
				15.7		1274.39		unid.
				10.0		1274.83		unid.
Ni v	216596	294939.6	$2.88 \times 10^{-1}$		1276.428			
				11.8		1276.72		unid.
Ni v	164525.9	242837	$2.13 \times 10^{-1}$	17.9	1276.958	1277.06	24.0	
				9.7		1277.64		unid.
				8.2		1278.29		unid.
				16.9		1279.04		unid.
Ni v	212095.8	290262	$2.31 \times 10^{-1}$	10.6	1279.325	1279.45	29.3	
Ni v	208151.5	286293.6	$3.95 \times 10^{-1}$		1279.720			
Ni v	247104.9	325222.9	$1.05 \times 10^{-1}$		1280.115			
Ni v	240959.6	319076.2	$2.26 \times 10^{-1}$		1280.138			
Xe vi	$5p^2 \ ^4P_{5/2}$	$4f \ ^2F_{7/2}^o$			1280.213			newly identified
Zn iv	131805	209899	$1.71 \times 10^{-1}$	13.0	1280.500	1280.58	18.7	newly identified
				7.2		1280.78		unid.
				6.8		1281.26		unid.
				7.3		1281.49		unid.
				7.0		1281.62		unid.
				7.5		1281.76		unid.
				4.5		1281.99		unid.
Ni v	229408.8	307399.7	$1.14 \times 10^{-1}$		1282.201			
Ni v	229413	307399.7	$1.08 \times 10^{-1}$		1282.270			
Zn iv	151250	229231	$1.22 \times 10^{-1}$		1282.357			newly identified
Ni v	251654.9	329614.3	$1.78 \times 10^{-3}$		1282.719			
Zn v	212471	290424	$9.80 \times 10^{-3}$		1282.832			newly identified
				3.5		1283.77		unid.
Sn v				18.2	1283.810	1283.91	23.4	
Ni v	216590.5	294443.3	$2.73 \times 10^{-1}$		1284.475			
Ni v	253905.2	331678.2	$3.87 \times 10^{-1}$		1285.793			
				9.8		1286.64		unid.
Ni v	232545.9	310212.6	$1.60 \times 10^{-1}$		1287.553			
Ni v	268273.9	345936.1	$3.03 \times 10^{-1}$		1287.628			
Ni v	216434.7	294086	$2.41 \times 10^{-1}$		1287.808			
				6.0		1288.22		unid.
				9.1		1288.37		unid.
Zn iv	132777	210187	$2.44 \times 10^{-1}$		1291.826			newly identified
				6.6		1292.01		unid.
				5.6		1292.19		unid.

Table A.3. Continued.

Ion	Levels		$f$	$W_\lambda /$ mÅ	Wavelength/Å		$v_{\text{rad}} /$ km/s	Comment
	Lower	Upper			Theoretical	Observed		
Zn iv	130366	207737	$1.11 \times 10^{-1}$		1292.476			newly identified
Sn v				25.8	1294.360	1294.45	20.8	
Ni v	212095.8	289298	$1.20 \times 10^{-1}$		1295.300			
Zn v	221631	298801	$1.03 \times 10^{-1}$		1295.850			newly identified
						1296.10		unid.
Ni v	212095.8	289247.1	$4.28 \times 10^{-2}$		1296.154			blend with C iii
Ni v	242504.3	319652.7	$8.59 \times 10^{-2}$		1296.203			blend with C iii
C iii	3d $^3D_2$	5f $^3F_3^0$	$2.04 \times 10^{-1}$		1296.322			
C iii	3d $^3D_1$	5f $^3F_2^0$	$2.29 \times 10^{-1}$		1296.327			
C iii	3d $^3D_3$	5f $^3F_4^0$	$2.10 \times 10^{-1}$		1296.333			
C iii	3d $^3D_2$	5f $^3F_2^0$	$2.59 \times 10^{-2}$		1296.345			
C iii	3d $^3D_3$	5f $^3F_3^0$	$1.85 \times 10^{-2}$		1296.369			
C iii	3d $^3D_3$	5f $^3F_2^0$	$4.21 \times 10^{-4}$		1296.392			
Zn iv	131805	208921	$1.67 \times 10^{-1}$		1296.734			newly identified
Ni v	242862.6	319860.4	$1.61 \times 10^{-1}$		1298.738			
Xe vi	5p $^2P_{3/2}^0$	5p $^4P_{1/2}$			1298.921			
Ga iv	153086	230040	$3.26 \times 10^{-1}$		1299.476			newly identified
Ni v	178019.8	254885	$1.79 \times 10^{-1}$		1300.979			
Zn iv	148180	225033	$3.10 \times 10^{-1}$		1301.189			newly identified
O i					1302.167			ISM multi-component
Ni v	242862.6	319652.7	$5.50 \times 10^{-2}$		1302.251			
Ni v	212095.8	288877.9	$7.57 \times 10^{-2}$		1302.387			
Zn v	222042	298801	$8.34 \times 10^{-2}$		1302.786			newly identified
Ni v	235736.5	312463.3	$2.32 \times 10^{-1}$	2.2	1303.326	1303.43	23.9	
Ga iv	150967	227681	$3.17 \times 10^{-1}$	5.4	1303.540	1303.66	27.6	newly identified
Zr v	378753	455444	$9.01 \times 10^{-1}$	16.1	1303.933	1304.05	26.9	
Ni v	247165	323853.1	$7.66 \times 10^{-2}$		1303.983			
				7.1		1304.19		unid.
				27.2		1304.44		unid.
Ni v	229408.8	306049	$4.36 \times 10^{-2}$		1304.798			
Ni v	229413	306049	$1.78 \times 10^{-1}$		1304.870			
Ni v	212253.4	288877.9	$1.26 \times 10^{-1}$		1305.066			
Ni v	229408.8	305996.3	$1.66 \times 10^{-1}$		1305.696			
Ni v	243370.5	319926.5	$1.30 \times 10^{-3}$		1306.233			
Ni v	229440.6	305996.3	$1.24 \times 10^{-1}$		1306.238			
Ni v	208046.4	284579.5	$2.83 \times 10^{-1}$		1306.624			blend with Zn iv, blend with Zr v
Zn iv	128730	205261	$3.80 \times 10^{-1}$		1306.657			blend with Ni v, blend with Zr v, newly identified
Zr v	395995	472520	1.00	16.1	1306.762			blend with Ni v, blend with Zn iv
Ni v	178019.8	254495.6	$2.94 \times 10^{-1}$	8.1	1307.603	1307.71	24.5	



Table A.3. Continued.

Ion	Levels		$f$	$W_\lambda /$ mÅ	Wavelength/Å		$v_{\text{rad}} /$ km/s	Comment
	Lower	Upper			Theoretical	Observed		
Ni v	225200.7	300918.1	$3.27 \times 10^{-1}$		1320.700			blend with Zn iv
Zn iv	128730	204447	$1.10 \times 10^{-1}$		1320.704			blend with Ni v, newly identified
Ni v	212253.4	287960	$4.38 \times 10^{-2}$		1320.889			blend with Zn iv
Zn iv	138479	214167	$2.77 \times 10^{-1}$	9.7 7.1	1321.215	1321.32 1322.25	23.8	blend with Ni v, newly identified unid.
Zn iv	130366	205991	$1.37 \times 10^{-1}$		1322.316			newly identified
Zn iv	135951	211570	$1.98 \times 10^{-1}$		1322.428			newly identified
Ni v	236454.1	312008.3	$9.08 \times 10^{-2}$	7.6	1323.553	1323.66	24.2	
Ni v	241773.6	317327.3	$1.52 \times 10^{-1}$	7.6	1323.562	1323.66	22.2	
Zr v	382985	458524	$7.96 \times 10^{-1}$	18.8	1323.826	1323.94	25.8	
Ni v	217101	292631	$3.50 \times 10^{-1}$		1323.977			
Zn v	208715	284116	$9.90 \times 10^{-3}$		1326.253			newly identified
Zn iv	131805	207175	$1.08 \times 10^{-1}$		1326.774			newly identified
N iv	2s3d $^3D_1$	2p( $^2P^o$ )3d $^3F_2^o$	$1.46 \times 10^{-2}$	12.8	1326.957	1327.08	27.8	uncertain
Zn iv	135951	211190	$1.11 \times 10^{-1}$		1329.110			newly identified
Ni v	217129.1	292353.4	$3.28 \times 10^{-1}$		1329.358			
Zn v	208715	283933	$4.42 \times 10^{-3}$		1329.471			newly identified
Zn iv	160919	236109	$2.17 \times 10^{-1}$		1329.959			newly identified
Zn iv	157075	232246	$2.56 \times 10^{-1}$		1330.302			newly identified
Zr v	327617	402688	$6.65 \times 10^{-2}$		1332.065			
Zn iv	157930	232938	$5.48 \times 10^{-1}$		1333.180			newly identified
Zn iv	138479	213480	$1.59 \times 10^{-1}$	13.3	1333.326	1333.45	27.9	newly identified
Ni v	233839.2	308804.1	$1.31 \times 10^{-1}$		1333.958			
Ni v	241773.6	316726.6	$1.38 \times 10^{-1}$		1334.169			
Ni v	225616.5	300563.3	$4.14 \times 10^{-2}$		1334.280			
C II					1334.532			ISM multi-component
Ni v	241082.2	315990.5	$1.60 \times 10^{-1}$		1334.966			
				22.8		1335.83		unid.
Ni v	217048.7	291891.4	$3.25 \times 10^{-1}$	14.1	1336.136	1336.28	32.3	
Ga iv	149512	224243	$2.02 \times 10^{-1}$	9.0	1338.129	1338.25	27.1	newly identified
O iv	2s2p $^2$ $^2P_{1/2}$	2p $^3$ $^2D_{3/2}^o$	$1.17 \times 10^{-1}$	91.9 11.3	1338.615	1338.75 1339.18	30.2	unid.
Zn iv	157075	231693	$3.70 \times 10^{-1}$		1340.156			newly identified
Ni v	225616.5	300224.9	$1.26 \times 10^{-1}$		1340.332			
Ni v	216189.9	290757	$8.26 \times 10^{-2}$		1341.074			
Zn v	241829	316339	$1.10 \times 10^{-2}$		1342.104			newly identified
Ni v	217048.7	291554.6	$2.03 \times 10^{-1}$		1342.176			
O iv	2s2p $^2$ $^2P_{3/2}$	2p $^3$ $^2D_{3/2}^o$	$1.16 \times 10^{-2}$	54.9	1342.990	1343.12	29.0	
O iv	2s2p $^2$ $^2P_{3/2}$	2p $^3$ $^2D_{5/2}^o$	$1.04 \times 10^{-1}$	106.7	1343.514	1343.65	30.4	
Zn iv	149191	223609	$3.61 \times 10^{-1}$		1343.750			newly identified

Table A.3. Continued.

Ion	Levels		$f$	$W_\lambda /$ mÅ	Wavelength / Å		$v_{\text{rad}} /$ km/s	Comment
	Lower	Upper			Theoretical	Observed		
Ni v	240959.6	315370.1	$1.30 \times 10^{-1}$		1343.896			
Zn iv	132777	207175	$2.94 \times 10^{-1}$		1344.122			newly identified
Zn v	240446	314838	$4.45 \times 10^{-2}$		1344.241			newly identified
O iii	3p $^3P_2$	3p $^3D_3^o$	$7.89 \times 10^{-2}$		1344.943			
O iii	3p $^3P_1$	3p $^3D_2^o$	$7.05 \times 10^{-2}$		1344.962			
				14.4		1345.78		unid.
				16.0		1346.26		unid.
Ni v	217129.1	291328.5	$1.82 \times 10^{-1}$		1347.720			
C iii	3p $^1P_1^o$	3p' $^1D_2$	$3.03 \times 10^{-2}$	16.7	1347.947	1348.07	27.4	blend with Zn iv
Zn iv	131805	205991	$2.15 \times 10^{-1}$	16.7	1347.954	1348.07	25.8	blend with C iii, newly identified
Zn iv	130366	204447	$1.98 \times 10^{-1}$	7.9	1349.876	1350.00	27.5	newly identified
Ni v	216189.9	290262	$6.02 \times 10^{-2}$		1350.036			
C iv	4d $^2D_{3/2}$	4f $^2F_{5/2}^o$	$7.22 \times 10^{-2}$		1351.214			
C iv	4d $^2D_{5/2}$	4f $^2F_{5/2}^o$	$3.44 \times 10^{-3}$		1351.287			
C iv	4d $^2D_{5/2}$	4f $^2F_{7/2}^o$	$6.88 \times 10^{-2}$		1351.292			
C iv	4f $^2F_{7/2}^o$	7g $^2G_{9/2}$	$5.65 \times 10^{-2}$		1352.975			
C iv	4f $^2F_{7/2}^o$	7g $^2G_{7/2}$	$1.64 \times 10^{-3}$		1352.975			
C iv	4f $^2F_{5/2}^o$	7g $^2G_{7/2}$	$5.81 \times 10^{-2}$		1352.975			
C iv	4f $^2F_{5/2}^o$	7d $^2D_{3/2}$	$5.37 \times 10^{-4}$		1353.427			
C iv	4f $^2F_{7/2}^o$	7d $^2D_{5/2}$	$5.75 \times 10^{-4}$		1353.433			
C iv	4f $^2F_{5/2}^o$	7d $^2D_{5/2}$	$3.85 \times 10^{-5}$		1353.433			
Zr v	402688	476677	1.05		1355.216			
				9.7		1355.74		unid.
Zr v	328941	402688	$4.39 \times 10^{-2}$		1355.975			
Zn iv	160886	234623	$3.72 \times 10^{-1}$		1356.171			newly identified
				7.4		1357.45		unid.
Zn iv	131805	205453	$1.79 \times 10^{-1}$	23.0	1357.801	1357.92	26.3	newly identified
Zn iv	148180	221737	$2.35 \times 10^{-1}$	11.2	1359.477	1359.61	29.3	newly identified
Zn iv	138479	211824	$1.39 \times 10^{-1}$		1363.432			newly identified
Zn iv	130366	203685	$2.01 \times 10^{-1}$	12.7	1363.912	1364.06	32.5	newly identified
				3.9		1364.33		unid.
						1364.65		unid.
				9.7		1364.97		unid.
Zn iv	148180	221426	$1.18 \times 10^{-1}$	11.7	1365.253	1365.38	27.9	newly identified
Zn iv	135951	208970	$3.07 \times 10^{-1}$	9.3	1369.510	1369.63	26.3	newly identified
				15.3		1370.26		unid.
				2.5		1370.61		unid.
O v	2s2p $^1P_1^o$	2p $^2$ $^1D_2$	$1.57 \times 10^{-1}$	90.9	1371.294	1371.43	29.7	
Sr v				8.3	1372.838	1372.96	26.6	

Table A.3. Continued.

Ion	Levels		$f$	$W_\lambda /$ mÅ	Wavelength / Å		$v_{\text{rad}} /$ km/s	Comment
	Lower	Upper			Theoretical	Observed		
Zn iv	138479	211190	$2.47 \times 10^{-1}$		1375.325			newly identified
				5.3		1376.45		unid.
Zr v	382985	455631	$3.17 \times 10^{-1}$		1376.544			unid.
				6.3		1376.79		unid.
Zn iv	128730	201319	$2.29 \times 10^{-1}$	15.7	1377.615	1377.75	29.4	newly identified
				9.8		1379.19		unid.
C iii	3d $^1D_2$	5f $^1F_3$	$3.46 \times 10^{-1}$	37.7	1381.652	1381.76	23.4	
Kr v	211336.57	283559	$5.14 \times 10^{-2}$	10.6	1384.611	1384.72	23.6	
Zn iv	160919	232981	$3.61 \times 10^{-1}$		1387.694			newly identified
Kr v	213932.87	285981	$7.46 \times 10^{-2}$	7.5	1387.961	1388.07	23.5	
				14.1		1390.73		unid.
				14.2		1390.94		unid.
Ni v	221087.6	292983	$1.41 \times 10^{-1}$		1390.910			
Kr v	216874.54	288683	$4.28 \times 10^{-2}$		1392.594	1392.77	38.3	
Kr v	219381.57	291138	$9.66 \times 10^{-2}$		1393.603			
Si iv	3s $^2S_{1/2}$	3p $^2P_{3/2}$	$5.13 \times 10^{-1}$	82.1	1393.755	1393.87	24.7	
				12.8		1395.98		unid.
						1396.48		unid.
Kr v	219823.27	291138	$2.40 \times 10^{-2}$	8.0	1402.235	1402.32	18.2	newly identified
				14.5		1402.53		unid.
Si iv	3s $^2S_{1/2}$	3p $^2P_{1/2}$	$2.55 \times 10^{-1}$	62.4	1402.770	1402.90	27.8	
				13.0		1408.56		unid.
				13.9		1409.60		unid.
				17.4		1413.09		unid.
				7.0		1413.31		unid.
Sr v				12.8	1413.882	1414.02	29.3	
						1423.36		unid.
						1423.48		unid.
				9.9		1424.44		unid.
				7.0		1424.95		unid.
C iii	3d $^3D_1$	3d' $^3P_0^o$	$3.40 \times 10^{-2}$		1425.903			
C iii	3d $^3D_1$	3d' $^3P_1^o$	$3.56 \times 10^{-2}$		1426.194			
C iii	3d $^3D_2$	3d' $^3P_1^o$	$4.60 \times 10^{-2}$		1426.216			
C iii	2s3s $^3S_1$	2p( $^2P^o$ )3s $^3P_1^o$	$1.62 \times 10^{-1}$	27.0	1426.446	1426.58	28.2	
C iii	3d $^3D_1$	3d' $^3P_2^o$	$1.03 \times 10^{-3}$		1426.716			
C iii	3d $^3D_2$	3d' $^3P_2^o$	$1.10 \times 10^{-2}$		1426.739			
C iii	3d $^3D_3$	3d' $^3P_2^o$	$4.77 \times 10^{-2}$		1426.796			
Mo vi	316477	386552	$7.53 \times 10^{-4}$	7.6	1427.030	1427.15	25.2	
C iii	2s3s $^3S_1$	2p( $^2P^o$ )3s $^3P_1^o$	$9.78 \times 10^{-2}$	39.5	1427.839	1427.97	27.5	
C iii	3p $^3P_1^o$	3p' $^3P_2$	$4.56 \times 10^{-2}$		1427.911			

Table A.3. Continued.

Ion	Levels		$f$	$W_\lambda /$ mÅ	Wavelength / Å		$v_{\text{rad}} /$ km/s	Comment
	Lower	Upper			Theoretical	Observed		
C III	3p $^3P_2^o$	3p' $^3P_2$	$8.22 \times 10^{-2}$	23.8	1428.178	1428.31	27.7	
C III	2s3s $^3S_1$	2p( $^2P^o$ )3s $^3P_0^o$	$3.26 \times 10^{-2}$		1428.498			
C III	3p $^3P_0^o$	3p' $^3P_1$	$1.10 \times 10^{-1}$		1428.553			
C III	3p $^3P_1^o$	3p' $^3P_1$	$2.74 \times 10^{-2}$		1428.668			
C III	3p $^3P_2^o$	3p' $^3P_1$	$2.74 \times 10^{-2}$		1428.935			
C III	3p $^3P_1^o$	3p' $^3P_0$	$3.66 \times 10^{-2}$		1429.099			
				22.2		1431.72		unid.
Sn IV	5s $^2S_{1/2}$	5p $^2P_{1/2}^o$	$3.00 \times 10^{-1}$	15.1	1437.525	1437.64	24.0	
Kr V	213932.87	283439.05	$1.10 \times 10^{-2}$	8.0	1438.722	1438.83	22.5	newly identified
C IV	4s $^2S_{1/2}$	6p $^2P_{3/2}^o$	$4.70 \times 10^{-2}$		1440.283			
C IV	4s $^2S_{1/2}$	6p $^2P_{1/2}^o$	$2.35 \times 10^{-2}$		1440.364			
				7.7		1447.25		unid.
						1451.78		unid.
						1454.45		unid.
Ba VII	173154	241412	$1.46 \times 10^{-2}$		1465.045			newly identified
						1475.13		unid.
						1475.29		unid.
						1475.41		unid.
						1475.50		unid.
						1477.59		unid.
C III	3d $^3D_2$	3d' $^3D_3^o$	$1.92 \times 10^{-2}$		1477.626			
C III	3d $^3D_3$	3d' $^3D_3^o$	$1.10 \times 10^{-1}$	32.2	1477.688	1477.810	24.8	
Ba VII	156151	223820	$1.72 \times 10^{-2}$		1477.775			newly identified
C III	3d $^3D_1$	3d' $^3D_2^o$	$3.09 \times 10^{-2}$		1478.021			
C III	3d $^3D_2$	3d' $^3D_2^o$	$8.56 \times 10^{-2}$	38.7	1478.045	1478.170	25.4	
C III	3d $^3D_3$	3d' $^3D_2^o$	$1.37 \times 10^{-2}$		1478.106			
C III	3d $^3D_1$	3d' $^3D_1^o$	$9.25 \times 10^{-2}$		1478.303			
C III	3d $^3D_2$	3d' $^3D_1^o$	$1.86 \times 10^{-2}$		1478.327			
Mo VI	119726	187331	$6.15 \times 10^{-1}$	38.8	1479.168	1479.30	26.8	
				15.6		1479.49		unid.
				21.8		1485.53		unid.
Ge IV	4d $^2D_{3/2}$	4f $^2F_{5/2}^o$			1494.889	1494.97	16.2	
C III	3d $^1D_2$	5p $^1P_1^o$	$2.98 \times 10^{-2}$		1497.563			
Ge IV	4d $^2D_{5/2}$	4f $^2F_{5/2}^o$			1500.519			newly identified
Ge IV	4d $^2D_{5/2}$	4f $^2F_{7/2}^o$			1500.609			newly identified
S V	3p $^1P^o$	3p $^2$ $^1D$	$1.04 \times 10^{-1}$	45.0	1501.799	1501.92	24.2	
				78.5		1511.07		unid.
Zr VI	393555	459581	$2.70 \times 10^{-1}$		1514.568			
Kr V	278928	344908	$8.37 \times 10^{-1}$		1515.611			
Zr VI	369712	435428	$1.99 \times 10^{-1}$		1521.699			



Table A.3. Continued.

Ion	Levels		$f$	$W_\lambda /$ mÅ	Wavelength / Å		$v_{\text{rad}} /$ km/s	Comment
	Lower	Upper			Theoretical	Observed		
Ba VII	178316	243933	$1.07 \times 10^{-2}$		1524.009			newly identified
				21.4		1526.05		unid.
Si II					1526.707			ISM multi-component
C III	3p $^1P_1^o$	4d $^1D_2$	$2.03 \times 10^{-1}$	23.4	1531.835	1531.97	26.4	
				22.9		1536.23		unid.
C III	3d $^1D_2$	3d' $^1F_3^o$	$6.86 \times 10^{-2}$	56.6	1541.115	1541.26	28.2	
C IV	2s $^2S_{1/2}$	2p $^2P_{3/2}^o$	$1.90 \times 10^{-1}$	245.9	1548.203	1548.33	24.6	
C IV	2s $^2S_{1/2}$	2p $^2P_{1/2}^o$	$9.52 \times 10^{-2}$	217.7	1550.772	1550.90	24.8	
						1561.93		unid.
						1563.99		unid.
Kr V	288683	352537	$6.65 \times 10^{-1}$		1566.073			
				27.1		1567.70		unid.
C III	3d $^3D_3$	3d' $^3F_4^o$	$2.28 \times 10^{-1}$	36.5	1576.479	1576.61	24.9	
C III	3p $^3P_2^o$	3p' $^3D_3$	$1.07 \times 10^{-2}$		1576.888			
C III	3d $^3D_2$	3d' $^3F_3^o$	$2.21 \times 10^{-1}$		1577.297			
C III	3d $^3D_3$	3d' $^3F_3^o$	$2.01 \times 10^{-1}$		1577.366			
C III	3p $^3P_1^o$	3p' $^3D_2$	$9.58 \times 10^{-1}$		1577.532			
C III	3p $^3P_2^o$	3p' $^3D_2$	$1.92 \times 10^{-3}$		1577.858			
C III	3d $^3D_1$	3d' $^3F_2^o$	$2.49 \times 10^{-1}$		1577.880			
C III	3d $^3D_2$	3d' $^3F_2^o$	$2.81 \times 10^{-2}$		1577.907			
C III	3d $^3D_3$	3d' $^3F_2^o$	$4.56 \times 10^{-4}$		1577.977			
C III	3p $^3P_0^o$	3p' $^3D_1$	$1.28 \times 10^{-2}$		1578.001			
C III	3p $^3P_1^o$	3p' $^3D_1$	$3.20 \times 10^{-3}$		1578.142			
Ba VII	178140	241412	$4.22 \times 10^{-3}$		1580.480			newly identified
Ba VII	156256	219528	$2.05 \times 10^{-3}$		1580.483			newly identified
						1582.54		unid.
Kr V	291138	354291	$3.56 \times 10^{-1}$		1583.456			
C IV	4p $^2P_{1/2}^o$	6d $^2D_{3/2}$	$1.36 \times 10^{-1}$		1585.811			
C IV	4p $^2P_{3/2}^o$	6d $^2D_{5/2}$	$1.22 \times 10^{-1}$		1586.111			
C IV	4p $^2P_{3/2}^o$	6d $^2D_{3/2}$	$1.35 \times 10^{-2}$		1586.141			
Mo V	94835	157851	$1.46 \times 10^{-1}$		1586.898			
Kr V	283677	346599	$9.57 \times 10^{-1}$		1589.269			
Mo V	99380	162257	$1.66 \times 10^{-1}$		1590.414			
C III	3s $^1S_0$	3s' $^1P_1^o$	$6.85 \times 10^{-1}$	37.5	1591.443	1591.59	27.7	
Zr VI	364827	427649	$4.28 \times 10^{-1}$		1591.799			
Kr V	291138	353957	$6.18 \times 10^{-1}$		1591.875			
Mo VI	119726	182404	$2.81 \times 10^{-1}$	27.3	1595.435	1595.58	27.2	
Zr IV	84461	147002	$9.73 \times 10^{-1}$		1598.948			
						1600.88		unid.
						1610.42		unid.

Table A.3. Continued.

Ion	Levels		$f$	$W_\lambda /$ mÅ	Wavelength / Å		$v_{\text{rad}} /$ km/s	Comment
	Lower	Upper			Theoretical	Observed		
						1610.70		unid.
						1616.99		unid.
C III	3p $^3P_2^o$	4d $^3D_3$	$4.57 \times 10^{-1}$	46.1	1620.069	1620.18	20.5	
C III	3p $^3P_1^o$	4d $^3D_2$	$4.03 \times 10^{-1}$	19.9	1620.338	1620.46	22.6	
C III	3p $^3P_0^o$	4d $^3D_1$	$5.44 \times 10^{-1}$		1620.594			
C III	3p $^3P_2^o$	4d $^3D_2$	$8.18 \times 10^{-2}$		1620.681			
C III	3p $^3P_1^o$	4d $^3D_1$	$1.36 \times 10^{-1}$		1620.743			
C III	3p $^3P_2^o$	4d $^3D_1$	$5.49 \times 10^{-3}$		1621.087			
Zr V	327617	388853	$1.21 \times 10^{-1}$		1633.027			
C IV	4d $^2D_{3/5}$	6f $^2F_{5/2}^o$	$1.86 \times 10^{-1}$		1637.543			
C IV	4d $^2D_{5/2}$	6f $^2F_{5/2}^o$	$8.85 \times 10^{-3}$		1637.650			
C IV	4d $^2D_{5/2}$	6f $^2F_{7/2}^o$	$1.77 \times 10^{-1}$		1637.650			
He II	2	3	$6.41 \times 10^{-1}$	254.3	1640.377	1640.54	29.8	
Mo V	99380	159857	$3.81 \times 10^{-1}$		1653.541			
C IV	4p $^2P_{1/2}^o$	6s $^2S_{1/2}$	$2.46 \times 10^{-2}$		1653.633			
C IV	4p $^2P_{3/2}^o$	6s $^2S_{1/2}$	$2.46 \times 10^{-2}$		1653.992			
C IV	4d $^2D_{3/2}$	6p $^2P_{3/2}^o$	$1.35 \times 10^{-3}$		1654.457			
C IV	4d $^2D_{3/2}$	6p $^2P_{1/2}^o$	$6.75 \times 10^{-3}$		1654.564			
C IV	4d $^2D_{5/2}$	6p $^2P_{3/2}^o$	$8.10 \times 10^{-3}$		1654.566			
				29.5		1659.43		unid.
Mo V	94835	155032	$3.93 \times 10^{-1}$		1661.215	1661.37	28.0	
Xe VI	5p <sup>2</sup> $^2D_{3/2}$	4f $^2F_{5/2}^o$			1663.116			newly identified
Xe VI	5d' $^2F_{5/2}^o$	5g $^2G_{7/2}$	$3.02 \times 10^{-1}$		1663.146			newly identified
				58.4		1667.83		unid.
Mo V	93111	153040	$2.83 \times 10^{-1}$		1668.662			
				30.4		1669.99		unid.
						1673.23		unid.
Zr VI	393555	453000	$4.00 \times 10^{-1}$		1682.241			
N IV	2s2p $^1P_1^o$	2p <sup>2</sup> $^1D_2$	$1.71 \times 10^{-1}$	106.7	1718.550	1718.69	24.4	
Zr V	325015	382985	$2.14 \times 10^{-1}$		1725.024			uncertain
Zr VI	364827	421991	$2.77 \times 10^{-1}$	79.8	1749.350	1749.50	26.7	uncertain
						1751.72		unid.
						1752.87		unid.
						1757.05		unid.
				138.8		1757.86		unid.
				37.6		1760.23		unid.
						1761.20		unid.
Kr V	250993	307667	$2.31 \times 10^{-1}$		1764.478			
				27.0		1767.98		unid.

Table A.3. Continued.

Ion	Levels		$f$	$W_\lambda /$ mÅ	Wavelength / Å		$v_{\text{rad}} /$ km/s	Comment		
	Lower	Upper			Theoretical	Observed				
Ba VII	157675	213712	$2.22 \times 10^{-2}$		1784.535			newly identified		
						49.4	1796.62		unid.	
						34.9	1803.15		unid.	
							1807.71		unid.	
						33.0	1808.36		unid.	
Ba VII	152397	206668	$1.50 \times 10^{-2}$		1842.595			newly identified		
							1849.26		unid.	
							1851.95		unid.	
							1855.49		unid.	
						27.3	1855.77		unid.	
Xe VI	$5p^2 \ ^2D_{5/2}$	$5d \ ^2D_{5/2}$			1884.016			newly identified		
						23.6	1885.53		unid.	
						10.2	1888.08		unid.	
C III	$2s3p \ ^1P_1^o$	$2s4s \ ^1S_0$	$9.68 \times 10^{-2}$		1894.290					
						30.9	1901.53		unid.	
						16.3	1901.77		unid.	
						25.6	1901.97		unid.	
						37.5	1902.29		unid.	
C III	$3d \ ^3D_3$	$4f \ ^3F_4^o$	$5.77 \times 10^{-1}$		1922.957					
C III	$3d \ ^3D_2$	$4f \ ^3F_3^o$	$5.58 \times 10^{-1}$		1923.164					
C III	$3d \ ^3D_3$	$4f \ ^3F_3^o$	$5.08 \times 10^{-2}$		1923.268					
C III	$3d \ ^3D_1$	$4f \ ^3F_2^o$	$6.29 \times 10^{-1}$		1923.341					
C III	$3d \ ^3D_2$	$4f \ ^3F_2^o$	$7.11 \times 10^{-2}$		1923.382					
C III	$3d \ ^3D_3$	$4f \ ^3F_2^o$	$1.15 \times 10^{-3}$		1923.486					
Kr VI	275380	326657	$6.59 \times 10^{-1}$		19.3		1937.28	unid.		
						93.3	1950.192		newly identified	
						20.3	1957.24		unid.	
						37.7	1967.57		unid.	
C III	$3p \ ^3P_0^o$	$4s \ ^3S_1$	$1.39 \times 10^{-1}$			2009.985				
							2010.214			
						45.0	2010.743	2010.91	24.9	
						15.9		2011.39		unid.
						17.9		2011.83		unid.
						12.7		2012.15		unid.
								2029.38		unid.
						19.9		2051.02		unid.
						38.8		2051.89		unid.
						23.3		2066.42		unid.

Table A.3. Continued.

Ion	Levels		$f$	$W_\lambda /$ mÅ	Wavelength / Å		$v_{\text{rad}} /$ km/s	Comment
	Lower	Upper			Theoretical	Observed		
C III	3d $^3D_1$	4p $^3P_2^0$	$7.22 \times 10^{-4}$		2092.467			
C III	3d $^3D_2$	4p $^3P_2^0$	$7.69 \times 10^{-3}$		2092.516			
C III	3d $^3D_3$	4p $^3P_2^0$	$3.34 \times 10^{-2}$		2092.639			
C III	3d $^3D_1$	4p $^3P_1^0$	$1.80 \times 10^{-2}$		2092.677			
C III	3d $^3D_2$	4p $^3P_1^0$	$3.23 \times 10^{-2}$		2092.725			
C III	3d $^3D_1$	4p $^3P_0^0$	$2.39 \times 10^{-2}$		2092.776			
				27.3		2098.66		unid.
C IV	4s $^2S_{1/2}$	5p $^2P_{3/2}^0$	$1.43 \times 10^{-1}$		2104.607			
C IV	4s $^2S_{1/2}$	5p $^2P_{1/2}^0$	$7.14 \times 10^{-2}$		2104.922			
Xe VI	6s $^2S_{1/2}$	6p $^2P_{3/2}^0$	$7.40 \times 10^{-1}$		2135.479			newly identified
						2146.69		unid.
C III	3d $^1D_2$	4f $^1F_3^0$	$7.96 \times 10^{-1}$	76.5	2163.605	2163.84	32.6	
				8.3		2212.24		unid.
				5.9		2212.49		unid.
				5.5		2212.92		unid.
				19.1		2240.01		unid.
C III	2p $^1P_1^0$	2p <sup>2</sup> $^1D_2$	$1.80 \times 10^{-1}$	109.9	2297.578	2297.78	26.4	
				21.5		2314.97		unid.
C IV	5d $^2D_{3/2}$	8f $^2F_{5/2}^0$	$8.12 \times 10^{-2}$		2333.504			
C IV	5d $^2D_{5/2}$	8f $^2F_{5/2}^0$	$3.87 \times 10^{-3}$		2333.597			
C IV	5d $^2D_{5/2}$	8f $^2F_{7/2}^0$	$7.73 \times 10^{-2}$		2333.597			
C IV	5f $^2F_{7/2}^0$	8g $^2G_{7/2}$	$2.39 \times 10^{-3}$		2336.247			
C IV	5f $^2F_{7/2}^0$	8g $^2G_{9/2}$	$8.23 \times 10^{-2}$		2336.247			
C IV	5f $^2F_{5/2}^0$	8g $^2G_{7/2}$	$8.46 \times 10^{-2}$		2336.247			
C IV	5g $^2G_{7/2}$	8h $^2H_{9/2}^0$	$5.98 \times 10^{-2}$		2336.700			
C IV	5g $^2G_{9/2}$	8h $^2H_{9/2}^0$	$1.12 \times 10^{-3}$		2336.700			
C IV	5g $^2G_{9/2}$	8h $^2H_{11/2}^0$	$5.87 \times 10^{-2}$		2336.700			
C IV	5p $^2P_{1/2}^0$	8s $^2S_{1/2}$	$1.32 \times 10^{-2}$		2336.722			
C IV	5g $^2G_{7/2}$	8f $^2F_{5/2}^0$	$3.77 \times 10^{-4}$		2336.787			
C IV	5g $^2G_{7/2}$	8f $^2F_{7/2}^0$	$1.42 \times 10^{-5}$		2336.787			
C IV	5g $^2G_{9/2}$	8f $^2F_{7/2}^0$	$3.91 \times 10^{-4}$		2336.787			
C IV	5f $^2F_{5/2}^0$	8d $^2D_{5/2}$	$1.11 \times 10^{-4}$		2337.066			
C IV	5f $^2F_{5/2}^0$	8d $^2D_{3/2}$	$1.56 \times 10^{-3}$		2337.066			
C IV	5f $^2F_{7/2}^0$	8d $^2D_{5/2}$	$1.67 \times 10^{-3}$		2337.066			
C IV	5p $^2P_{3/2}^0$	8s $^2S_{1/2}$	$1.32 \times 10^{-2}$		2337.109			
				46.5		2344.31		unid.
				73.5		2382.82		unid.
He II	3	8	$1.60 \times 10^{-2}$		2386.221			

Table A.3. Continued.

Ion	Levels		$f$	$W_\lambda /$ mÅ	Wavelength / Å		$v_{\text{rad}} /$ km/s	Comment
	Lower	Upper			Theoretical	Observed		
C IV	4p $^2P^o_{1/2}$	5d $^2D_{3/2}$	$5.23 \times 10^{-1}$		2405.170			
C IV	4p $^2P^o_{3/2}$	5d $^2D_{5/2}$	$4.61 \times 10^{-1}$		2405.830			
C IV	4p $^2P^o_{3/2}$	5d $^2D_{3/2}$	$5.12 \times 10^{-2}$		2405.928			
O IV	4f $^2F^o_{5/2}$	5g $^2G_{7/2}$	1.20		2450.116			
O IV	4f $^2F^o_{7/2}$	5g $^2G_{7/2}$	$3.38 \times 10^{-2}$		2450.782			
O IV	4f $^2F^o_{7/2}$	5g $^2G_{9/2}$	1.17		2450.782			
				17.6		2460.82		unid. newly identified
Ge IV	5p $^2P^o_{3/2}$	5d $^2D_{5/2}$			2488.691			
He II	3	7	$2.77 \times 10^{-2}$		2512.059			
						2524.41		unid.
						2524.72		unid.
C IV	4d $^2D_{3/2}$	5f $^2F^o_{5/2}$	$8.86 \times 10^{-1}$		2525.017			
C IV	4d $^2D_{5/2}$	5f $^2F^o_{5/2}$	$4.22 \times 10^{-2}$		2525.272			
C IV	4d $^2D_{5/2}$	5f $^2F^o_{7/2}$	$8.44 \times 10^{-1}$		2525.272			
C IV	4f $^2F^o_{7/2}$	5g $^2G_{9/2}$	1.30		2530.736			
C IV	4f $^2F^o_{7/2}$	5g $^2G_{7/2}$	$3.78 \times 10^{-2}$		2530.736			
C IV	4f $^2F^o_{5/2}$	5g $^2G_{7/2}$	1.34		2530.736			
C IV	4f $^2F^o_{7/2}$	5d $^2D_{5/2}$	$9.08 \times 10^{-3}$		2534.488			
C IV	4f $^2F^o_{5/2}$	5d $^2D_{5/2}$	$6.05 \times 10^{-4}$		2534.488			
C IV	4f $^2F^o_{5/2}$	5d $^2D_{3/2}$	$8.47 \times 10^{-3}$		2534.597			
				6.7		2586.31		unid.
						2586.65		unid.
						2586.83		unid.
				18.4		2595.53		unid.
C IV	4d $^2D_{3/2}$	5p $^2P_{3/2}$	$6.74 \times 10^{-3}$		2595.596			
C IV	4d $^2D_{5/2}$	5p $^2P_{3/2}$	$4.06 \times 10^{-2}$		2595.865			
C IV	4d $^2D_{3/2}$	5p $^2P_{1/2}$	$3.38 \times 10^{-2}$		2596.074			
				23.6		2597.57		unid.
				33.0		2598.08		unid.
				45.4		2599.11		unid.
				44.3		2599.80		unid.
				67.1		2600.27		unid.
C IV	4p $^2P^o_{1/2}$	5s $^2S_{1/2}$	$1.28 \times 10^{-1}$		2698.516			
C IV	4p $^2P^o_{3/2}$	5s $^2S_{1/2}$	$1.28 \times 10^{-1}$		2699.471			
He II	3	6	$5.59 \times 10^{-2}$		2734.220			
Mg II					2796.352			ISM multi-component
Mg II					2803.531			ISM multi-component
C IV	5p $^2P^o_{1/2}$	7d $^2D_{3/2}$	$1.40 \times 10^{-1}$		2819.687			

Table A.3. Continued.

Ion	Levels		$f$	$W_\lambda /$ mÅ	Wavelength / Å		$v_{\text{rad}} /$ km/s	Comment
	Lower	Upper			Theoretical	Observed		
C iv	5p $^2P_{3/2}^o$	7d $^2D_{3/2}$	$1.40 \times 10^{-2}$		2820.251			
C iv	5p $^2P_{3/2}^o$	7d $^2D_{5/2}$	$1.26 \times 10^{-1}$		2820.278			
O iv	3s $^4P_{5/2}^o$	3p $^4S_{3/2}$	$6.83 \times 10^{-2}$		2837.105			
				54.5		2881.55		unid.
C iv	5d $^2D_{3/2}$	7f $^2F_{5/2}^o$	$1.96 \times 10^{-1}$		2902.303			
C iv	5d $^2D_{5/2}$	7f $^2F_{5/2}^o$	$9.34 \times 10^{-3}$		2902.446			
C iv	5d $^2D_{5/2}$	7f $^2F_{7/2}^o$	$1.87 \times 10^{-1}$		2902.466			
C iv	5f $^2F_{7/2}^o$	7g $^2G_{9/2}$	$2.21 \times 10^{-1}$		2906.502			
C iv	5f $^2F_{7/2}^o$	7g $^2G_{7/2}$	$6.42 \times 10^{-3}$		2906.502			
C iv	5f $^2F_{5/2}^o$	7g $^2G_{7/2}$	$2.27 \times 10^{-1}$		2906.502			
C iv	5g $^2G_{7/2}$	7h $^2H_{9/2}^o$	$2.00 \times 10^{-1}$		2907.193			
C iv	5g $^2G_{9/2}$	7h $^2H_{9/2}^o$	$3.73 \times 10^{-3}$		2907.193			
C iv	5g $^2G_{9/2}$	7h $^2H_{11/2}^o$	$1.96 \times 10^{-1}$		2907.193			
C iv	5g $^2G_{7/2}$	7f $^2F_{5/2}^o$	$1.13 \times 10^{-3}$		2907.382			
C iv	5g $^2G_{7/2}$	7f $^2F_{7/2}^o$	$4.24 \times 10^{-5}$		2907.402			
C iv	5g $^2G_{9/2}$	7f $^2F_{7/2}^o$	$1.17 \times 10^{-3}$		2907.402			
C iv	5f $^2F_{5/2}^o$	7d $^2D_{5/2}$	$3.01 \times 10^{-4}$		2907.589			
C iv	5f $^2F_{5/2}^o$	7d $^2D_{3/2}$	$4.21 \times 10^{-3}$		2907.589			
C iv	5f $^2F_{7/2}^o$	7d $^2D_{5/2}$	$4.52 \times 10^{-3}$		2907.617			
				60.1		2958.83		unid.
O iii	3p $^1P_1$	3d $^1D_2^o$	$4.20 \times 10^{-1}$		2960.559			
C iii	3d $^1D_2$	3s' $^1P_1^o$	$6.72 \times 10^{-2}$	36.9	2982.986	2983.23	24.5	

Table A.4. Like Table A.1, for the optical observations.

Ion	Levels		$f$	$W_\lambda /$ mÅ	Wavelength / Å		$v_{\text{rad}} /$ km/s	Comment
	Lower	Upper			Theoretical	Observed		
O iv	3s $^2P_{1/2}^o$	3p $^2D_{3/2}$	$2.84 \times 10^{-1}$		3348.055			newly identified
O iv	3s $^2P_{3/2}^o$	3p $^2D_{5/2}$	$2.55 \times 10^{-1}$		3349.110			newly identified
O iv	3s $^4P_{3/2}^o$	3p $^4D_{5/2}$	$1.83 \times 10^{-1}$		3381.212			newly identified
O iv	3s $^4P_{1/2}^o$	3p $^4D_{3/2}$	$1.45 \times 10^{-1}$		3381.304			newly identified
O iv	3s $^4P_{5/2}^o$	3p $^4D_{7/2}$	$2.32 \times 10^{-1}$		3385.518			newly identified
O iv	3s $^4P_{1/2}^o$	3p $^4D_{1/2}$	$1.45 \times 10^{-1}$		3390.191			newly identified
O iv	3s $^4P_{3/2}^o$	3p $^4D_{3/2}$	$9.29 \times 10^{-2}$		3396.803			newly identified
S v	4s $^1S$	4p $^1P^o$	$6.37 \times 10^{-1}$		3397.334			blend with O iv, newly identified
O iv	3p $^2P_{1/2}^o$	3d $^2D_{3/2}$	$2.95 \times 10^{-1}$		3403.545			newly identified

Table A.4. Continued.

Ion	Levels		$f$	$W_\lambda /$ mÅ	Wavelength / Å		$v_{\text{rad}} /$ km/s	Comment		
	Lower	Upper			Theoretical	Observed				
O IV	3s	$4P_{5/2}^o$	3p	$4D_{5/2}$	$5.22 \times 10^{-2}$	49.1	3409.698			newly identified
O IV	3p	$2P_{3/2}^o$	3d	$2D_{5/2}$	$2.65 \times 10^{-1}$		3411.688	3412.02	29.2	newly identified
O IV	3p	$2P_{3/2}^o$	3d	$2D_{3/2}$	$2.95 \times 10^{-2}$		3413.633			newly identified
C III	4p	$3P_0^o$	5d	$3D_1$	$3.17 \times 10^{-1}$		3608.778			newly identified
C III	4p	$3P_1^o$	5d	$3D_2$	$2.38 \times 10^{-1}$		3609.051			newly identified
C III	4p	$3P_1^o$	5d	$3D_1$	$7.96 \times 10^{-2}$		3609.071			newly identified
C III	4p	$3P_2^o$	5d	$3D_3$	$2.67 \times 10^{-1}$		3609.620			newly identified
C III	4p	$3P_2^o$	5d	$3D_2$	$4.78 \times 10^{-2}$		3609.676			newly identified
C III	4p	$3P_2^o$	5d	$3D_1$	$3.20 \times 10^{-3}$		3609.695			newly identified
C IV	6f	$2F_{5/2}^o$	9g	$2G_{7/2}$	$9.78 \times 10^{-2}$		3689.263			newly identified
C IV	6f	$2F_{7/2}^o$	9g	$2G_{7/2}$	$2.76 \times 10^{-3}$		3689.263			newly identified
C IV	6f	$2F_{7/2}^o$	9g	$2G_{9/2}$	$9.51 \times 10^{-2}$		3689.263			newly identified
C IV	6g	$2G_{9/2}$	9h	$2H_{11/2}^o$	$9.15 \times 10^{-2}$		3689.635			newly identified
C IV	6g	$2G_{9/2}$	9h	$2H_{9/2}^o$	$1.74 \times 10^{-3}$		3689.636			newly identified
C IV	6g	$2G_{7/2}$	9h	$2H_{9/2}^o$	$9.32 \times 10^{-2}$		3689.636			newly identified
C IV	6h	$2H_{9/2}^o$	9i	$2I_{11/2}$	$5.77 \times 10^{-2}$		3689.717			newly identified
C IV	6h	$2H_{11/2}^o$	9i	$2I_{11/2}$	$8.54 \times 10^{-4}$		3689.717			newly identified
C IV	6h	$2H_{11/2}^o$	9i	$2I_{13/2}$	$5.69 \times 10^{-2}$		3689.717			newly identified
C IV	6h	$2H_{9/2}^o$	9g	$2G_{7/2}$	$2.73 \times 10^{-4}$		3689.753			newly identified
C IV	6h	$2H_{9/2}^o$	9g	$2G_{9/2}$	$6.36 \times 10^{-6}$		3689.753			newly identified
C IV	6h	$2H_{11/2}^o$	9g	$2G_{9/2}$	$2.79 \times 10^{-4}$		3689.753			newly identified
C IV	6g	$2G_{7/2}$	9f	$2F_{5/2}^o$	$1.15 \times 10^{-3}$		3689.785			newly identified
C IV	6g	$2G_{7/2}$	9f	$2F_{7/2}^o$	$4.34 \times 10^{-5}$		3689.785			newly identified
C IV	6g	$2G_{9/2}$	9f	$2F_{7/2}^o$	$1.20 \times 10^{-3}$		3689.785			newly identified
O IV	3p	$4D_{1/2}$	3d	$4F_{3/2}^o$	$2.31 \times 10^{-1}$		3725.889			newly identified
O IV	3p	$4D_{3/2}$	3d	$4F_{5/2}^o$	$1.85 \times 10^{-1}$		3725.945			newly identified
O IV	3p	$4D_{5/2}$	3d	$4F_{7/2}^o$	$1.89 \times 10^{-1}$		3729.030			newly identified
O IV	3p	$4D_{3/2}$	3d	$4F_{3/2}^o$	$4.62 \times 10^{-2}$		3736.682			newly identified
O IV	3p	$4D_{7/2}$	3d	$4F_{9/2}^o$	$2.06 \times 10^{-1}$		3736.850			newly identified
He I	2s	$3S$	3p	$3P^o$	$6.45 \times 10^{-2}$		3888.643			newly identified
H I	2		8		$8.04 \times 10^{-3}$		3889.049			newly identified
C III	4d	$3D_3$	5f	$3F_4^o$	$3.28 \times 10^{-1}$		3889.137			blend with H I, newly identified
C III	4d	$3D_3$	5f	$3F_3^o$	$2.89 \times 10^{-2}$		3889.462			blend with H I, newly identified
C III	4d	$3D_3$	5f	$3F_2^o$	$6.57 \times 10^{-4}$		3889.670			blend with H I, newly identified
C IV	5s	$2S_{1/2}$	6p	$2P_{3/2}^o$	$1.52 \times 10^{-1}$		3934.283			newly identified
C IV	5s	$2S_{1/2}$	6p	$2P_{1/2}^o$	$7.62 \times 10^{-2}$		3934.887			newly identified
C III	4d	$1D_2$	5f	$1F_3^o$	$3.70 \times 10^{-1}$	94.2	4056.061	4056.33	19.9	uncertain, newly identified

Table A.4. Continued.

Ion	Levels		$f$	$W_\lambda /$ mÅ	Wavelength/Å		$v_{\text{rad}} /$ km/s	Comment		
	Lower	Upper			Theoretical	Observed				
N iv	3p	$^1P_1^o$	3d	$^1D_2$	$2.74 \times 10^{-1}$	4057.757		newly identified		
C iii	4f	$^3F_2^o$	5g	$^3G_3$	1.02	4067.939		newly identified		
C iii	4f	$^3F_3^o$	5g	$^3G_3$	$6.50 \times 10^{-2}$	4068.916		newly identified		
C iii	4f	$^3F_3^o$	5g	$^3G_4$	$9.78 \times 10^{-1}$	4068.916		newly identified		
C iii	4f	$^3F_4^o$	5g	$^3G_5$	$9.92 \times 10^{-1}$	4070.260		newly identified		
C iii	4f	$^3F_4^o$	5g	$^3G_3$	$9.92 \times 10^{-4}$	4070.306		newly identified		
C iii	4f	$^3F_4^o$	5g	$^3G_4$	$5.06 \times 10^{-2}$	4070.306		newly identified		
C iii	4p	$^1P_1^o$	5d	$^1D_2$	$3.40 \times 10^{-1}$	4121.845		newly identified		
C iii	3p'	$^3D_2$	5f	$^3F_3^o$	$2.23 \times 10^{-1}$	4156.504		newly identified		
C iii	3p'	$^3D_2$	5f	$^3F_2^o$	$2.84 \times 10^{-2}$	4156.741		newly identified		
C iii	3p'	$^3D_3$	5f	$^3F_4^o$	$2.31 \times 10^{-1}$	4162.877		newly identified		
C iii	4f	$^1F_3^o$	5g	$^1G_4$	1.18	4186.900		newly identified		
C iii	3s'	$^1P_1^o$	3p'	$^1D_2$	$5.03 \times 10^{-1}$	4325.561		newly identified		
He ii	4		10		$1.20 \times 10^{-2}$	4338.659		Barstow et al. (2000)		
C iv	5p	$^2P_{1/2}^o$	6d	$^2D_{3/2}$	$4.14 \times 10^{-1}$	4440.335		newly identified		
C iv	5p	$^2P_{3/2}^o$	6d	$^2D_{5/2}$	$4.62 \times 10^{-1}$	4441.499		newly identified		
C iv	5p	$^2P_{3/2}^o$	6d	$^2D_{3/2}$	$5.13 \times 10^{-2}$	4441.736		newly identified		
C iii	4p	$^3P_0^o$	5s	$^3P_1$	$1.74 \times 10^{-1}$	4515.352		newly identified		
C iii	4p	$^3P_1^o$	5s	$^3P_1$	$1.74 \times 10^{-1}$	4515.811		newly identified		
C iii	4p	$^3P_2^o$	5s	$^3P_1$	$1.74 \times 10^{-1}$	4516.788		newly identified		
C iv	5f	$^2F_{5/2}^o$	6g	$^2G_{7/2}$	1.18	4657.474		Barstow et al. (2000)		
C iv	5f	$^2F_{7/2}^o$	6g	$^2G_{9/2}$	1.15	4657.606		Barstow et al. (2000)		
C iv	5f	$^2F_{7/2}^o$	6g	$^2G_{7/2}$	$3.32 \times 10^{-2}$	4657.690		Barstow et al. (2000)		
C iv	5g	$^2G_{7/2}$	6h	$^2H_{9/2}^o$	1.66	4658.147		Barstow et al. (2000)		
C iv	5g	$^2G_{9/2}$	6h	$^2H_{11/2}^o$	1.63	4658.228		Barstow et al. (2000)		
C iv	5g	$^2G_{9/2}$	6h	$^2H_{9/2}^o$	$3.10 \times 10^{-2}$	4658.278		Barstow et al. (2000)		
C iii	3s'	$^3P_1^o$	3p'	$^3P_1$	$7.53 \times 10^{-2}$	4659.058		newly identified		
C iii	3s'	$^3P_2^o$	3p'	$^3P_2$	$2.26 \times 10^{-1}$	4665.860		newly identified		
He ii	3		4		$8.43 \times 10^{-1}$	4686.059		Barstow et al. (2000)		
He ii	4		8		$3.23 \times 10^{-2}$	4859.299		Barstow et al. (2000)		
He ii	4		7		$6.55 \times 10^{-2}$	5411.492		Barstow et al. (2000)		
C iii	3p	$^1P_1^o$	3d	$^1D_2$	$3.47 \times 10^{-1}$	53.9	5695.916	5696.47	29.2	newly identified
C iv	3s	$^2S_{1/2}$	3p	$^2P_{3/2}^o$	$3.19 \times 10^{-1}$	159.2	5801.313	5801.78	24.1	Barstow et al. (2000)
C iv	3s	$^2S_{1/2}$	3p	$^2P_{1/2}^o$	$1.59 \times 10^{-1}$		5811.970			Barstow et al. (2000)
N iv	3p'	$^3P_{1/2}$	3d'	$^3P_{2/3}^o$	$1.12 \times 10^{-2}$		5812.308			blend with C iv, newly identified
He i	2p	$^3P^o$	3d	$^3D$	$6.11 \times 10^{-1}$	264.8	5875.661	5876.10	22.4	Barstow et al. (2000)
He ii	4		6		$1.79 \times 10^{-1}$		6560.049			Barstow et al. (2000)

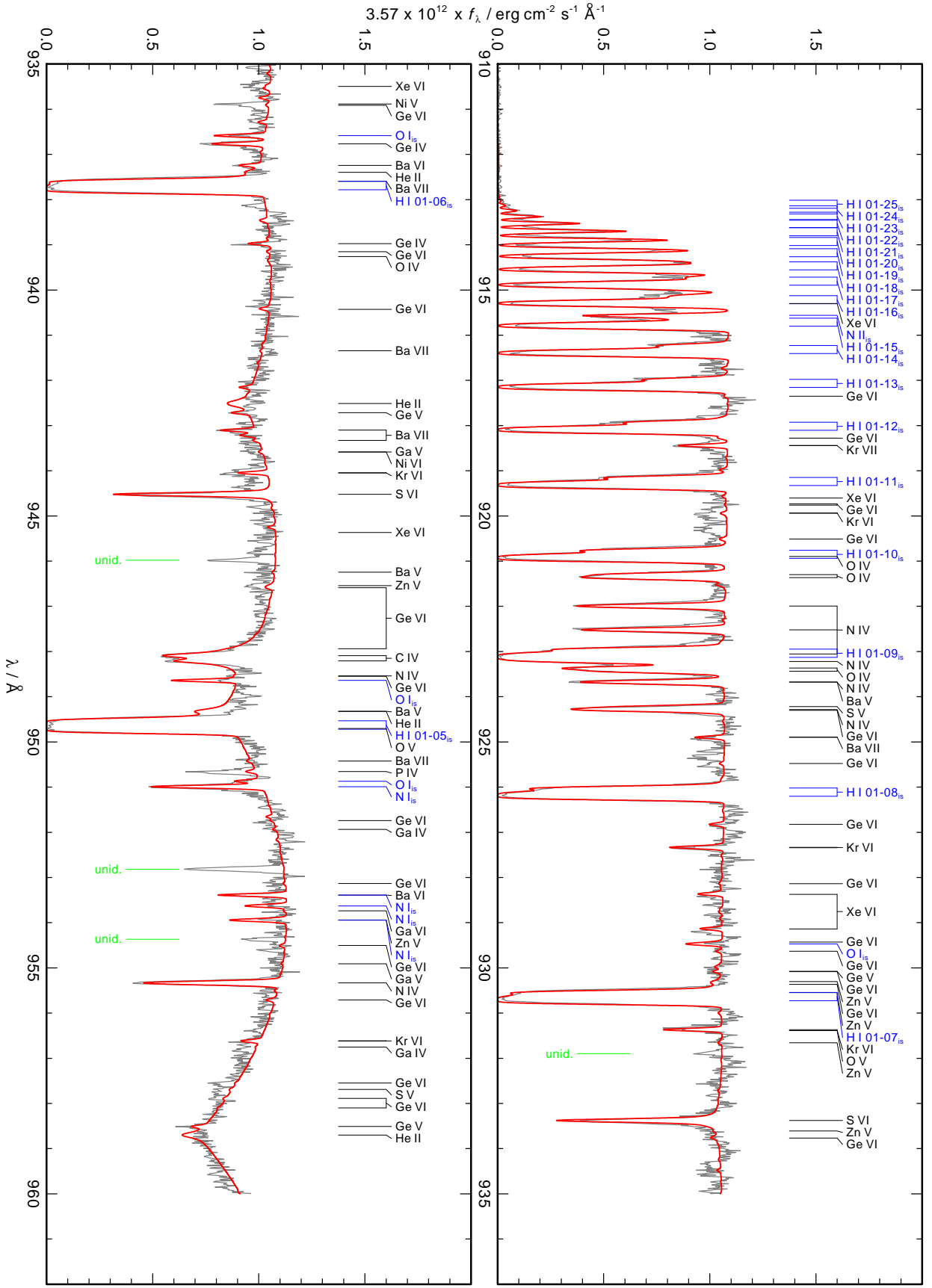


**Table A.5.** Like Table A.1, for the SofI observations.

Ion	Levels		$f$	$W_\lambda /$ mÅ	Wavelength/Å		$v_{\text{rad}} /$ km/s	Comment
	Lower	Upper			Theoretical	Observed		
He II	4	5	1.04		10123.499			
He II	5	7	$2.07 \times 10^{-1}$		11626.406			

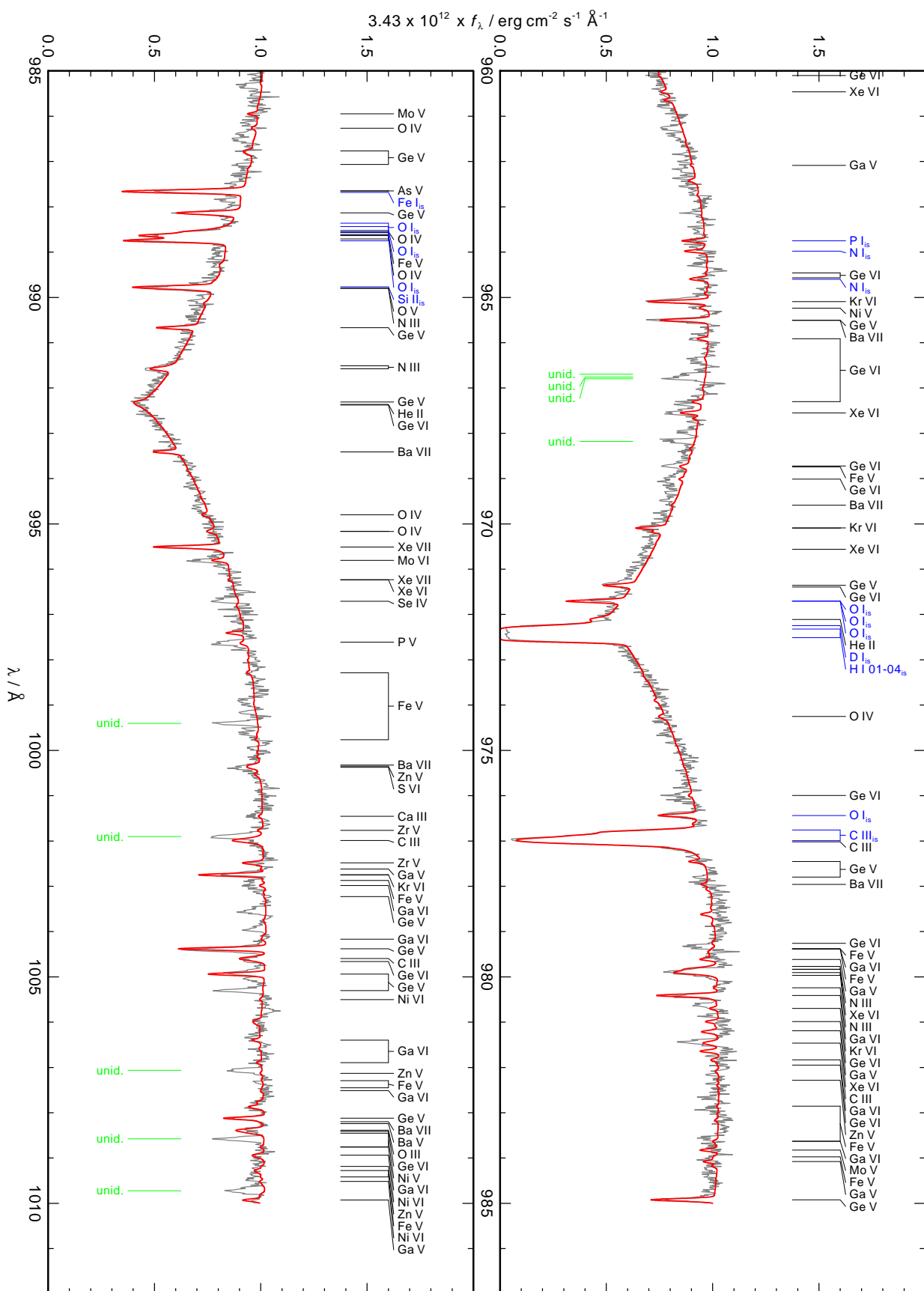
## **Appendix B: Observed spectra of RE 0503–289 compared with our best model**

In the following figures, we show the comparison of our synthetic spectra with the FUSE (Fig.B.1, HST/STIS (Fig.B.2, and optical (Fig.B.3 observations. A visualization via TVIS is available at <http://astro.uni-tuebingen.de/~TVIS/objects/RE0503-289>.



**Fig. B.1.** FUSE observation (gray) compared with the best model (red). Stellar lines are identified at top. "unid." denotes unidentified lines.

Fig. B.1. Figure B.1 continued.



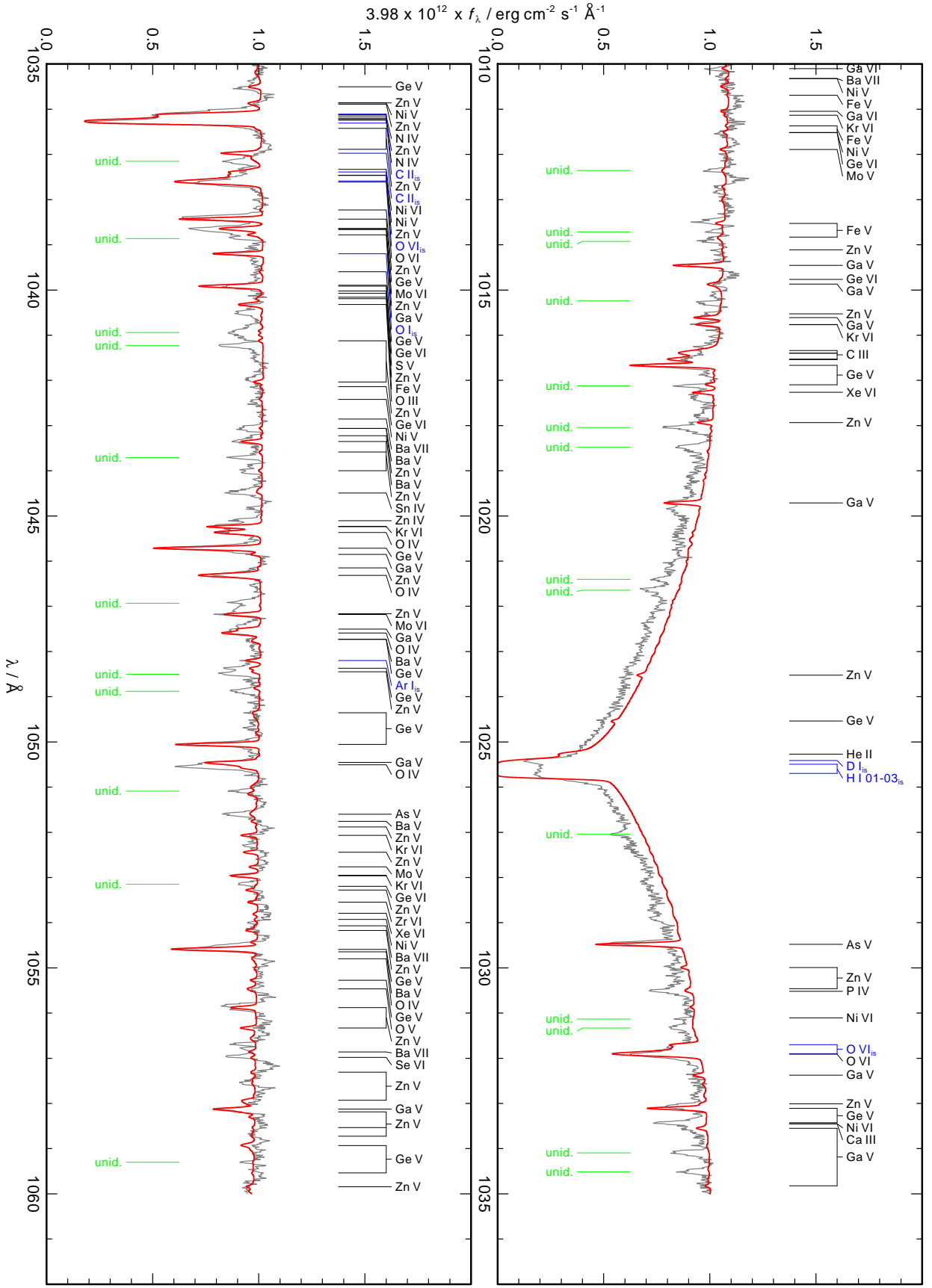


Fig. B.1. Figure B.1 continued.



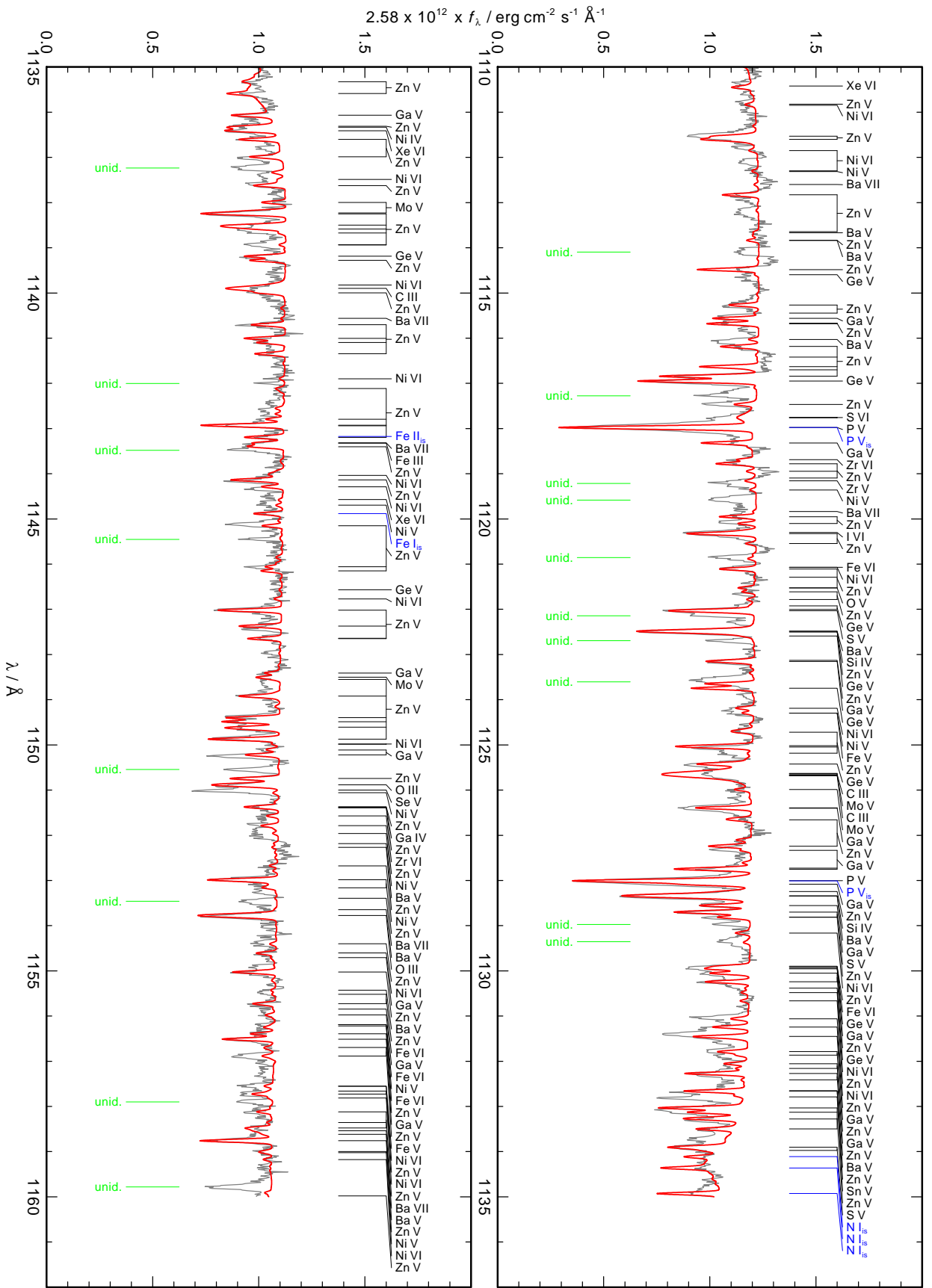
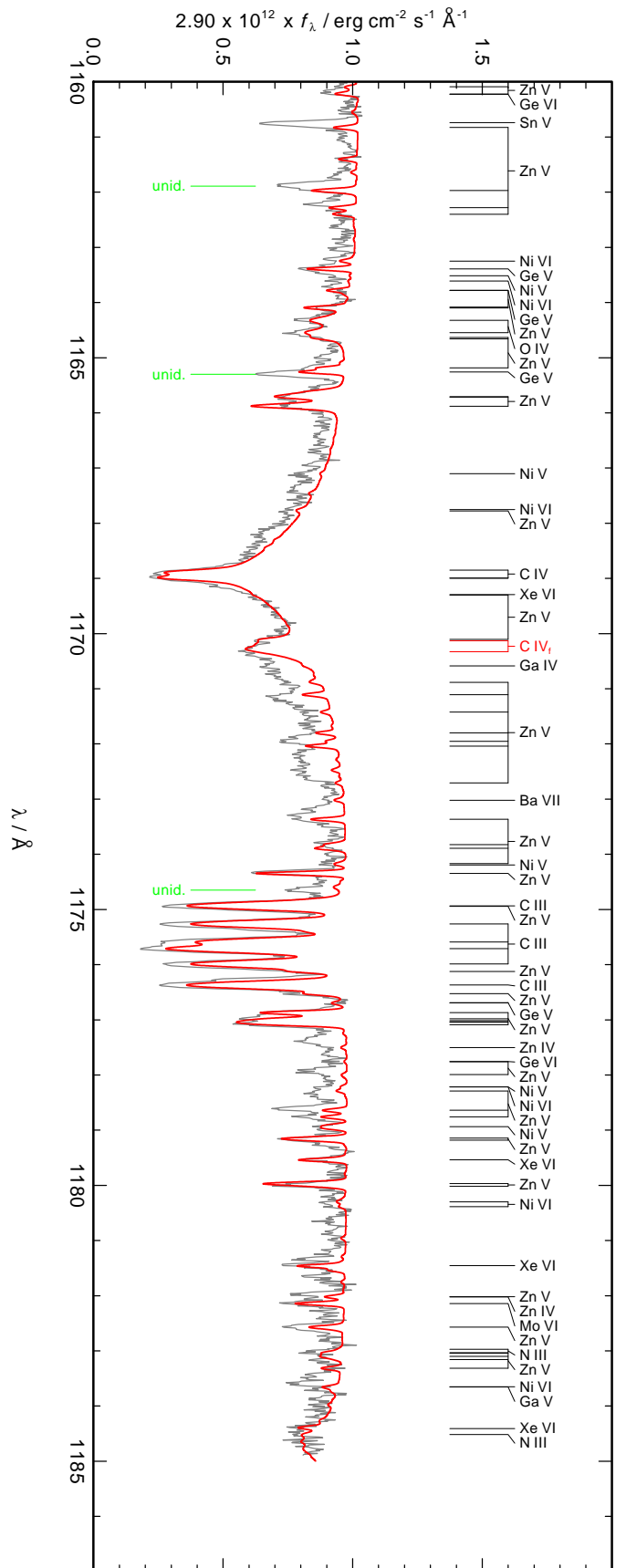


Fig. B.1. Figure B.1 continued.

Fig. B.1. Figure B.1 continued.









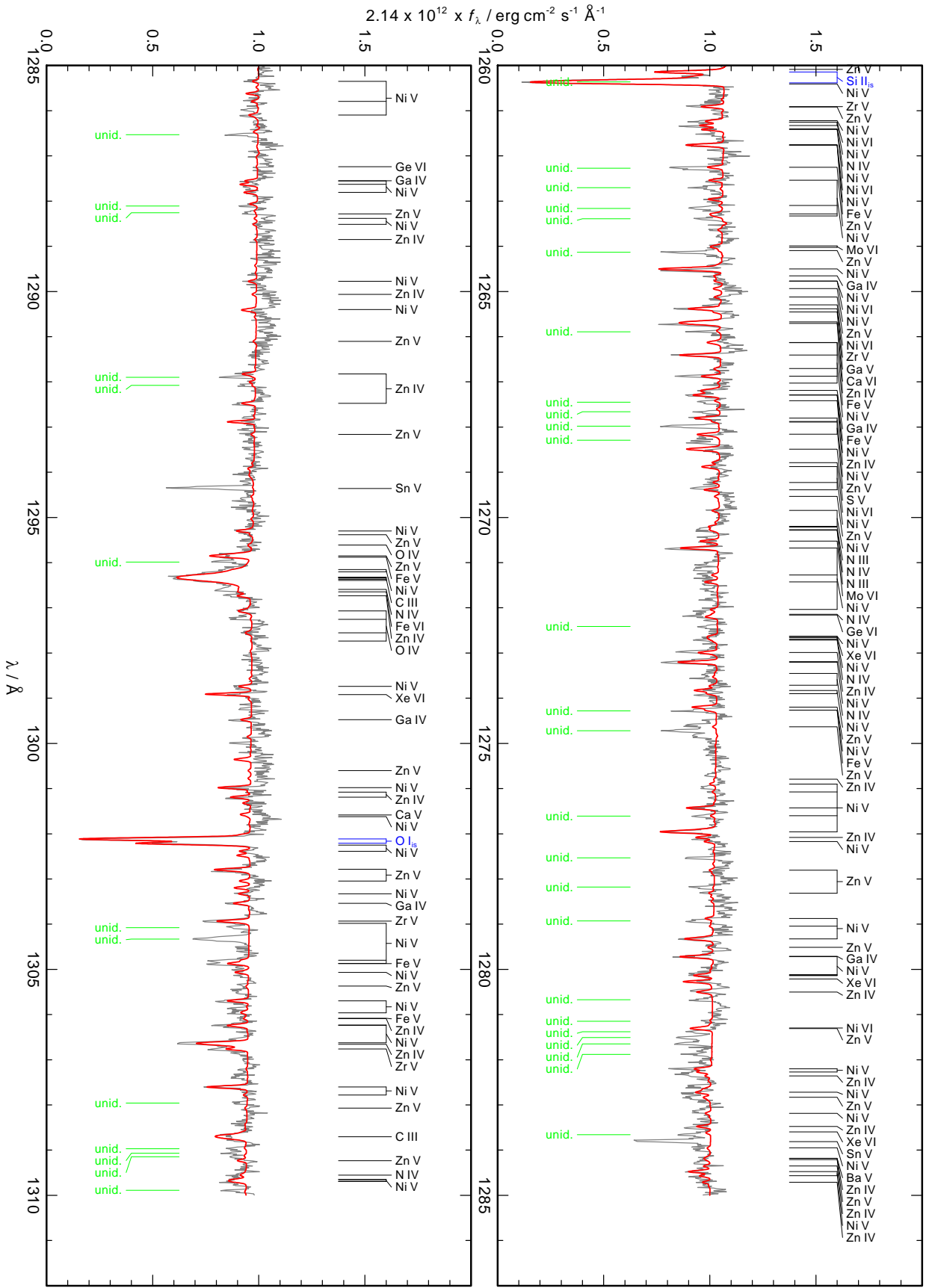
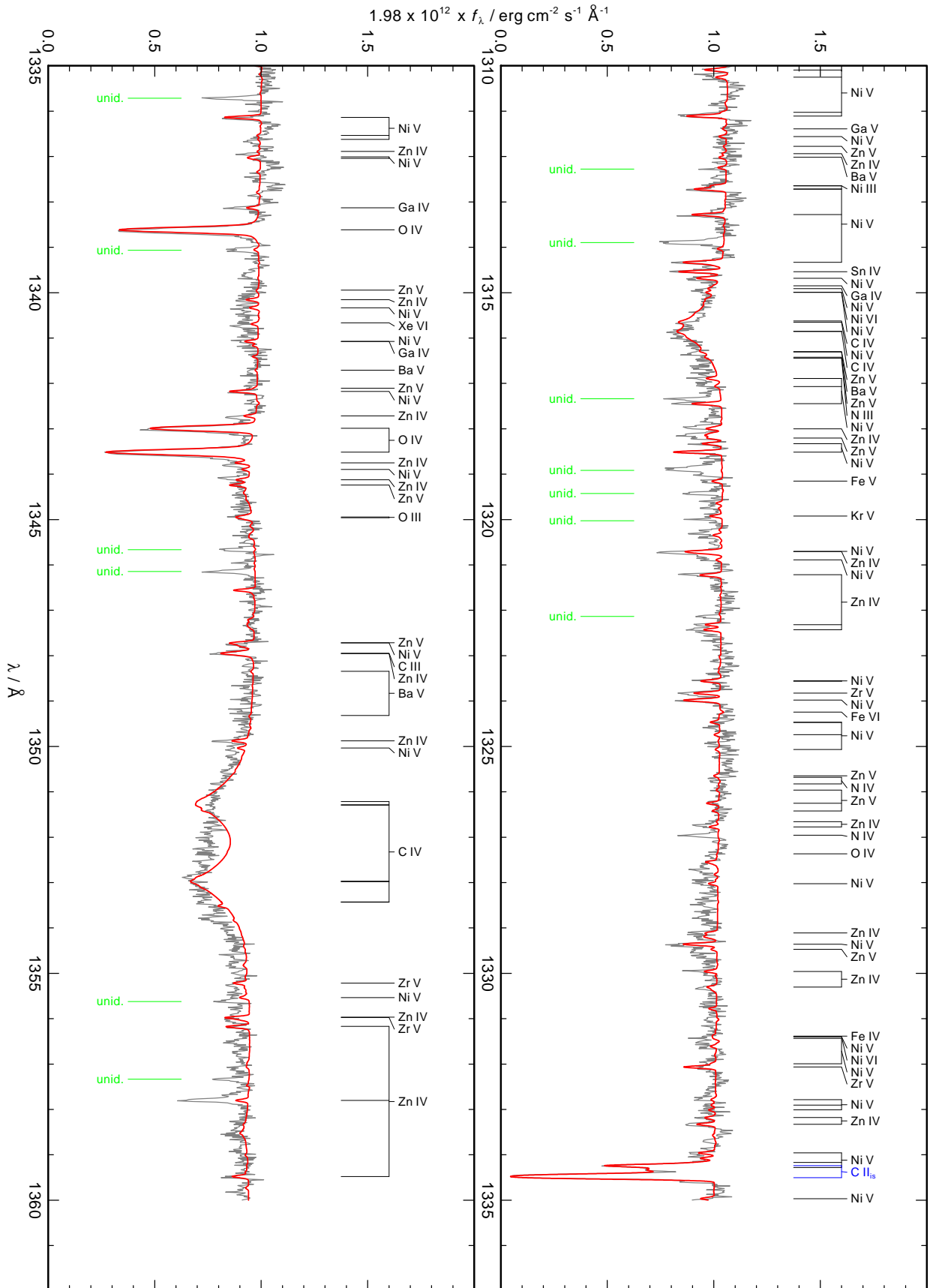


Fig. B.2. Figure B.2 continued.

Fig. B.2. Figure B.2 continued.



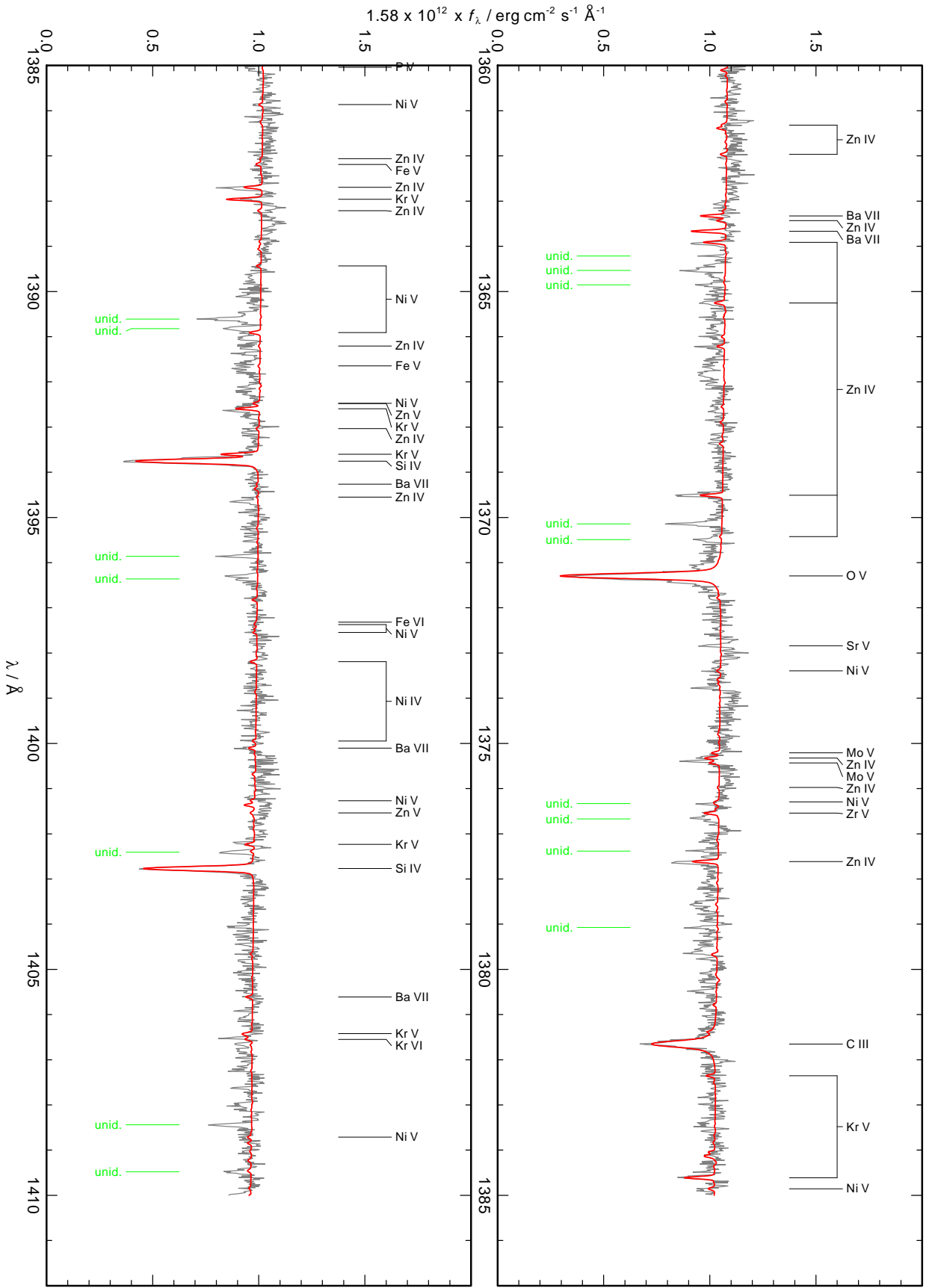
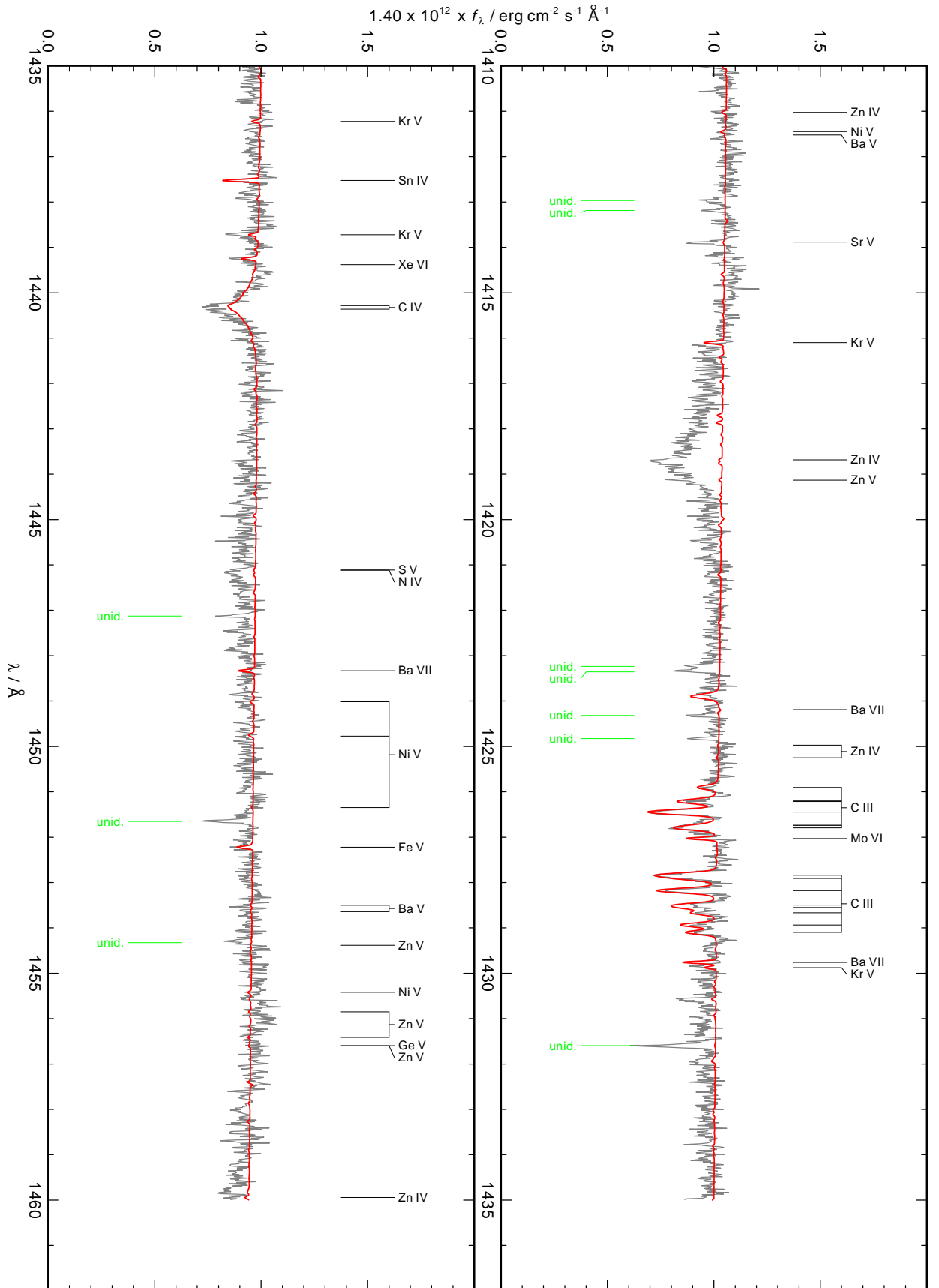


Fig. B.2. Figure B.2 continued.

Fig. B.2. Figure B.2 continued.



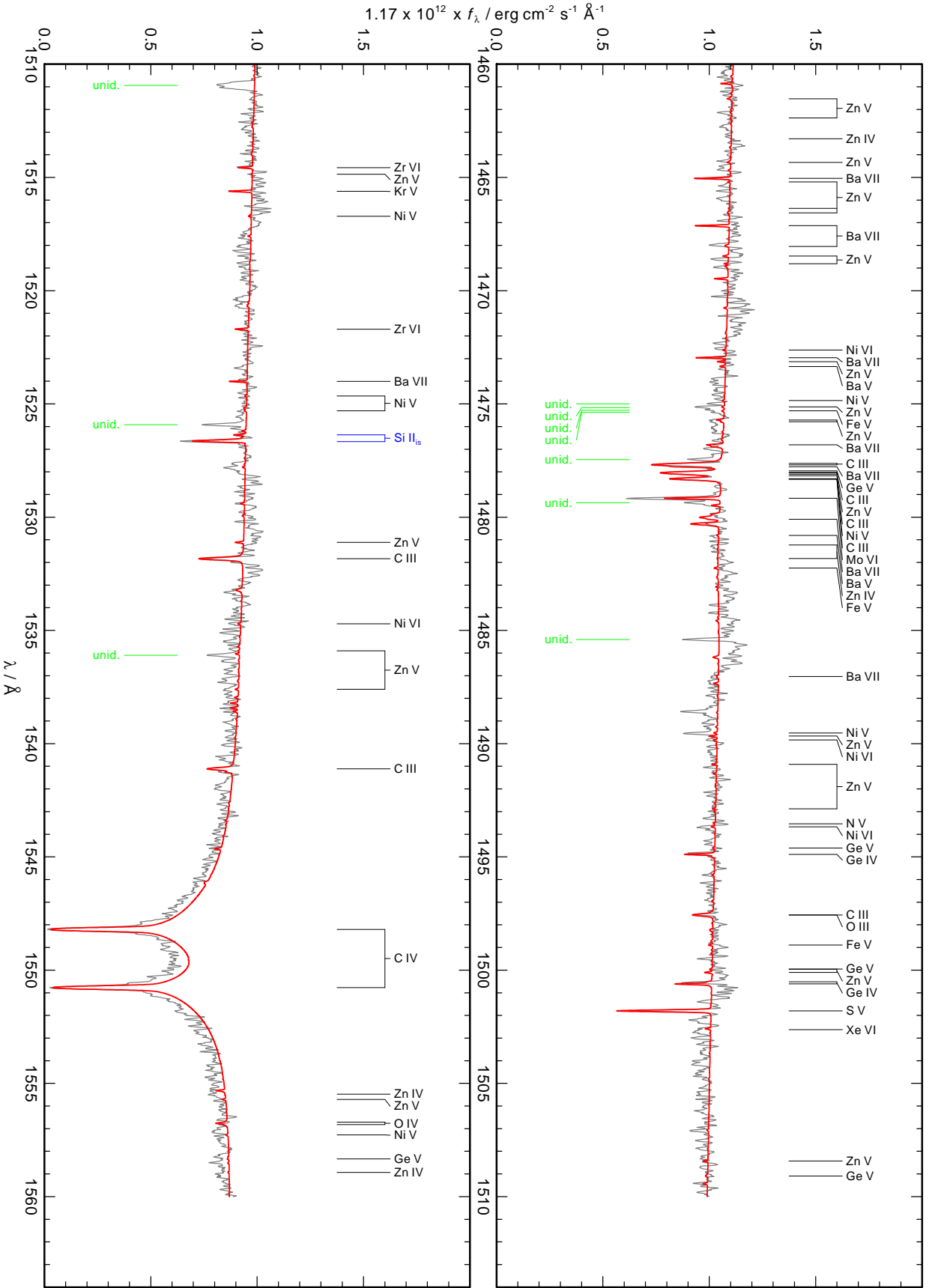
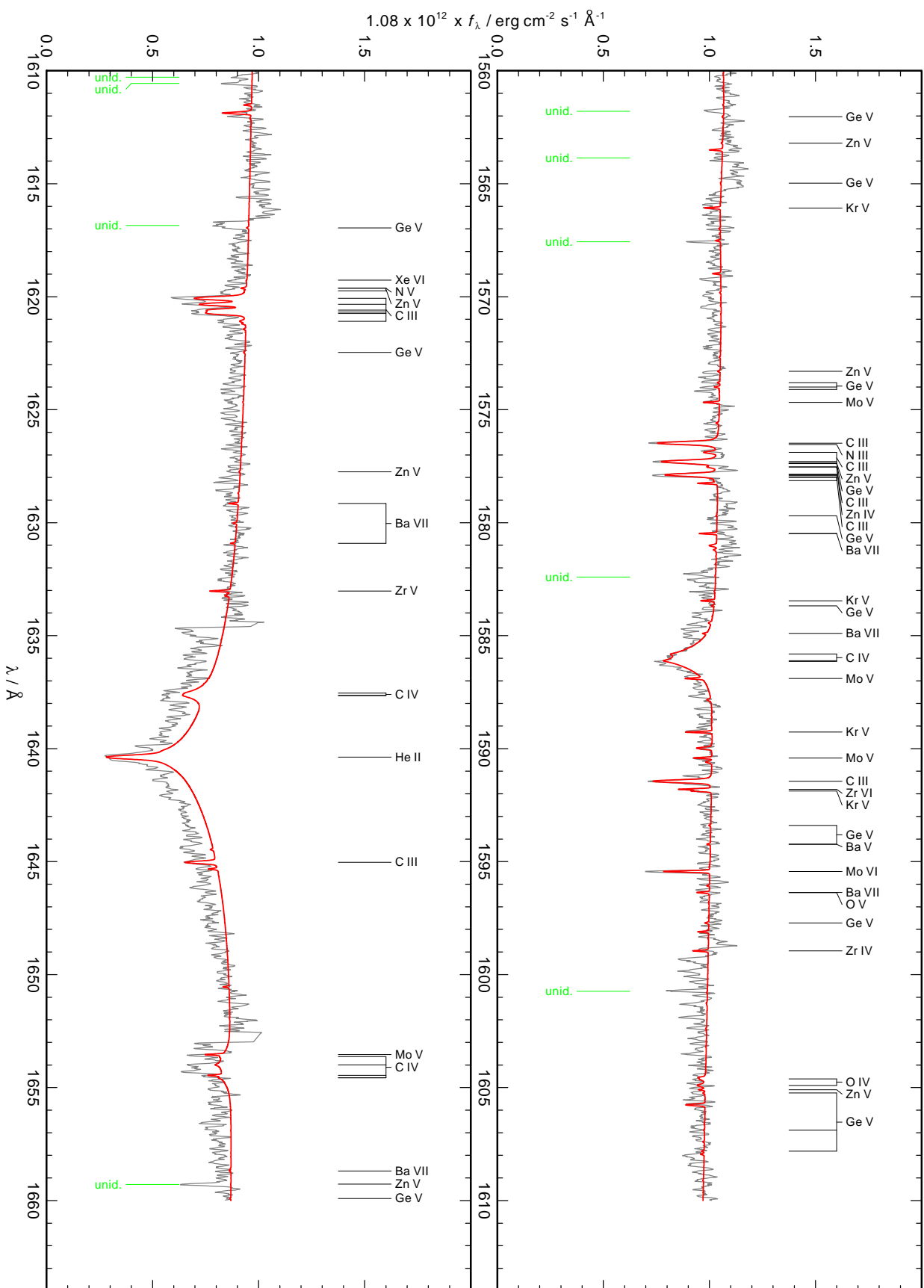


Fig. B.2. Figure B.2 continued.

Fig. B.2. Figure B.2 continued.





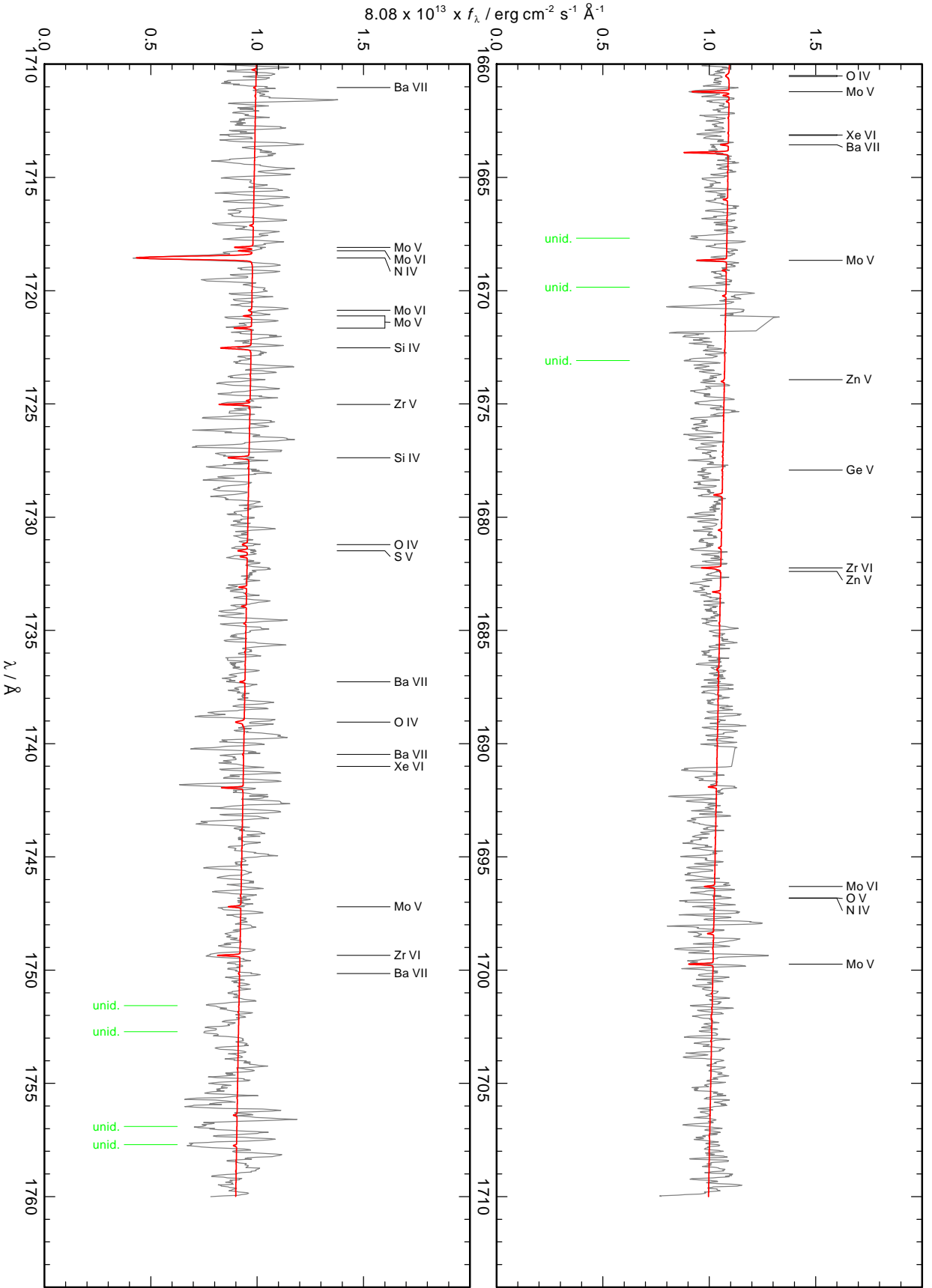
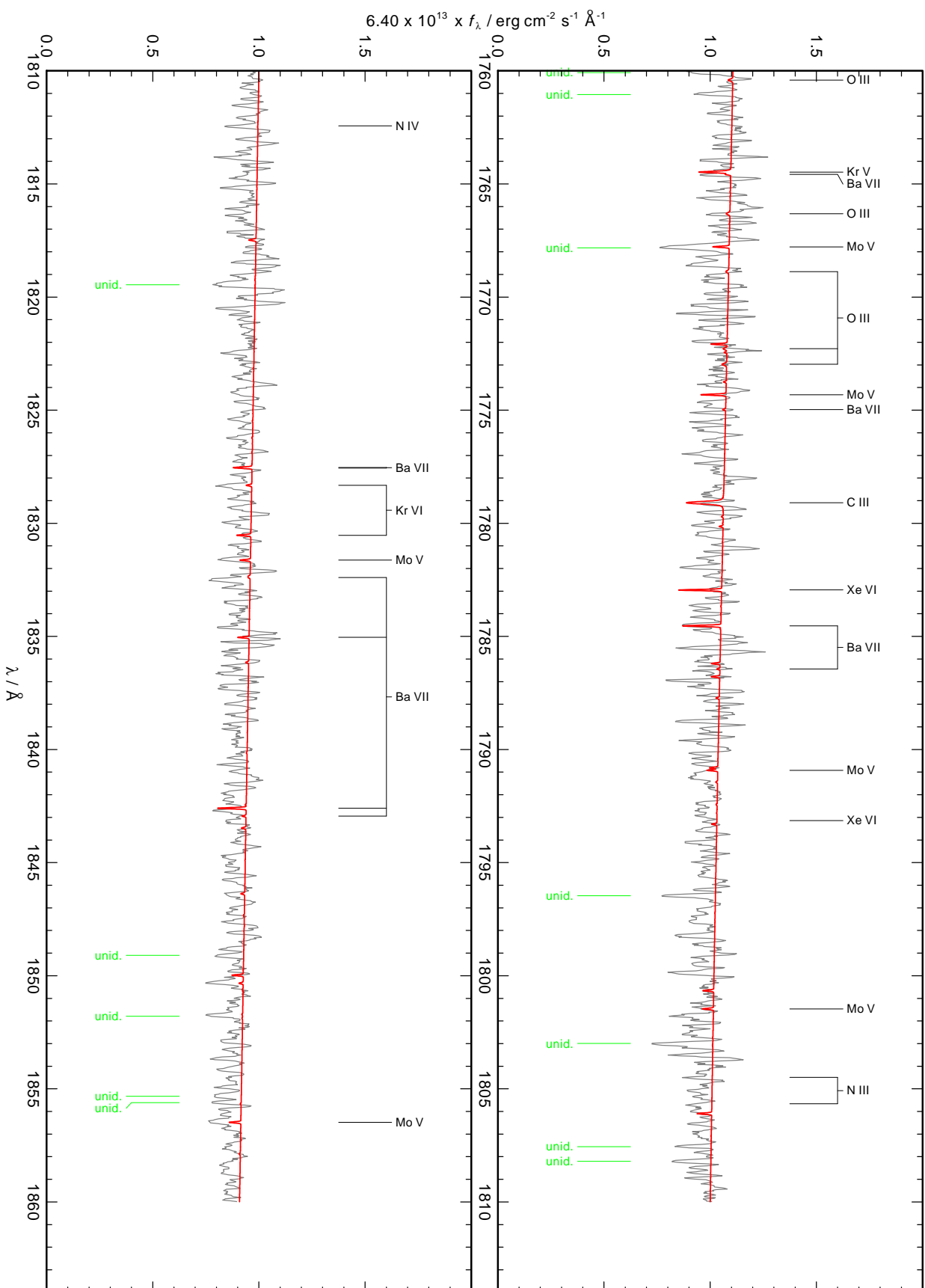


Fig. B.2. Figure B.2 continued.

Fig. B.2. Figure B.2 continued.



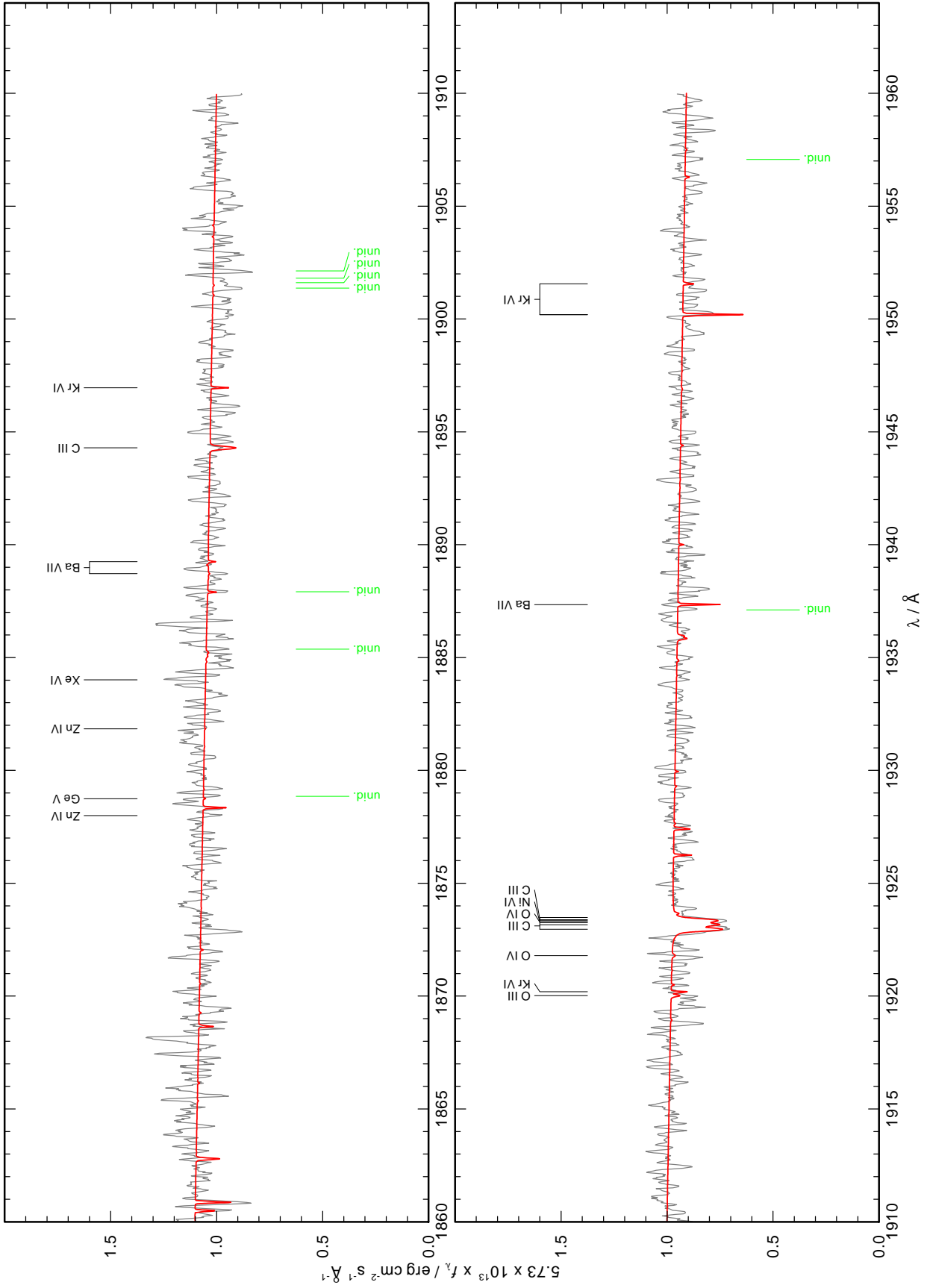


Fig. B.2. Figure B.2 continued.



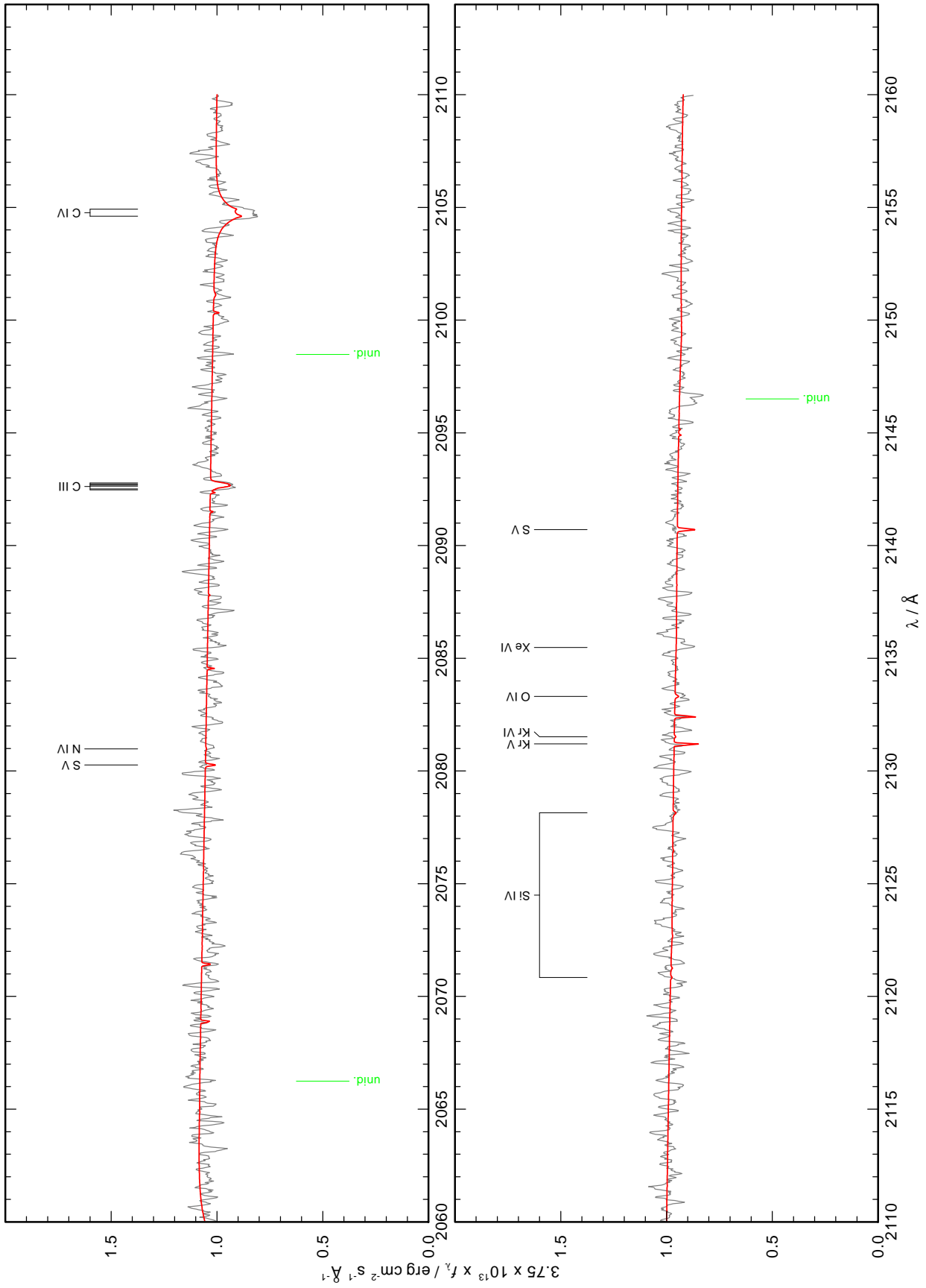


Fig. B.2. Figure B.2 continued.

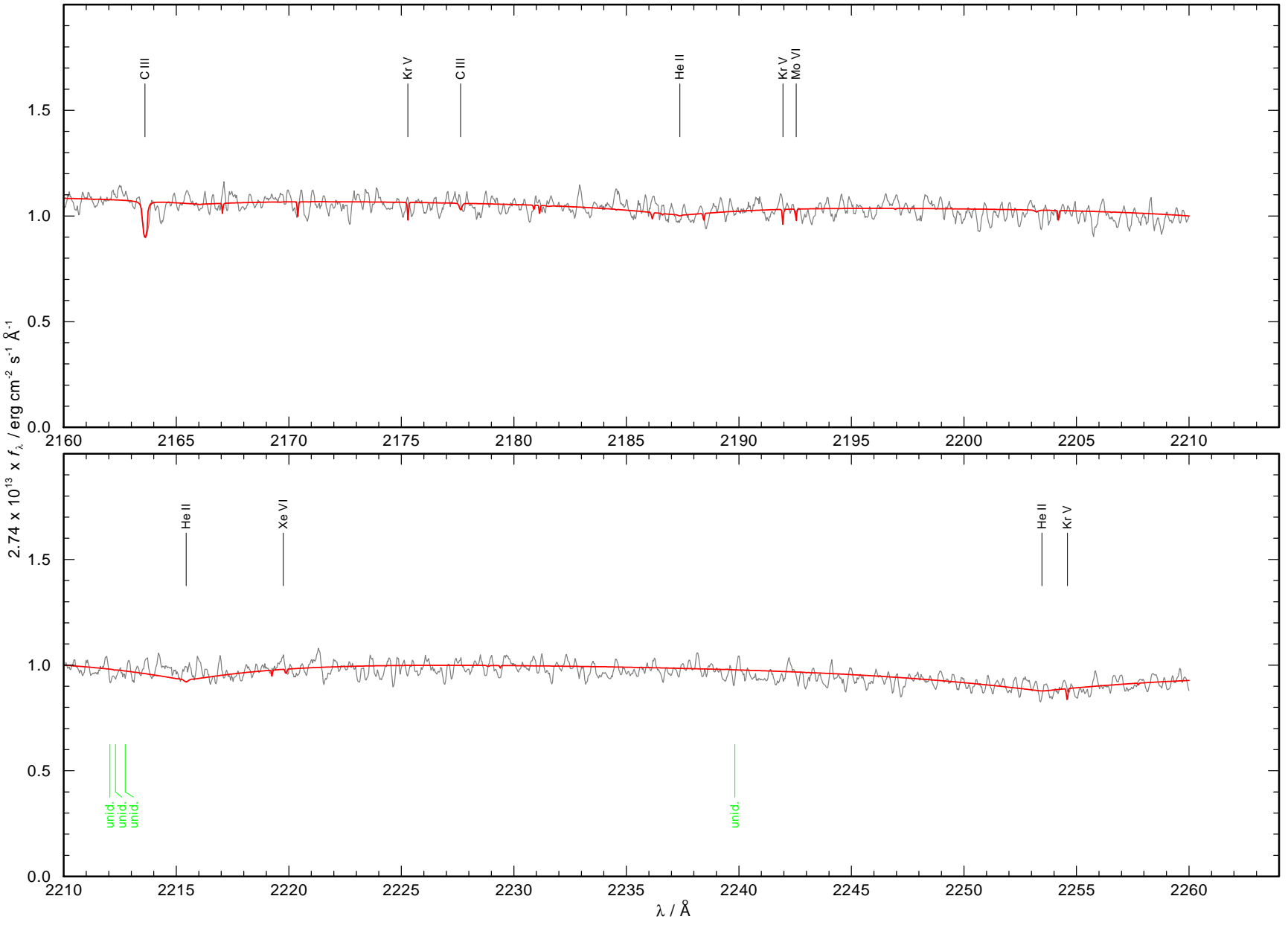


Fig. B.2. Figure B.2 continued.

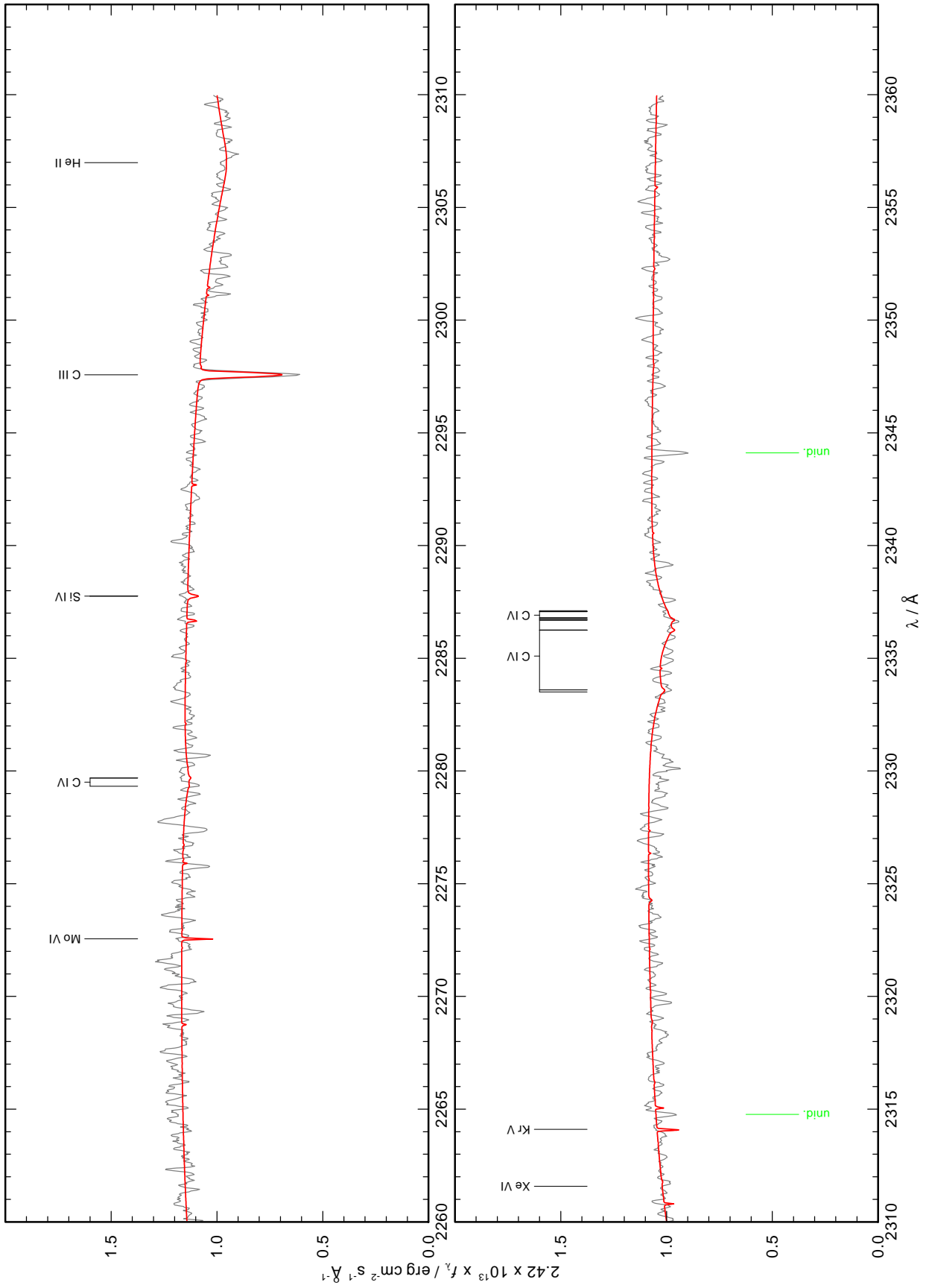
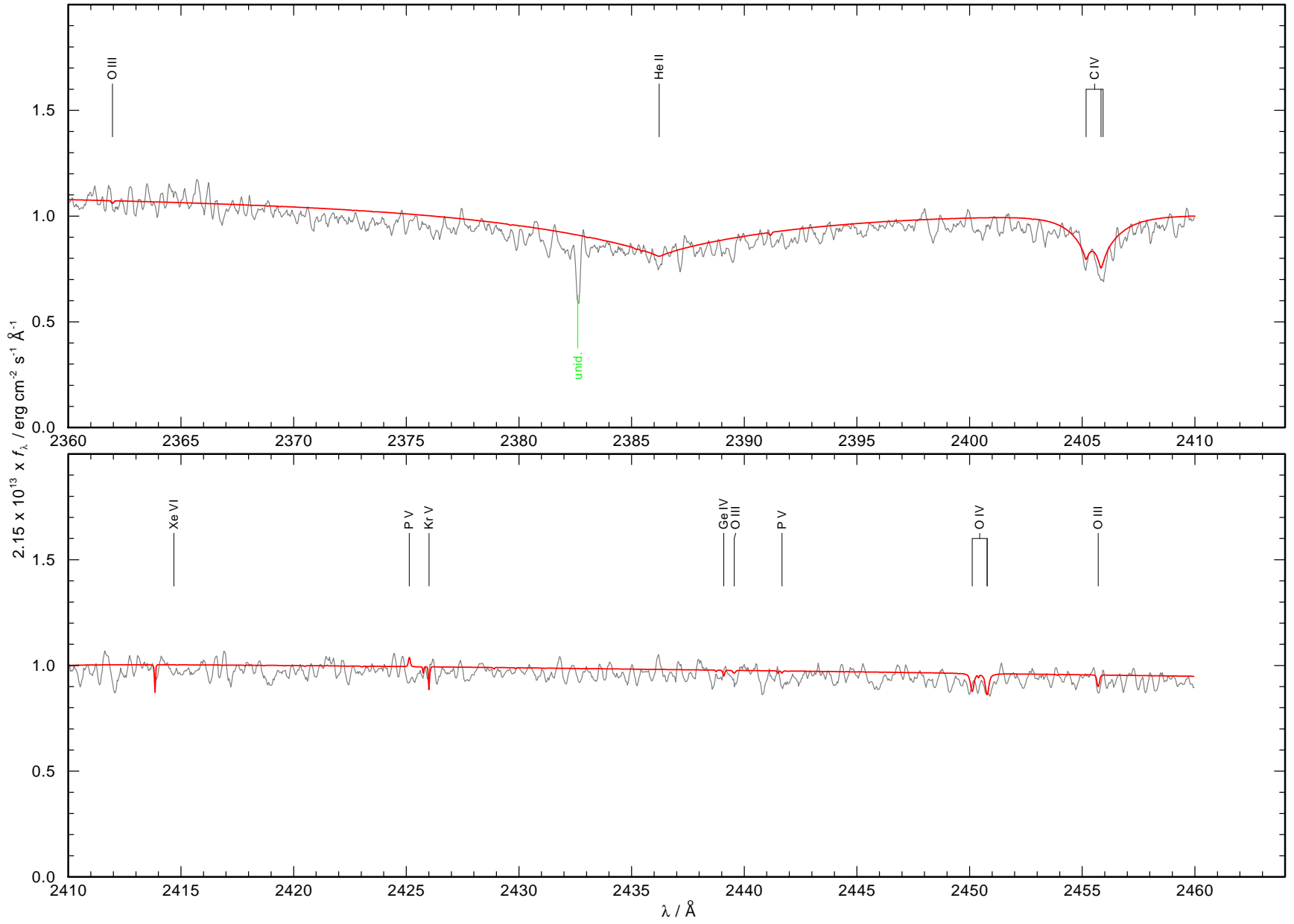


Fig. B.2. Figure B.2 continued.

Fig. B.2. Figure B.2 continued.





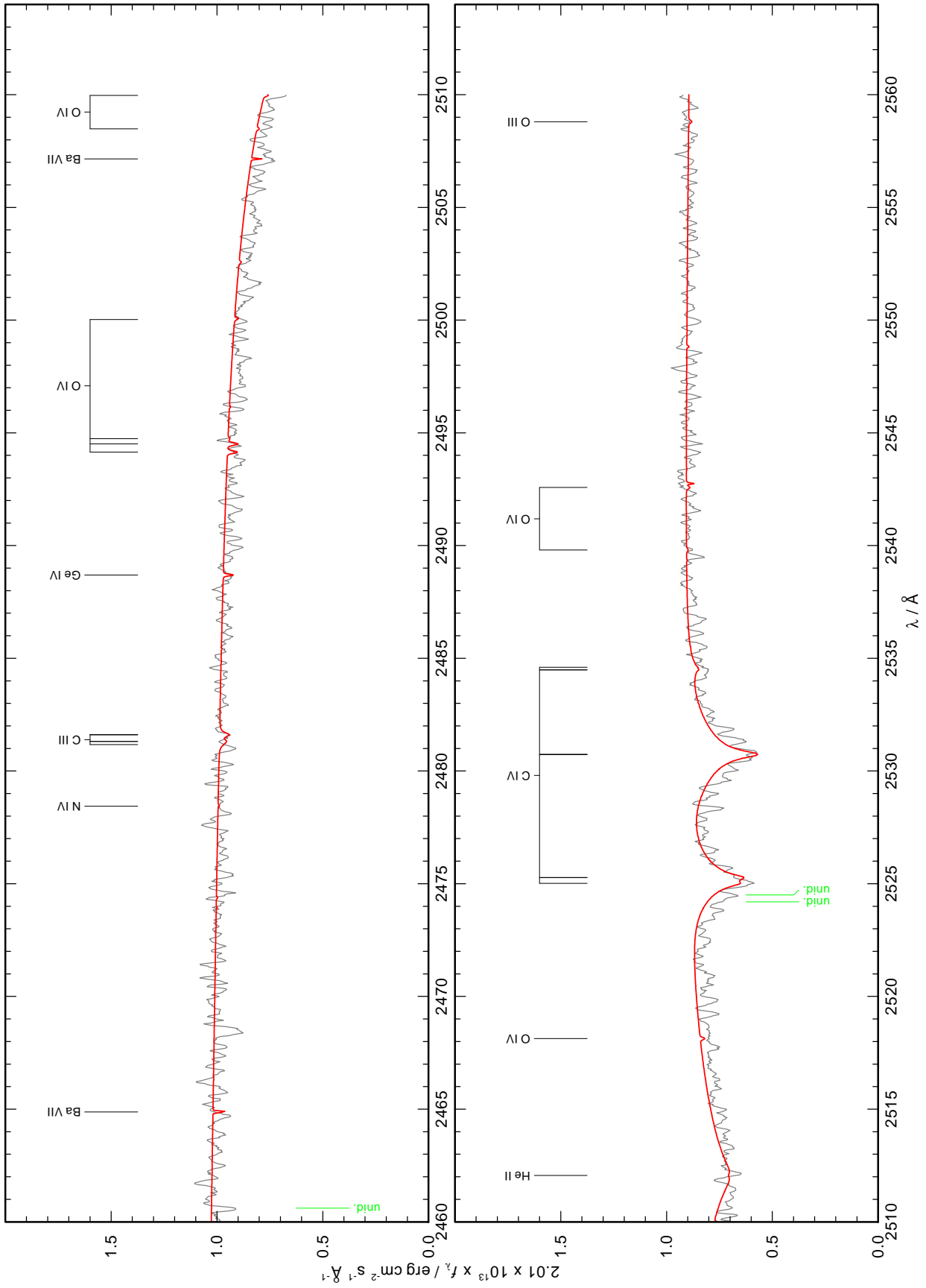
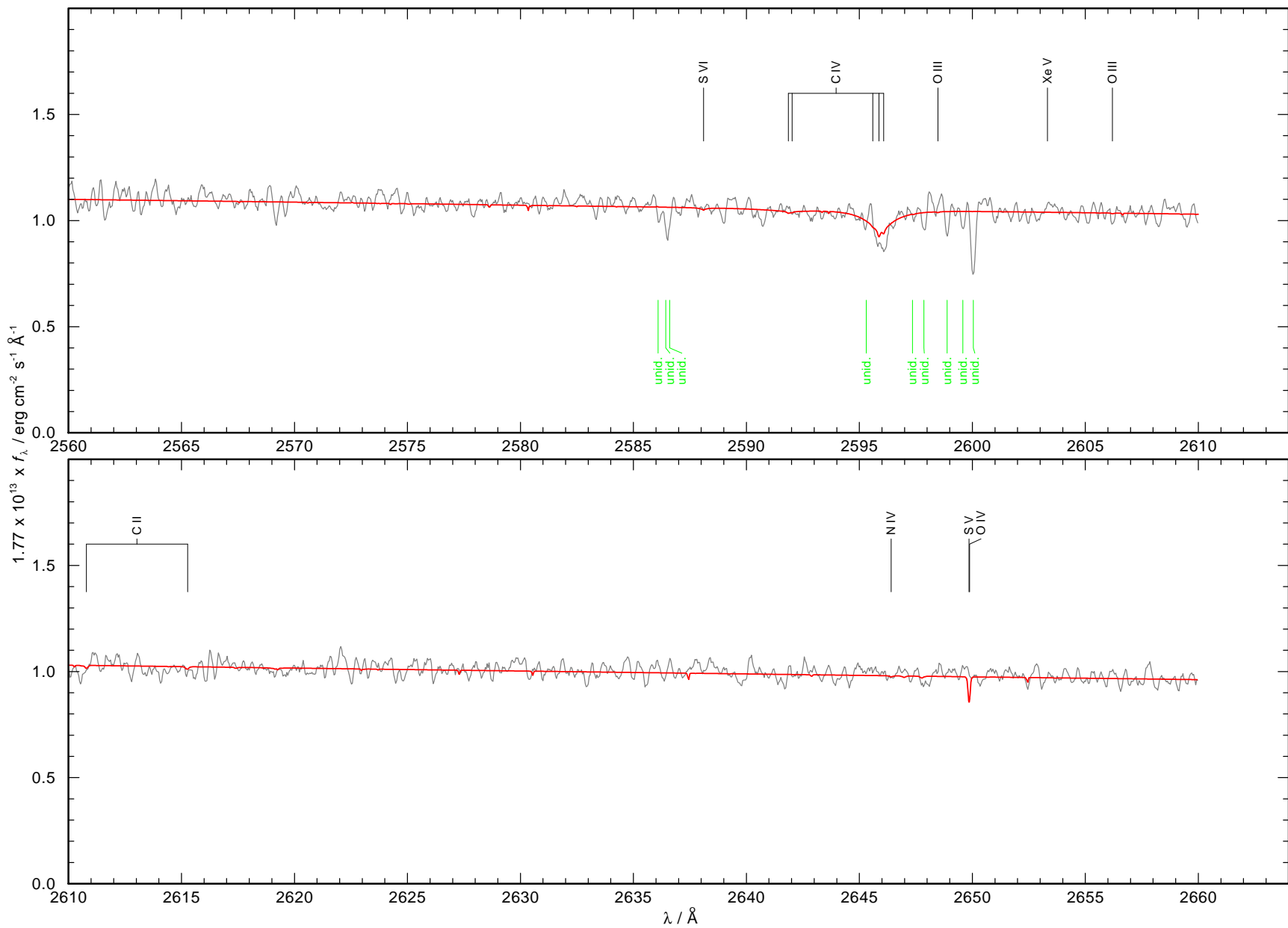


Fig. B.2. Figure B.2 continued.

Fig. B.2. Figure B.2 continued.



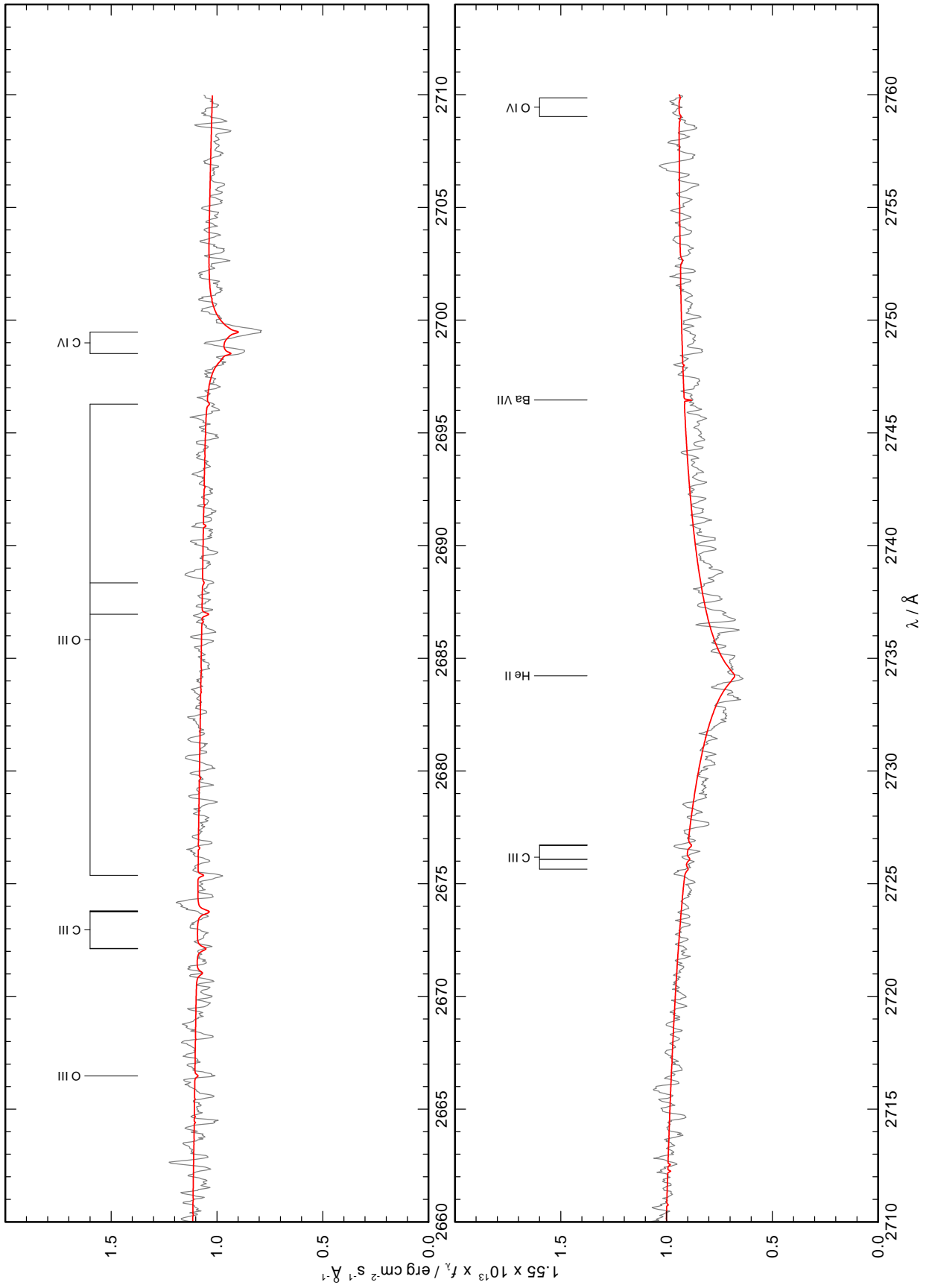


Fig. B.2. Figure B.2 continued.

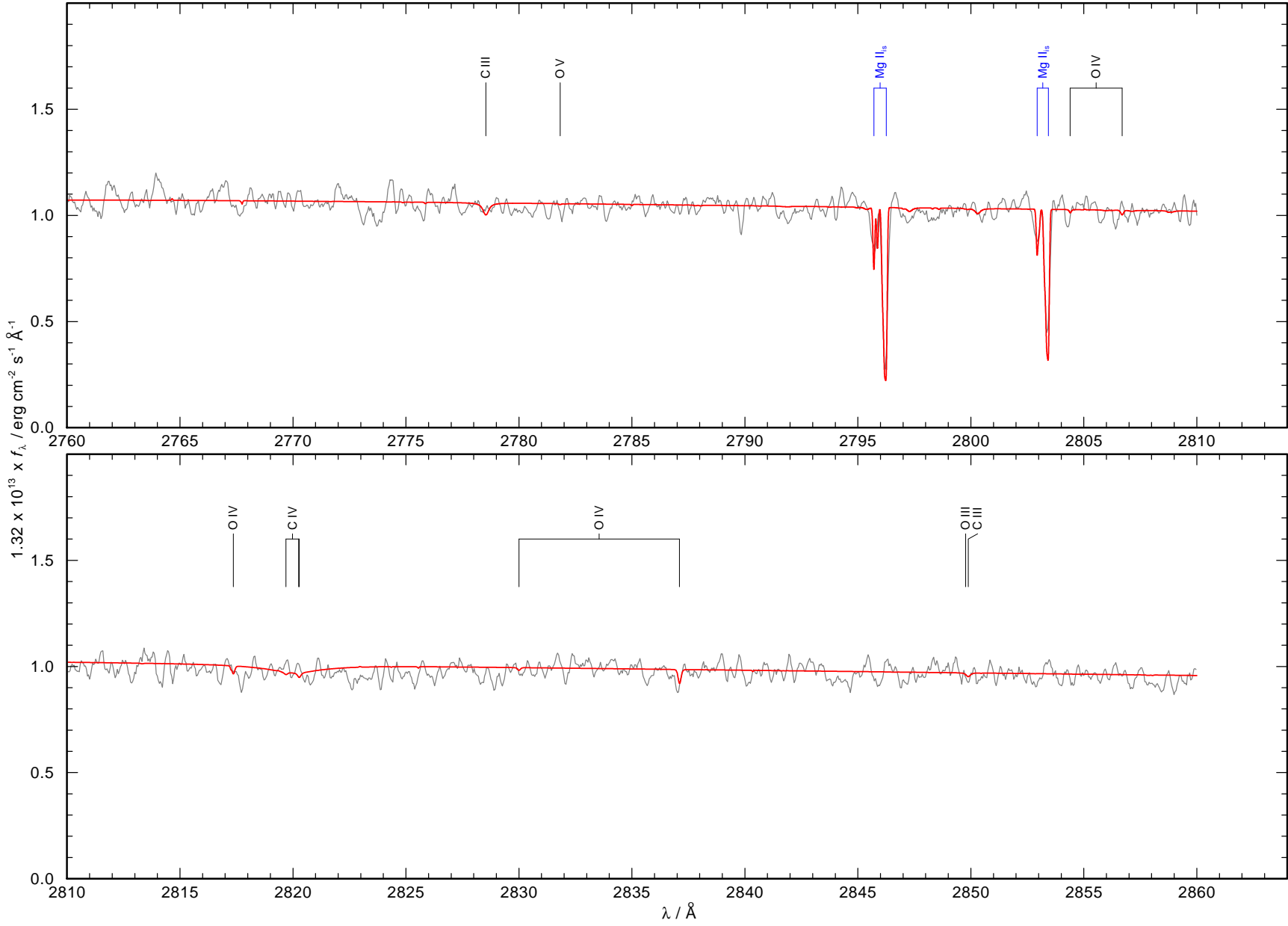


Fig. B.2. Figure B.2 continued.

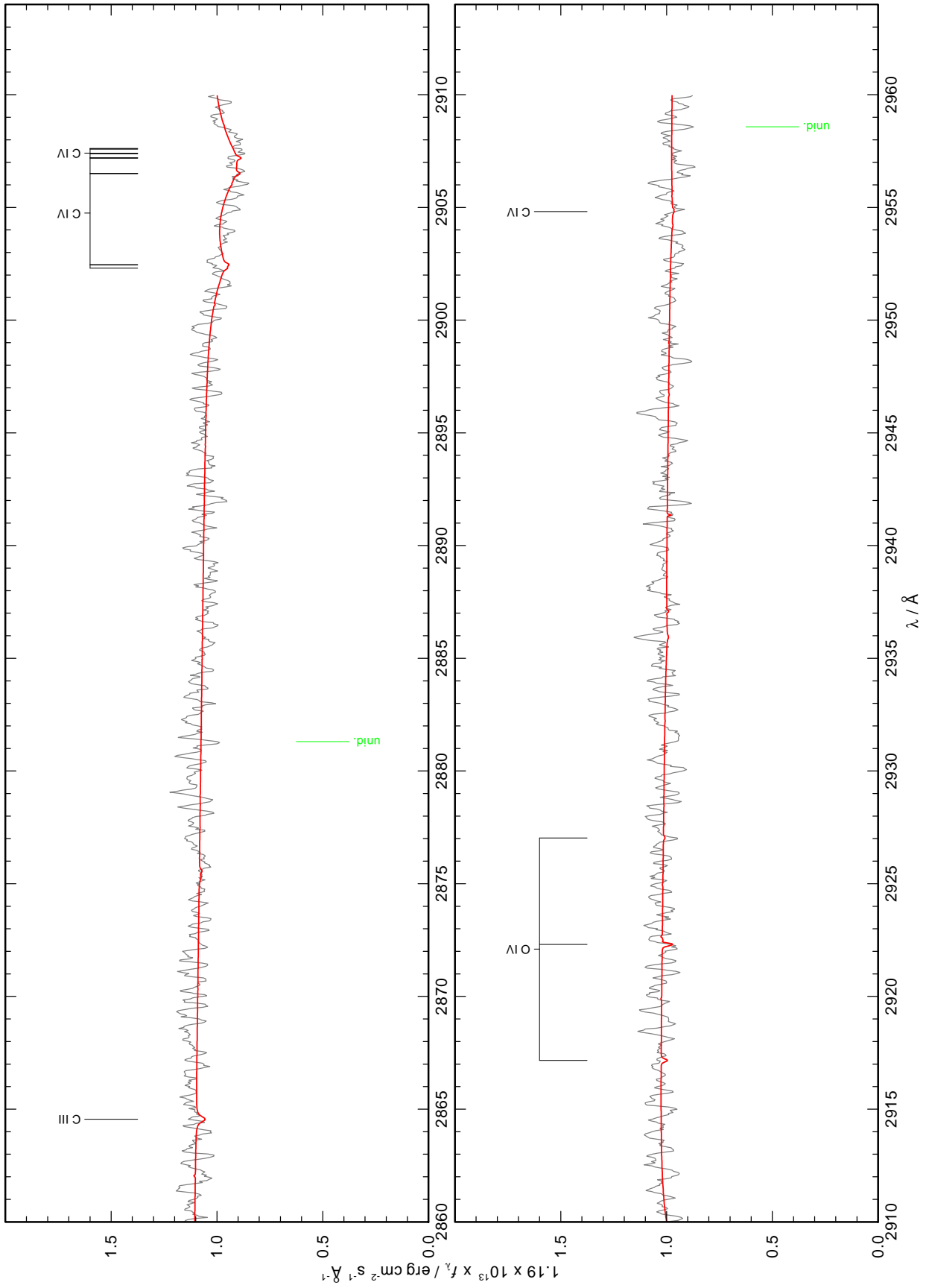


Fig. B.2. Figure B.2 continued.

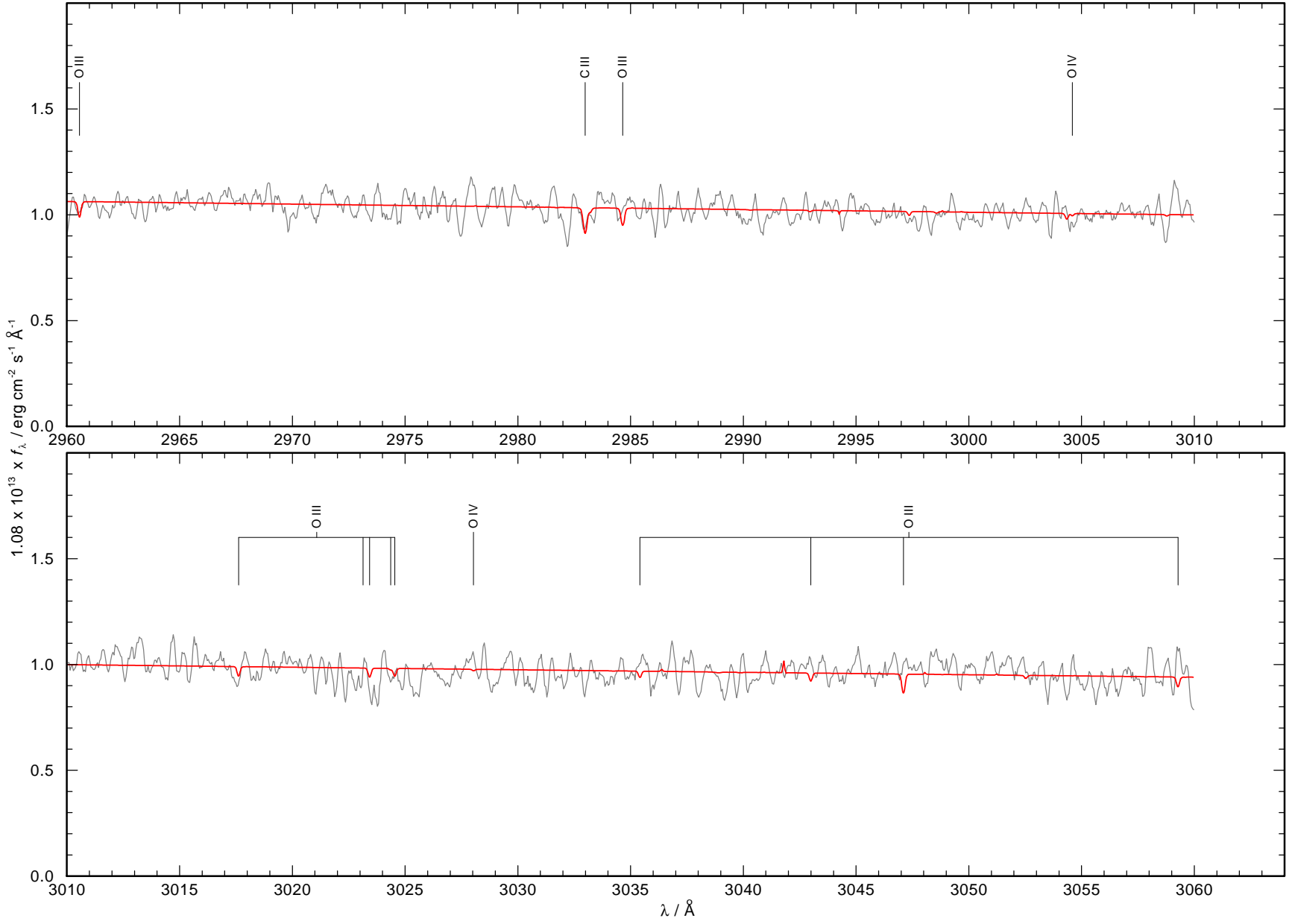
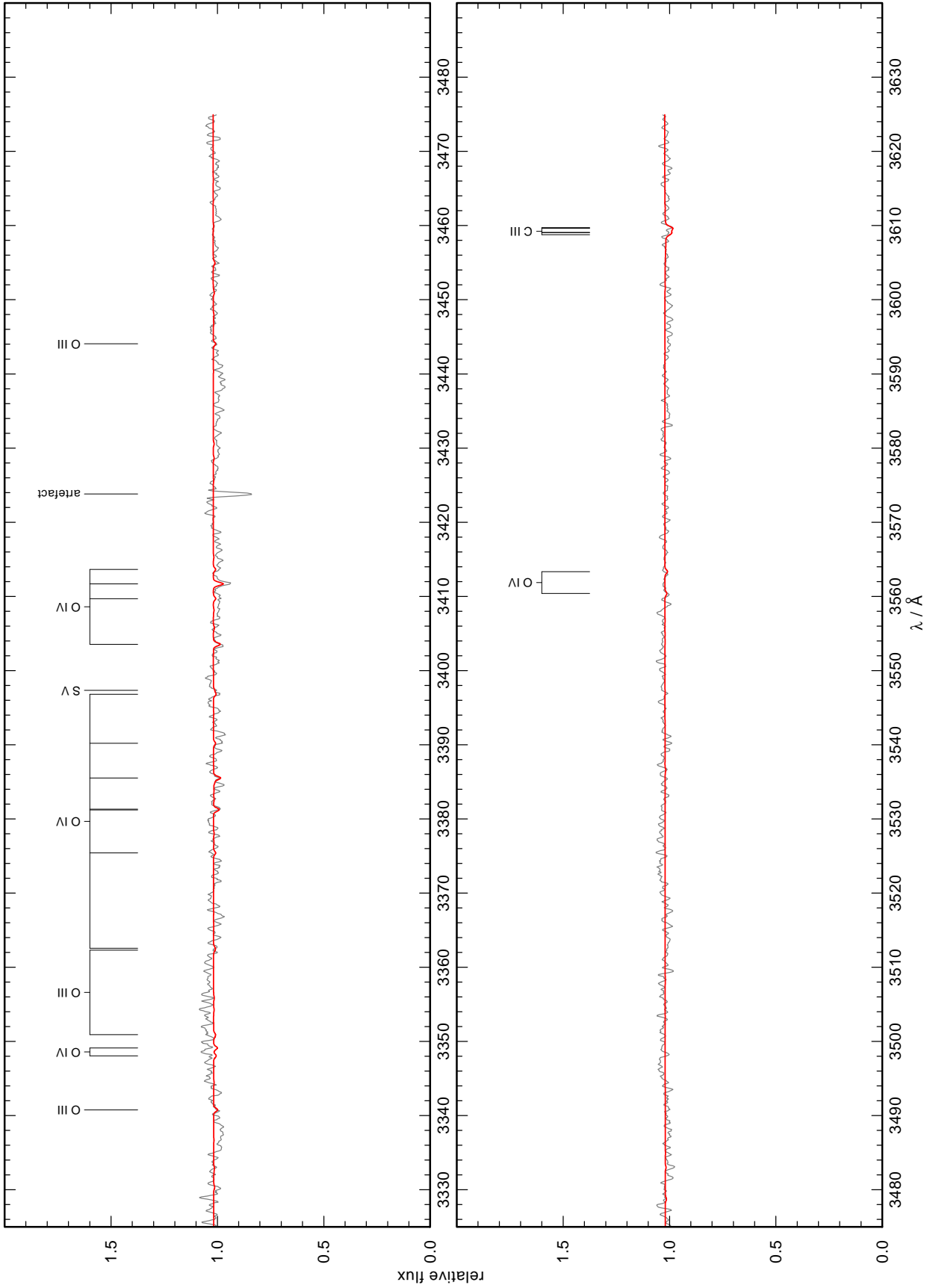


Fig. B.2. Figure B.2 continued.



**Fig. B.3.** Optical (SPY) observation (gray) compared with the best model (red). Stellar lines are identified at top. “unid.” denotes unidentified lines.

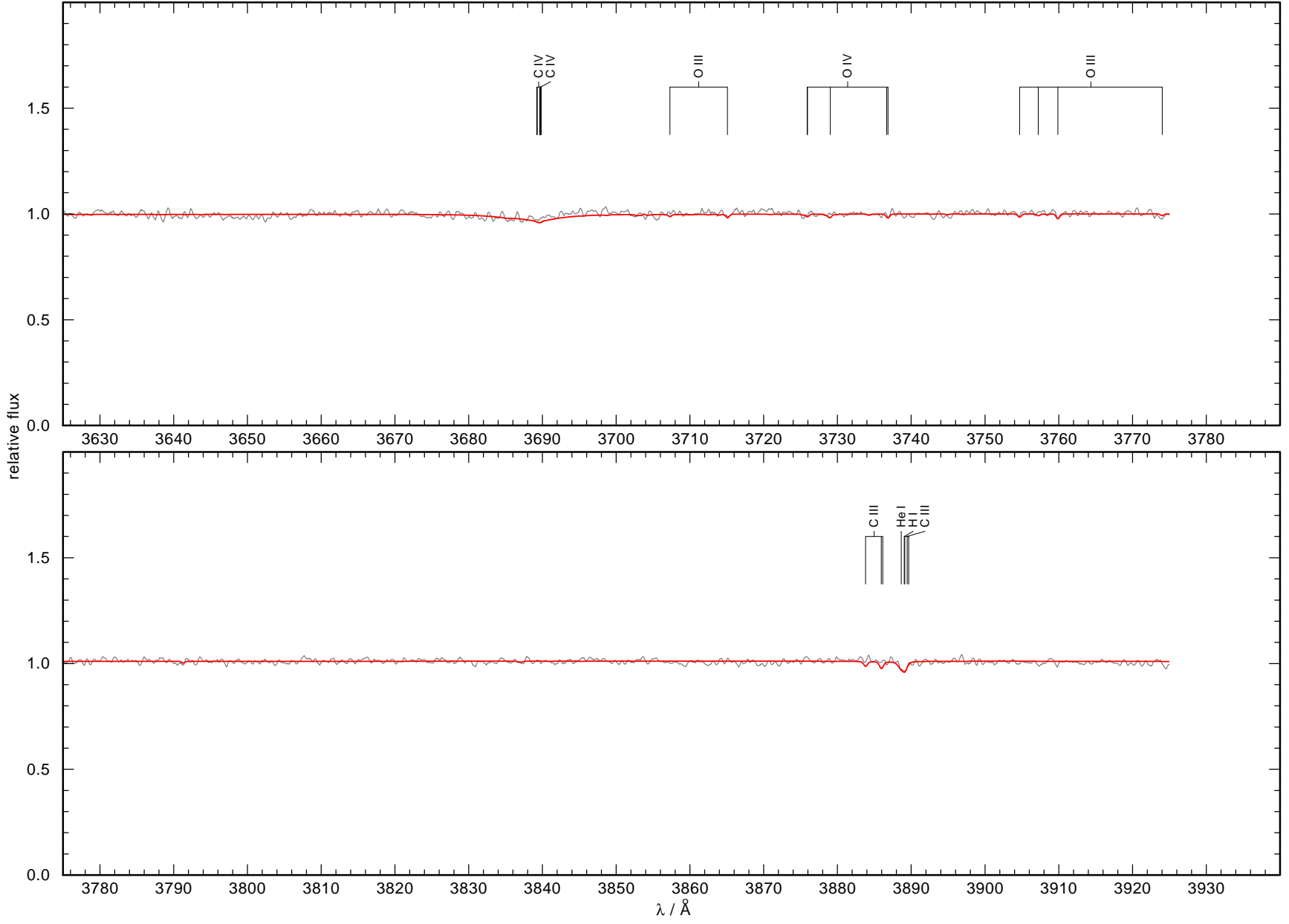


Fig. B.3. Figure B.3 continued.



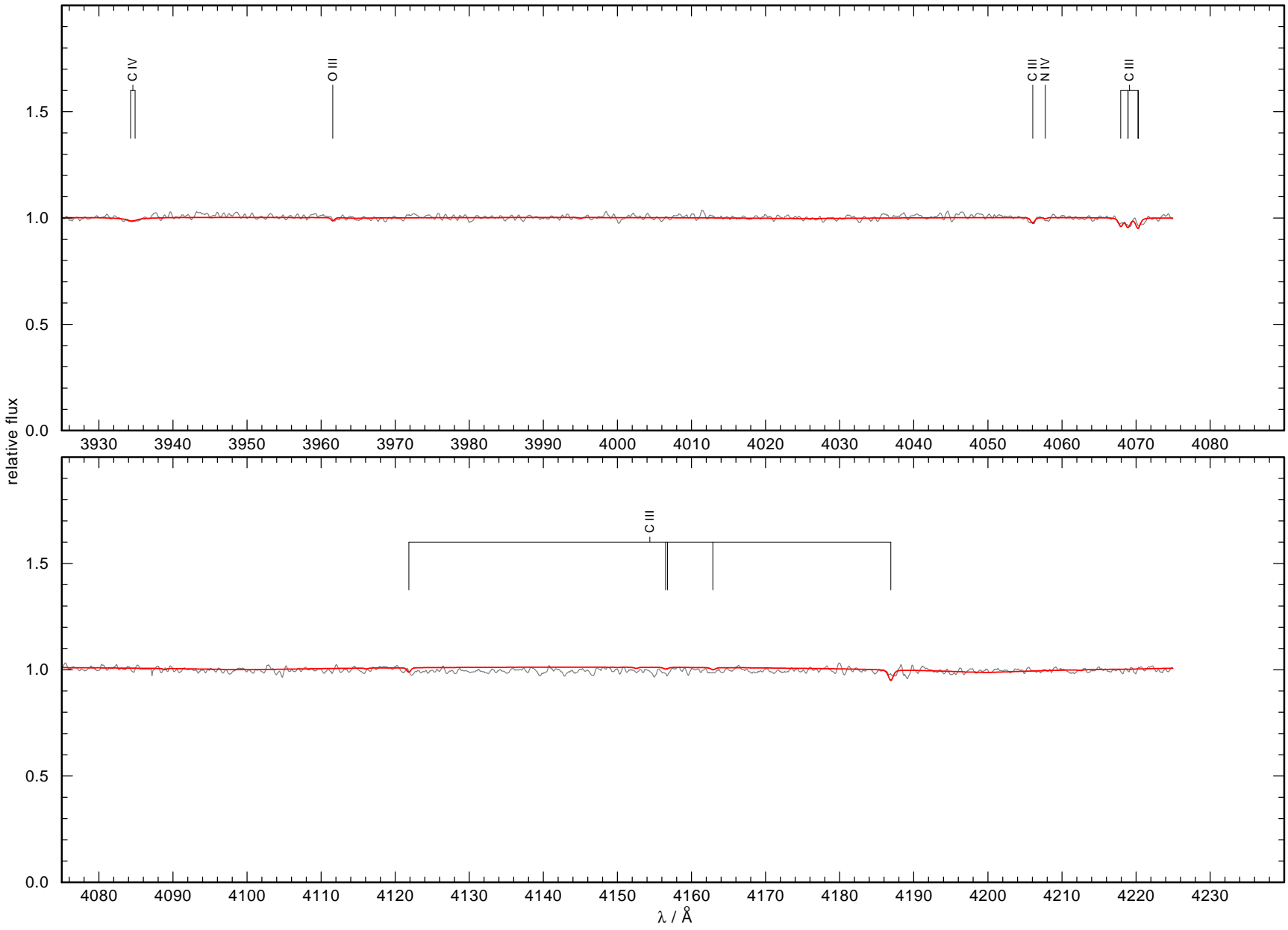


Fig. B.3. Figure B.3 continued.

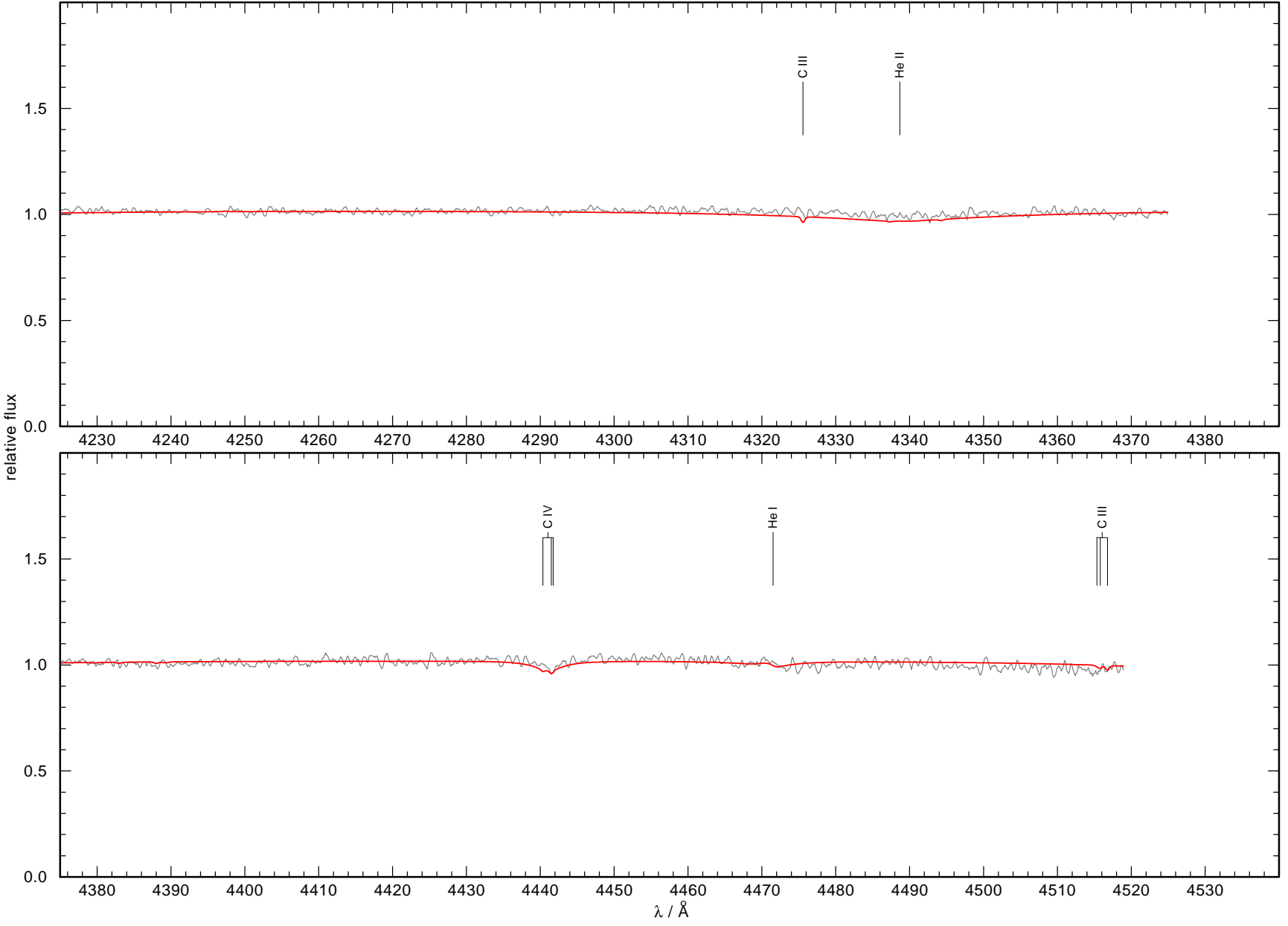


Fig. B.3. Figure B.3 continued.

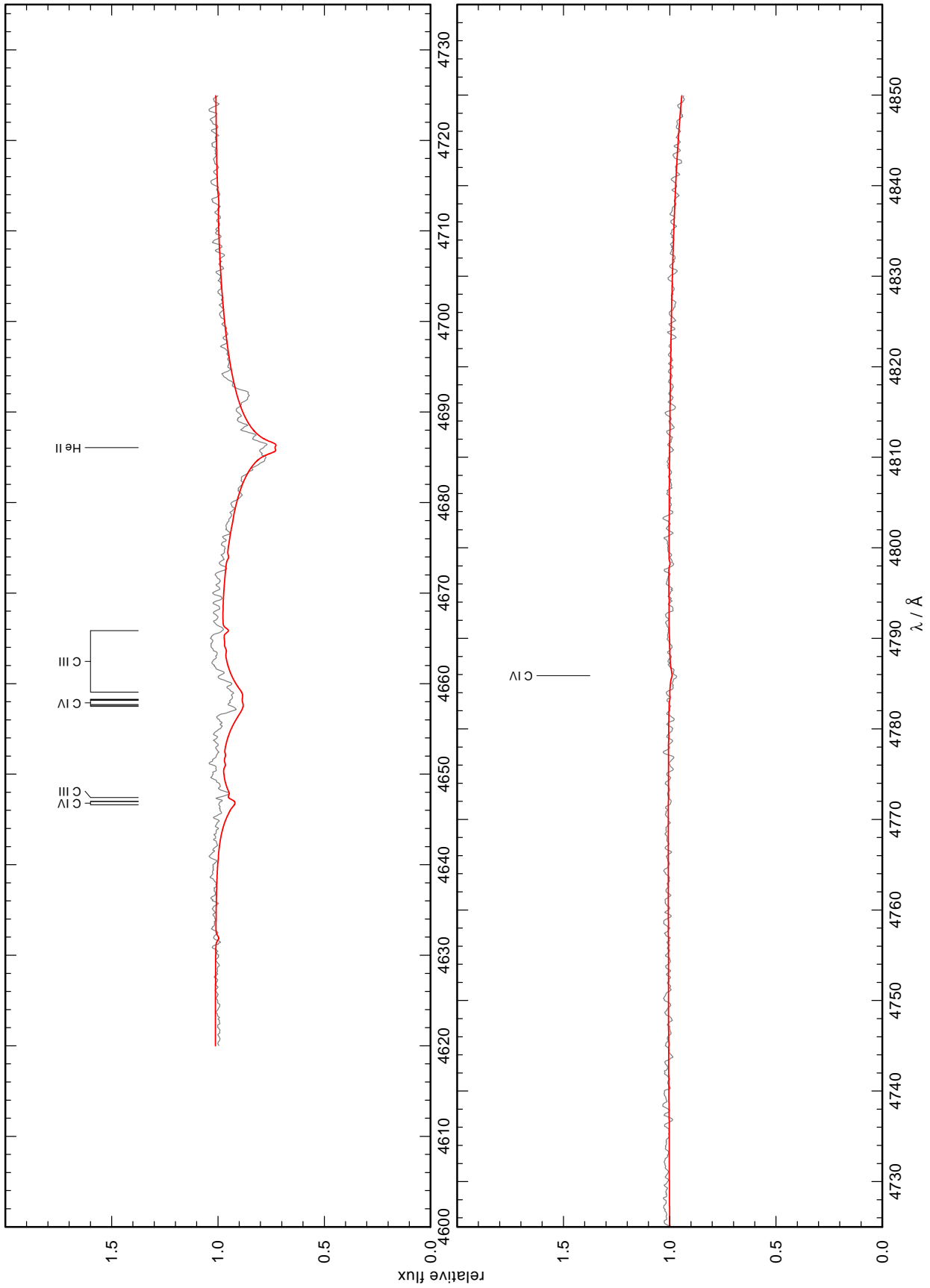


Fig. B.3. Figure B.3 continued.

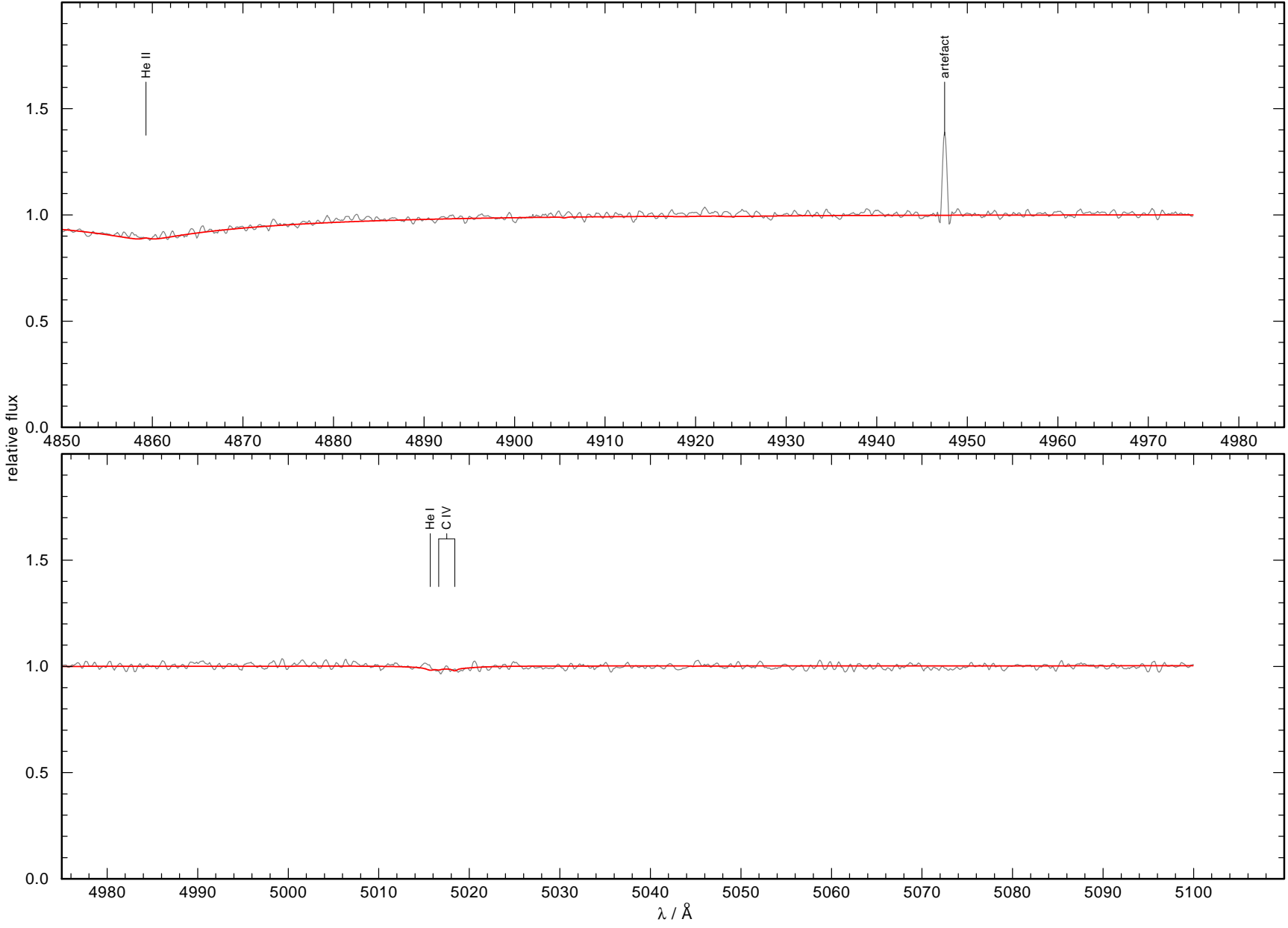


Fig. B.3. Figure B.3 continued.

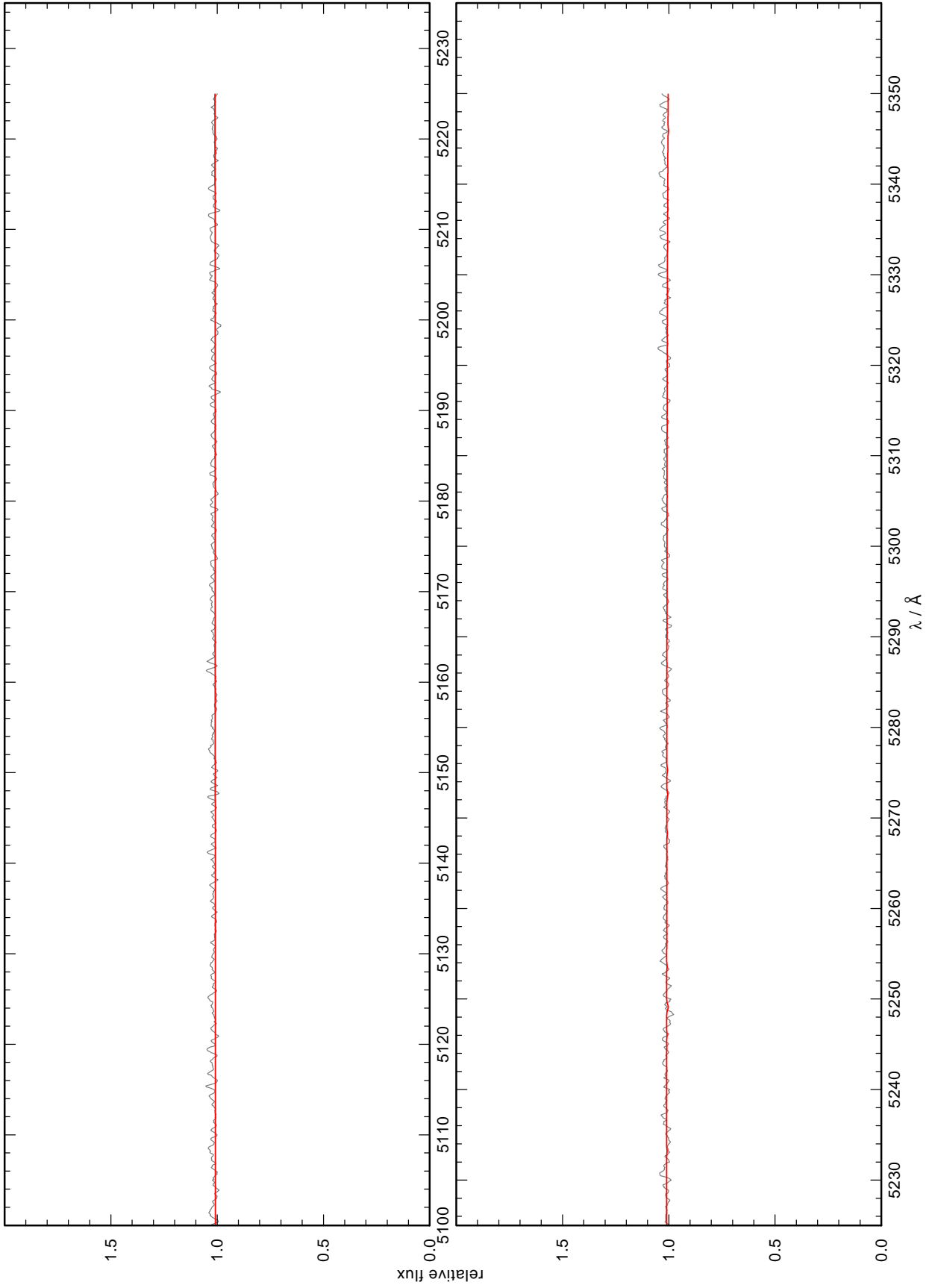


Fig. B.3. Figure B.3 continued.

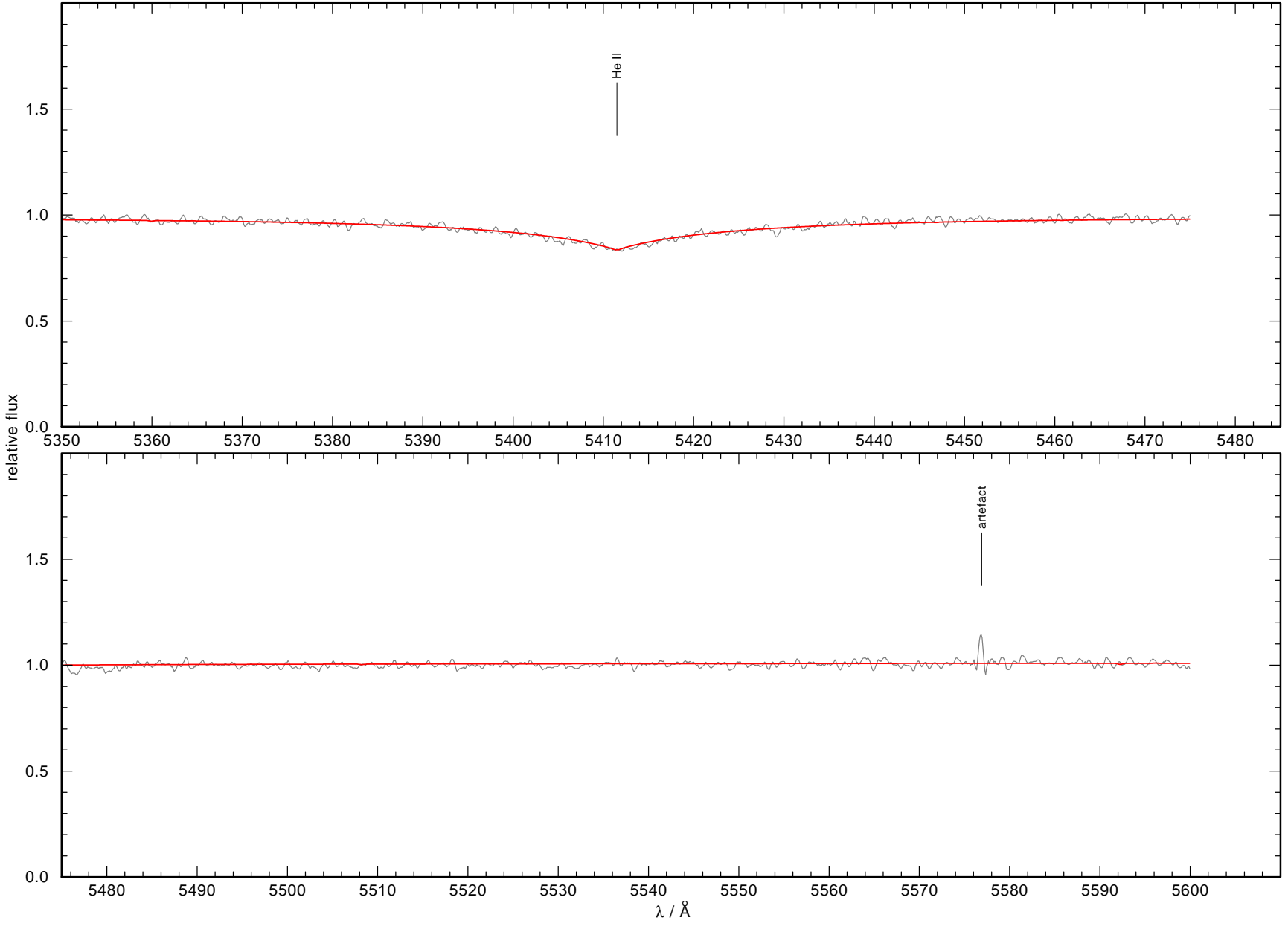


Fig. B.3. Figure B.3 continued.

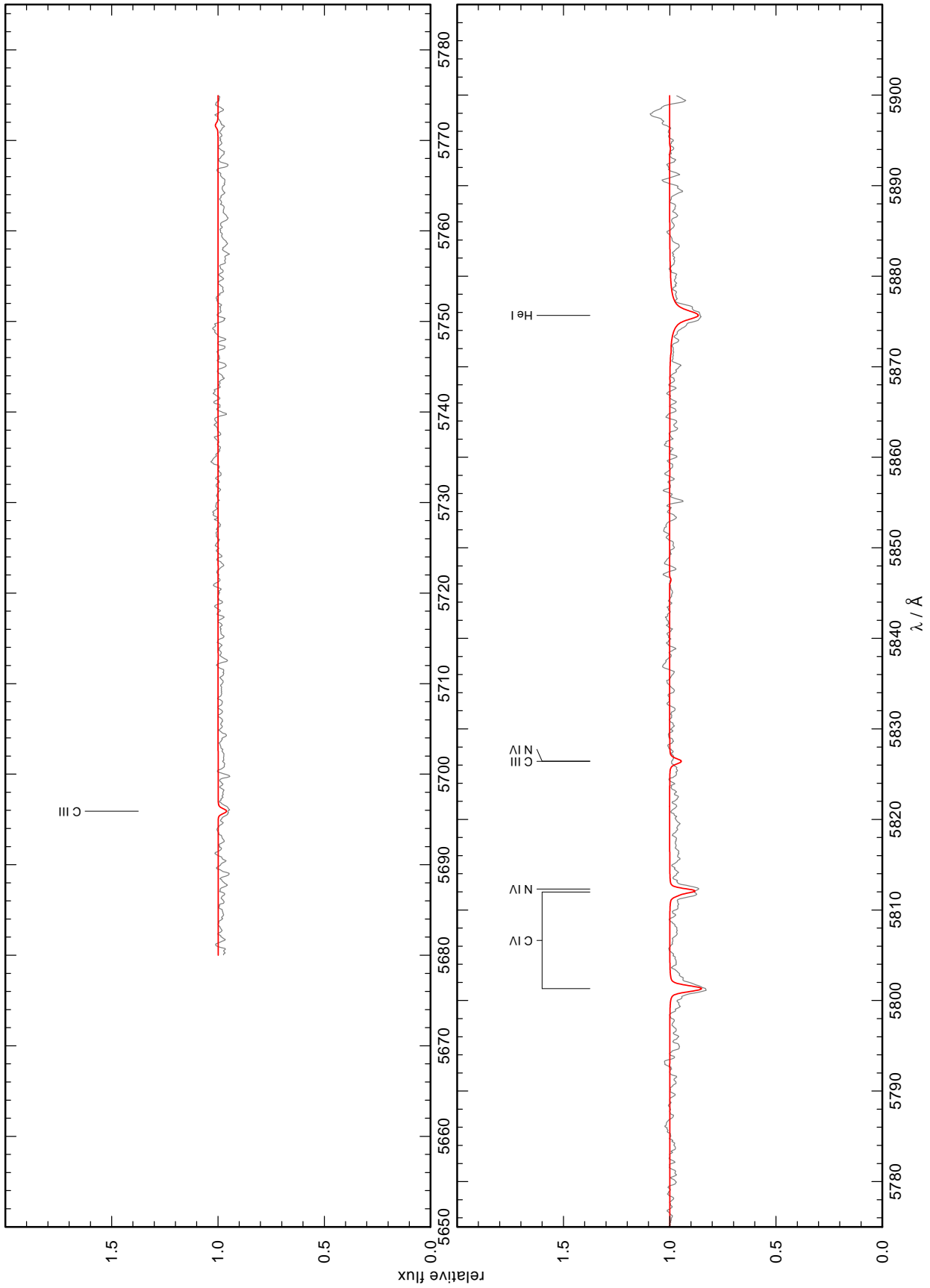


Fig. B.3. Figure B.3 continued.

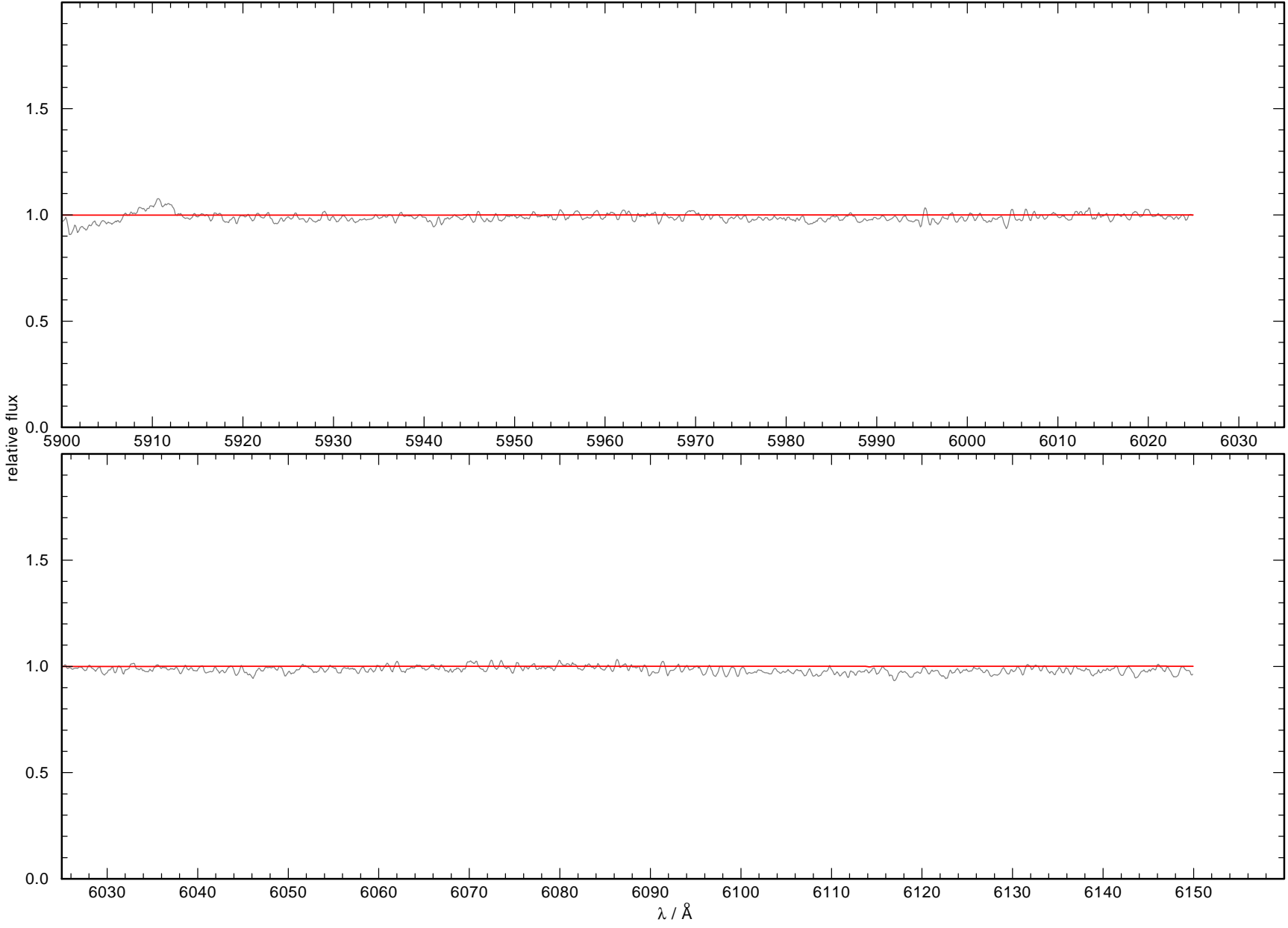


Fig. B.3. Figure B.3 continued.



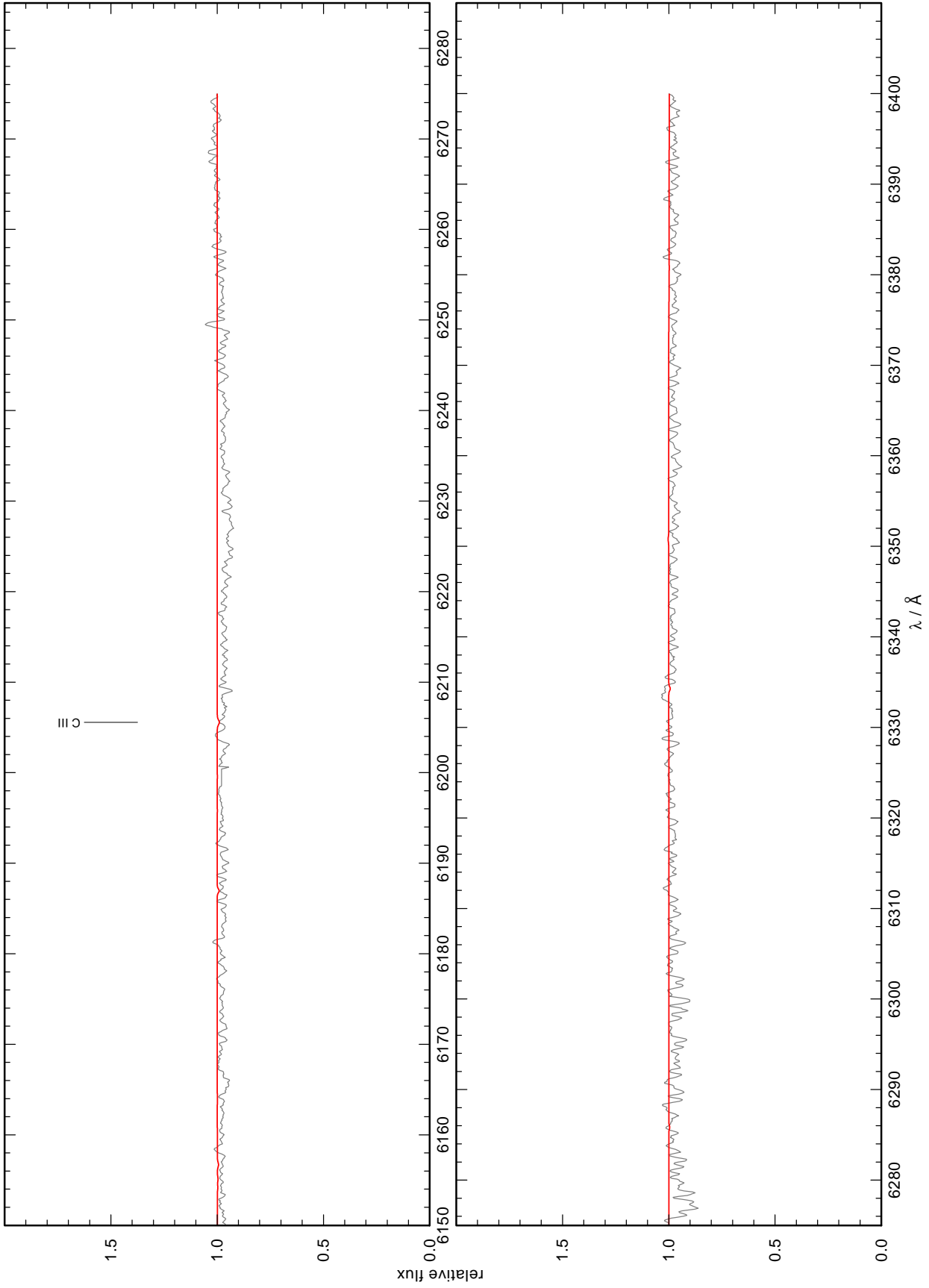


Fig. B.3. Figure B.3 continued.

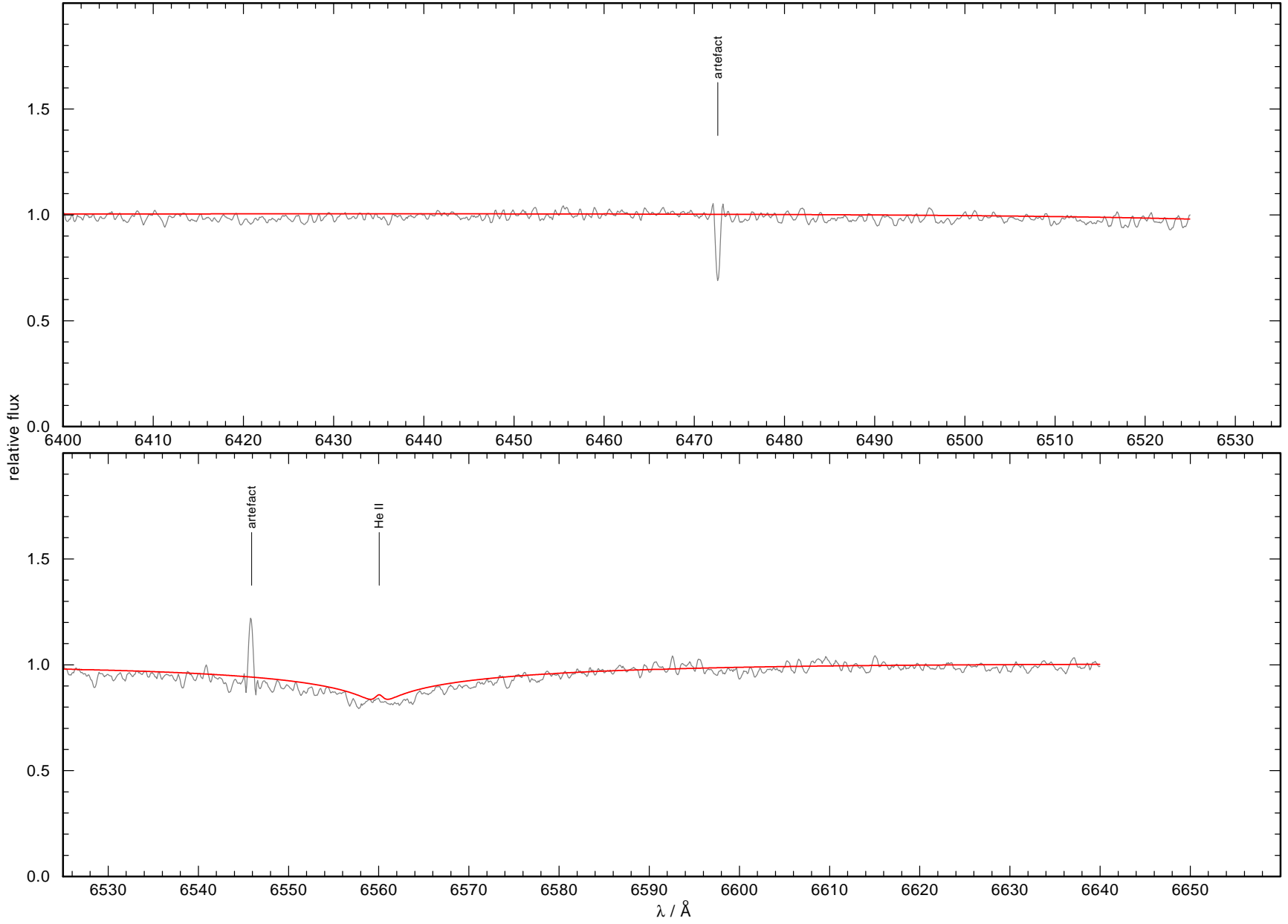


Fig. B.3. Figure B.3 continued.

## **Appendix C: WWW interfaces of TEUV, TGRED, and TVIS**

**Fig. C.1.** TEUV WWW interface. Not shown on astro-ph, please visit the WWW page.

**Fig. C.2.** TGRED WWW interface. Not shown on astro-ph, please visit the WWW page.

**Fig. C.3.** TVIS WWW interface. Not shown on astro-ph, please visit the WWW page.